THE EFFECTS OF BAICALEIN ON CHLORIDE TRANSPORT AND AQUEOUS HUMOUR FORMATION OF PORCINE CILIARY EPITHELIUM

XIAO JINGRU

Ph.D

The Hong Kong Polytechnic University

2015

The Hong Kong Polytechnic University
School of Optometry

The Effects Of Baicalein On Chloride Transport And Aqueous Humour Formation Of Porcine Ciliary Epithelium

XIAO JINGRU

A thesis submitted in partial fulfilment of the requirements

for the degree of Doctor of Philosophy

November 2013

CERTIFICATE OF ORIGINALITY

I hereby declare that this thesis is my own work and that, to the best of my knowledge and belief, it reproduces no material previously published or written, nor material that has been accepted for the award of any other degree or diploma, except where due acknowledgement has been made in the text.

Xiao Jingru

Abstract

Glaucoma is among the worldwide leading causes of irreversible blindness, frequently associated with elevated intraocular pressure (IOP). Currently, reducing IOP by reducing aqueous humour formation (AHF), or enhancing the outflow, is the only effective treatment in retarding the progression of vision defect. However, several current anti-glaucoma drugs have shown fading effectiveness and multiple side effects, suggesting a need in developing of novel and more potent drugs. Baicalein is a major bioactive flavone derived from a medicinal herb Scutellariae radix, with multiple biological functions, such as anti-inflammation, anti-tumor and modulation of chloride transport. AHF is also driven by chloride transport. Therefore, this present study aimed to examine if baicalein can regulate AHF and be a novel and potent medicinal for treating glaucoma.

The first part of present study employed Ussing chamber techniques to investigate the effect of baicalein on short-circuit current (Isc) across porcine ciliary body/epithelium (CBE), and its underlying transport mechanisms. Addition of baicalein on aqueous side elicited significant reduction of Isc dose-dependently. Baicalein induced Isc inhibition was strongly dependent on Cl^- concentration in the bath solution. Blocking Cl^- channels, instead of Na^+-K^+-$2Cl^-$ cotransporter, almost abolished the inhibition caused by baicalein, suggesting baicalein may inhibit Isc by reducing Cl^- secretion via Cl^- channels. Inhibition of protein kinase C

(PKC), not protein kinase A or lipoxygenase, dramatically suppressed baicalein induced Isc inhibition, indicating PKC was likely involved in the signalling pathway mediating the responses.

Fluid flow (FF) measurements showed that baicalein significantly reduced FF across porcine CBE, indicating the fluid secretion was markedly inhibited by baicalein.

Due to undesirable interaction with intracellular dye, the effects of baicalein on intracellular Cl^- concentration ($[Cl^-]_i$) and membrane potential of porcine ciliary epithelial cells could not be precisely quantified. Nevertheless, the electrical properties of these cells were successfully characterized by using the potential-sensitive dye bis (1,3-dibutylbarbituric acid) trimethine oxonol [DiBAC4(3)]. Both pigmented (PE) and non-pigmented (NPE) ciliary epithelial cells showed similar responses towards different interventions. Depolarization was noticed after Cl^- replacement. Both NFA and baicalein significantly inhibited the depolarization induced by Cl^- substitution, suggesting baicalein can also inhibit the Cl^- conductance upon Cl^- removal in porcine NPE cells.

Whole-cell current recordings in native porcine NPE cells showed that baicalein markedly reduced swelling-activated current and the basal current with normal and increased $[Cl^-]_i$. Only the inhibitory action on basal current with normal $[Cl^-]_i$ was completely blocked by PKC inhibitors (staurosporine and calphostin C), indicating under physiological condition, those active and PKC sensitive Cl^-

channels at NPE cells were probably the downstream cellular targets of baicalein in porcine CBE.

The involvements of PKC in the baicalein induced responses were further supported by the stimulation of phospho-PKC expression in baicalein treated-porcine ciliary epithelial cells.

In the final part, baicalein treated eyes showed significant lower IOP than contralateral eyes in guinea pigs from both topical administration and intravitreal injection groups.

In conclusion, baicalein can inhibit the transepithelial Cl^- transport and fluid secretion across porcine CBE, probably via down-regulating Cl^- channel activities. This inhibition may involve PKC associated signalling pathways. Baicalein has ocular hypotensive property and it may be developed into a novel anti-glaucoma drug in the future.

Publications arising from the thesis

Publication:

Xiao J.R., Li K.K., Do C.W., To C.H. (2014). Potential therapeutic effects of baicalein, baicalin, and wogonin in ocular disorders. *J Ocul Pharmacol Ther* 30(8):605-14

Abstracts:

Xiao J.R., Li K.K., Do C.W., Liu Q., Ge J., To C.H. (2009). The effects of baicalein on transepithelial electrical parameters of porcine ciliary body epithelium (CBE). *Invest Ophthalmol Vis Sci* 50: ARVO E-Abstract 94.

Xiao J.R., Li K.K., Tam W.S., Do C.W., To C.H. (2010). Modulation of chloride transport and aqueous humor secretion by baicalein. *Invest Ophthalmol Vis Sci* 52: ARVO E-Abstract 1519.

Xiao J.R., Li K.K., Do C.W., To C.H. (2012). A study of the intracellular electrical properties and transport mechanisms of porcine pigmented and non-pigmented ciliary epithelial cells. *Invest Ophthalmol Vis Sci* 53: ARVO E-Abstract 5339.

Acknowledgements

I would like to express my sincere thanks to Professor Chi-ho To, my supervisor, for his guidance and suggestions to my research study. He always shows great enthusiasm in research and in his life. It's his precious attitude that led me to a wonderful research life. I would also like to thank Dr Chi-wai Do, my co-supervisor, for his generous help and valuable suggestions during my PhD study.

I would also like to express my gratitude to the research team members of the laboratory, especially Mr K.K Li, for their support and encouragement. They have also brought me plenty of warmth and fun that have brightened up my research life.

Most importantly, I have to express my heartfelt thank to my husband and my family, for their care, patience, understanding and support throughout the period of my study. It's their endless love supports me to go for my degree without hesitation.

Xiao Jingru

Table of Contents

List of figures

List of tables

List of abbreviations

AE	Cl^-/ HCO_3^- antiport
AH	Aqueous humour
AHF	Aqueous humour formation
AQ	Aqueous side
AR	Adenosine receptor
ATP	Adenosine 5'-triphosphate
BAC	Benzalkonium chloride
BMT	Bumetanide
BS	Bilateral sides
BSA	Bovine serum albumin
$[Cl^-]_i$	Intracellular Cl^- concentration
CA	Carbonic anhydrase
CAI	Carbonic anhydrase inhibitor
cAMP	Cyclic 3',5'-adenosine monophosphate
CBE	Ciliary body/epithelium
CE	Ciliary epithelium
CFTR	Cystic fibrosis transmembrane conductance regulator
cGMP	Cyclic 3',5'-guanosine monophosphate
COX	Cyclooxygenases
Cx	Connexin
DAG	Diacylglycerol
DiBAC4(3)	Bis (1,3-dibutylbarbituric acid) trimethine oxonol

DIDS	4,4’-diisothiocyanatostilbene-2,2’-disulfonic acid
DMSO	Dimethyl sulfoxide
DPC	Diphenylamine-2-carboxylate
ELAM-1	Endothelial-leukocyte adhesion molecule 1
FBS	Fetal bovine serum
FF	Fluid flow
FSM	Furosemide
HETE	Hydroxyeicosatetraenoic acid
HP-β-CD	Hydroxypropyl beta-cyclodextrin
HRP	Horseradish peroxidase
IAA94	[(6,7-dichloro-2-cyclopentyl-2,3-dihydro-2-methyl-1-oxo-1H-inde n-5yl)-oxy] acetic acid
IL	Interleukins
IOP	Intraocular pressure
Isc	Short-circuit current
LOX	Lipoxygenases
MAPK	Mitogen-activated protein kinases
MQAE	*N*-(Ethoxycarbonylmethyl)-6-MethoxyquinoliniumBromide
NDGA	Nordihydroguaiaretic acid
NFA	Niflumic acid
NHE	Na^+/H^+ exchanger
NKCC	Na^+-K^+-$2Cl^-$ cotransporter
NMDA	N-methyl-D-aspartate
NO	Nitric oxide

NOS	Nitric oxide synthase
NPE	Non-pigmented epithelium
NPPB	5-Nitro-2-(3-phenylpropylamino)-benzoic acid
NRR	Normal Ringer solution
ORC	Open re-circulating chamber
PBS	Phosphate-buffered saline
PD	Potential difference
PE	Pigmented epithelium
PI3K	Phosphatidylinositol-4,5-bisphosphate 3-kinase
pHi	Intracellular pH
PKA	Protein kinase A or cAMP-dependent protein kinase
PKC	Protein kinase C
PKG	Protein kinase G
PLC	Phospholipase C
PMA	Phorbol 12-myristate 13-acetate
PVDF	Polyvinylidene difluoride
ROS	Reactive oxygen species
RGC	Retinal ganglion cell
Rt	Tissue resistance
RT-PCR	Reverse transcriptase polymerase chain reaction
RVD	Regulatory volume decrease
sGC	Soluable guanylate cyclase
SDS	Sodium dodecyl sulfate
SNP	Sodium nitroprusside

ST	Stromal side
TGF	Transforming growth factor
TM	Trabecular meshwork
TNF	Tumor necrosis factor

Chapter 1 Introduction

1.1 Background

Glaucoma is a chronic and progressive ocular disease, that is frequently, yet not always related to an elevated intraocular pressure (IOP). It is characterized by progressive optic neuropathy, vision loss and eventually blindness. For decades, glaucoma has been one of the leading causes of blindness all over the world (Quigley, 1996).

1.1.1 Pathogenesis of glaucoma

The pathophysiology of glaucoma is not clearly understood yet. It is believed to be the result of a complex interplay of multiple factors.

Elevated IOP

Elevated IOP has long been considered the mechanical force that causes irreversible damage of the retina and optical nerve system (Flammer and Mozaffarieh, 2007) and it is believed to be the primary factor in the initiation and progression of glaucoma. Intraocular pressure is normally maintained by balanced

aqueous humour (AH) dynamics between AH production and drainage. Abnormally high resistance in AH outflow facility increases IOP and thereby causes glaucoma (Brubaker, 1998). Reducing IOP by surgical and pharmacological intervention can significantly slow down progression of glaucomatous visual field loss (Kass et al., 2002).

There is a significant positive correlation between elevated IOP and retinal ganglion cell (RGC) loss according to a number of investigations in animal models (Morrison et al., 1997; Chauhan et al., 2002; Levkovitch-Verbin et al., 2002). Moreover, severe pressure has also been demonstrated to induce RGC apoptosis and axonal damages within hours (Naskar et al., 2002; Guo et al., 2005; Schlamp et al., 2006).

The underlying mechanism of the RGC death caused by elevated IOP is yet to be fully elucidated. Indeed, a direct induction of RGC apoptosis by IOP elevation has been reported (WoldeMussie et al., 2001). However, later studies suggested that more complicated mechanisms may contribute to the IOP induced RGC death. RGC apoptosis was found to be strongly related to the pressure induced excessive extracellular matrix remodeling in RGC layer (Guo et al., 2005). Moreover, in experimental glaucoma, activation of caspase 8 (McKinnon et al., 2002; Huang et

al., 2005b), caspase 9 (Hanninen et al., 2002; Huang et al., 2005b) and calcineurin cleavage (Huang et al., 2005a) has also been reported to be involved in RGC apoptosis.

Vascular insufficiency

Besides elevated IOP, insufficient vascular supply is another vital risk factor of the onset and development of glaucomatous neuropathy. Chronic reduction of blood flow in optical nerve head and retina has been observed in patients of primary open-angle glaucoma and normal tension glaucoma (Michelson et al., 1998; Chung et al., 1999). A positive association between vascular insufficiency and glaucoma has also been reported by several studies (Nicolela et al., 1996; Flammer et al., 2002; Satilmis et al., 2003; Akarsu et al., 2004). In a magnetic resonance imaging study, the incidences of pan-cerebral ischemia and cerebral infarcts in glaucoma patients are higher than that in the normal subjects further indicates that vascular insufficiency may be important in the pathophysiology of glaucoma (Ong et al., 1995).

Due to a decreasing ocular perfusion pressure, both age and reduced diastolic systematic pressure are recognized as risk factors for insufficient blood supply to

the retina and optical nerve head. The mechanism underlying RGC loss in response to vascular insufficiency is not fully understood. It is hypothesized that ischemia may directly impair the retina or induce apoptosis of RGC. In a rodent anterior ischemic optic neuropathy model, axonal ischemia was suggested to be one possible reason of RGC apoptosis (Slater et al., 2002).

Inflammatory response

Evidences have shown that there was continuous glial cell activation in the optical nerve head and retina of glaucomatous eyes, and that the cytokine level correlated well with optic neuropathy in POAG (Huang et al., 2009; Huang et al., 2010), suggesting neuron inflammatory process may be important in glaucoma (Medzhitov, 2008; Xu et al., 2009). In addition, a number of inflammation mediators have been detected in AH and outflow pathway of glaucoma patients, including transforming growth factor beta (TGF-β), interleukins (IL) IL-1α and IL-8, the tumor necrosis factor alpha (TNF-α), and endothelial-leukocyte adhesion molecule 1 (ELAM-1) (Fuchshofer and Tamm, 2012; Tezel, 2008; Sacca et al., 2012; Liton et al., 2012). These data further supported there is an active inflammatory response in glaucomatous eyes.

Oxidative stress

Increasing evidences have supported that reactive oxygen species (ROS) take an important part in the pathogenesis of glaucoma (Izzotti et al., 2006; Tezel, 2006; Sacca et al., 2007; Osborne et al., 2008). Reduced antioxidant capacity in glaucoma patients' blood plasma has been reported by several studies. For instance, the major antioxidant glutathione was significantly reduced, while malondialdehyde which is a product of oxidative stress was much higher in patients with glaucoma than normal subjects (Gherghel et al., 2005; Yildirim et al., 2005). ROS can also cause degeneration in trabecular meshwork (TM): both *in vitro* and *in vivo* treatment of hydrogen peroxide caused significant alteration in cell structure and drainage mechanisms (Kahn et al., 1983; Zhou et al., 1999). In glaucoma patients, more DNA damage induced by oxidative stress in TM cells was detected than normal subjects (Izzotti et al., 2003). The extent of these TM cell damages can even be correlated to the IOP increase and visual field loss (Sacca et al., 2005). Besides TM, degeneration in optical nerve was also prone to oxidative stress and may in turn induce apoptosis of ganglion cells (Moreno et al., 2004). To combat these oxidative damages, many antioxidants have been studied in animal models of glaucoma neuropathy. Indeed, RGC were protected by

neurotrophic factors and antioxidant agent in rats with experimental glaucoma (Ko et al., 2000). In another rat glaucoma model, topical administration of a novel free radical scavenger markedly reduced IOP by 29.6%. Furthermore, N-methyl-D-aspartate (NMDA) induced RGC loss was significantly reduced after co-administration of this antioxidant agent with NMDA (Hosseini et al., 2006).

1.1.2 Therapeutic approaches

Clinically, surgical and medical treatments are the two major options for glaucoma therapy based on the types and stages of glaucoma. Currently, lowering IOP is the only pharmacological treatment reported to effectively protect the optical nerve and slow down the progression of glaucomatous vision loss (Collaborative Normal-Tension Glaucoma Study Group, 1998b; Collaborative Normal-Tension Glaucoma Study Group, 1998a; The AIGS Investigators, 2000).

Intraocular pressure can be reduced through suppressing AH secretion or improving AH drainage. Clinically, there are several classes of anti-glaucoma drugs used to reduce IOP: α-adrenergic receptor agonists, β-adrenergic receptor

antagonists, carbonic anhydrase inhibitors, prostaglandin analogs and cholinergic agents. The first three classes function to reduce IOP by decreasing AH formation (AHF), while cholinergic agents and prostaglandin analogs act through enhancing AH outflow. However, due to drug resistance and individual variation in sensitivity to different drugs, a combination of two or three anti-glaucoma drugs is gradually required to improve the hypotensive effect. It was reported that the compliance of patients using multi-drug treatment is significantly reduced (Schwartz, 2005). Moreover, multiple-dose and long-term medication increases the risk of ocular and systemic adverse effects which may lower patients' compliance further (Detry-Morel, 2006). Although topical anti-glaucoma agents are relatively safer than systemic medications, they are not without sides effects: such as inflammatory responses (Yee, 2007), allergic reactions (Baudouin, 1996) and toxicity to TM (Samples et al., 1989). Therefore, to maximizing the patient compliance and efficacy, developing novel potent hyoptensive drugs with low toxicity should be the goal.

Besides IOP control, neuroprotective strategies have gained prominence recently by virtue of a better understanding of the pathogenesis of glaucoma. Recently, NMDA-type glutamate receptor antagonists have received extensive attention in

neuroprotection research. Memantine is a noncompetitive NMDA antagonist, which preferentially blocks ion channels that are excessively open. Because it essentially targets at pathological activity, without interfering with normal neuronal function, memantine was well tolerated for clinical treatment of neuron disorders such as Alzheimer's disease (Lipton, 2004). Memantine has been reported to effectively protect RGC cells (Chen et al., 1992; Chen et al., 1998), but the clinical trials for its efficacy and safety in treating glaucoma are yet to be characterized.

In addition, a number of agents have shown promising neuroprotective effects in animal models and *in vitro* studies, such as antiapoptic agents (erythropoietin) (Zhong et al., 2007; Zhang et al., 2013), neurotrophic factor such as BNDF (Ko et al., 2000), an antioxidant (N-ace-tyl-L-cysteine) (Hosseini et al., 2006) and nitric oxide synthase (NOS) inhibitors (L-NAME, aminoguinidine) (Koseki et al., 1994). Although none of them have progressed to the clinical trial phase, they may provide the breakthrough in therapeutic treatment of glaucoma in the future.

1.2 Mechanisms of AHF

AH is a transparent fluid exclusively secreted from the ciliary process of ciliary body. After AHF, AH leaves posterior chamber, flows into anterior chamber through pupil and finally exits from the eye via the trabecular pathway and the uveoscelaral pathway.

AHF of ciliary body was suggested to proceed through four steps (Bill, 1975):

1. Blood flows through the microvasculature within the ciliary stroma.

2. An ultrafiltrate is derived from the blood plasma via the fenestrated capillaries into the interstitial space of the ciliary stroma.

3. Solutes in the ultrafiltrate are selectively transported across the ciliary epithelium (CE) from the stroma into the posterior chamber.

4. The osmotic gradient created by the solute transferred across the CE drives a passive flow of fluid.

In theory, three possible pathways are involved in the process of AHF across CE:

1. Diffusion - the passive flow of solutes down the transmembrane electrochemical gradient;

2. Ultrafiltration - the passive transmembrane transport of water and solutes under the influence of the differential osmotic pressure of the ciliary body and the hydrostatic pressure in the blood;

3. Active secretion - the energy-dependent transport of solutes across the plasma membrane.

The concentrations of some solutes in AH, such as ascorbate and Cl^-, are much higher than predicted from the electrochemical equilibrium of the blood plasma, suggesting mechanisms besides diffusion may account for AHF (Davson, 1990; Krupin and Civan, 1996).

Since the ciliary processes have a great hydraulic conductivity, ultrafiltration was thought to be responsible for around 80% of AH secretion (Green and Pederson, 1972). However, subsequent observations proposed ultrafiltration may play a minor role in the process. Bill (1973) found that the hydrostatic pressure was lower than the sum of oncotic pressure and IOP, thus favoring reabsorption instead of secretion of AH. Moreover, AH secretion was hardly affected after the systemic arterial blood pressure was experimentally lowered by 25% (Reitsamer and Kiel, 2003).

Active transport process was then proposed to account for the major portion of AH secretion (Bill, 1975). Indeed, AH secretion was found to be inhibited by various metabolic blockers (Becker, 1963; Becker, 1980; Kodama et al., 1985; Shahidullah et al., 2003), hypothermia (Becker, 1960; Cole, 1969), and anoxia (Watanabe and Saito, 1978; Krupin et al., 1984; Chu and Candia, 1988), further supporting an active nature of AHF.

1.3 Transepithelial ion secretion across CE

AH is exclusively secreted by CE, which consists of the pigmented (PE) and the non-pigmented (NPE) ciliary epithelial layers. With PE layer facing the stroma and NPE layer facing AH, PE and NPE cells are coupled together through the intercellular gap junctions and constitute a functional syncytium (Raviola and Raviola, 1978).

The transepithelial ion transport produced an osmotic gradient that drives water to enter the posterior chamber and forms AH. The transepithelial ion transport across CE involves three steps: (1) uptake of ion by the PE cells, (2) ion transfer from PE to NPE cells via gap junctions, (3) ion secretion into the posterior chamber by the NPE cells (To et al., 2002).

Na^+, Cl^- and HCO_3^-, as the dominant ions in AH, are believed to be involved in the transepithelial ion transport. The transport of these ions across CE is focused and reviewed here.

1.3.1. Na^+ transport

Sodium-potassium adenosine triphosphatase (Na^+, K^+-ATPase) is a vital enzyme mediating active Na^+ transport across CE. It pumps 3 Na^+ ions out and pumps 2 K^+

ions into the cells, with the consumption of one Adenosine 5'-triphosphate (ATP) (Glynn, 1993). The presence of Na^+, K^+-ATPase in CE has been reported in various species including rat and mouse (Wetzel and Sweadner, 2001), rabbit (Cole, 1964; Flugel and Lutjen-Drecoll, 1988; Usukura et al., 1988), pig (Shahidullah et al., 2007), and ox (Ghosh et al., 1990). In CE, Na^+, K^+-ATPase is expressed mainly at the interdigitation and basolateral infoldings of PE and NPE cells (Usukura et al., 1988; Mori et al., 1991), with higher expression level in NPE cells (Riley and Kishida, 1986; Usukura et al., 1988). The isoforms of Na^+, K^+-ATPase also shows regional differences in locations. For instance, α- and β-isoforms are more abundantly detected in the pars plicata (Ghosh et al., 1991).

Besides regulating intracellular pH (pH_i), cell volume and membrane potential, Na^+, K^+-ATPase generates Na^+ and K^+ gradients for secondary transepithelial solutes transport. Several experimental observations supported the vital importance of Na^+, K^+-ATPase in ion transport across CE and AHF. Inhibition of its activity by ouabain almost abolished the Isc across porcine CE (Kong, 2006). The AH inflow was reduced by ouabain in cats (Oppelt and White, 1968; Garg and Oppelt, 1970), pig (Law et al., 2009), isolated perfused eye of rabbit (Kodama et

al., 1985) and ox (Shahidullah et al., 2003). In experimental animals, Ouabain was reported to reduce IOP as well (Becker, 1963; Waitzman and Jackson, 1965).

Cole was the first to report the presence of net Na^+ transport across CE. In rabbit and ox, a positive potential difference (PD) across CE at the aqueous side was detected. The magnitude of PD was significantly dependent on the Na^+ concentration in the bathing solution (Cole, 1961; Cole, 1962), indicating the involvement of active Na^+ transport in AHF. Later, several studies supported this hypothesis. The Na^+ accession rate from blood stroma into posterior chamber was found to be very close to the AHF rate in dog (Maren, 1976). Both the Na^+ accession rate and AHF were effectively suppressed by the administration of ouabain in various species including cat (Garg and Oppelt, 1970), monkey (Maren, 1977) and dog (Zimmerman et al., 1976; Maren, 1976).

However, subsequent electrophysiologic studies questioned the role of active Na^+ transport in AHF. An aqueous-side negative PD across CE was detected in several studies (Holland and Gipson, 1970; Watanabe and Saito, 1978; Kishida et al., 1981; Krupin et al., 1984; Iizuka et al., 1984; Chu et al., 1987), representing the presence of active anion transport instead of cation transport. Moreover, many studies failed to detect the net Na^+ transport across CE among different species

including toad (Saito and Watanabe, 1979), cat (Holland and Gipson, 1970), rabbit (Kishida et al., 1982) and ox (To et al., 1998a). Furthermore, ouabain caused minor stimulation, rather than inhibition, of Na^+ fluxes (Saito and Watanabe, 1979; Pesin and Candia, 1982). The detection of small net Na^+ transport was known to be difficult because the unidirectional Na^+ flux is very high. To address this problem, Candia et al. (1991) reduced the Na^+ concentration in the bathing solution, and finally detected a net Na^+ flux, yet the magnitude was too small to account for the *in vivo* AHF rate (Candia et al., 1991). This discrepancy may be due to a relatively slow delivery of solutes from the stroma into the aqueous side. The predicted AHF rate from excised CE preparation (Do et al., 2000) was much lower than the measured value from an arterially perfused eye (Wilson et al., 1993; Shahidullah et al., 2003).

1.3.2. HCO_3^- transport

Carbonic anhydrase (CA) is the vital enzyme in the regulation of HCO_3^- transport across CE, which catalyzes the reversible conversion from CO_2 and water into HCO_3^- and H^+. The presence (Lutjen-Drecoll and Lonnerholm, 1981; Lutjen-Drecoll et al., 1983) and activities (Dobbs et al., 1979; Wistrand and Garg,

1979; Muther and Friedland, 1980; Wu et al., 1997) of CA have been demonstrated by extensive histochemical and biochemical studies respectively. Two isoforms of CA (CA II and IV isoform) were identified (Wistrand et al., 1986; Matsui et al., 1996; Wu et al., 1997) and suggested to facilitate HCO_3^- transport into the AH (Maren, 1997).

The CA inhibitors (CAI) were found to be effective in reducing the rate of AHF and IOP in human (Dailey et al., 1982; Larsson and Alm, 1998) and animals (Stein et al., 1983; Bar-Ilan et al., 1984; Kishida et al., 1986; Wang et al., 1990; Wang et al., 1991), indicating the functional significance of CA in AH secretion. In fact, CAI has been used as anti-glaucoma drugs for several decades and the primary mechanism is believed to be the inhibition of AHF.

The CA-facilitated HCO_3^- release into AH was first proposed by Friedenwald (1949). Results from several subsequent studies supported the presence of this transport. In guinea pig and rabbit, the concentration of HCO_3^- in AH was higher than that in blood plasma (Davson and Luck, 1956), indicating the existence of active HCO_3^- accumulation or transport into AH. Moreover, a concomitant accession of Na^+ and HCO_3^- in AH was noticed (Maren, 1976), and this accession was suppressed by a CAI, acetazolamide (Maren, 1976).

By removing HCO_3^- in the solution, the polarity of PD across rabbit CE was reversed (Kishida et al., 1981; Krupin et al., 1984). Similar abolition of PD after the depletion of HCO3$^-$ was also noticed in porcine CE (Kong et al., 2006). However, eliminating bathing HCO_3^- only reduced the PD across bovine CE by 30-40% (Do and To, 2000). Although transepithelial ion transport showed different dependency on HCO_3^-, these results clearly supported an essential role of HCO_3^- in the maintenance of ionic movement across CE.

Na^+-HCO_3^- symport has been detected in the PE cells of rabbit and ox (Helbig et al., 1989b; Butler et al., 1994), which may be responsible for the entry of HCO_3^- into PE cells, while the Cl^-/HCO_3^- exchangers detected at the baselateral membrane of rabbit NPE cells (Wolosin et al., 1991; Wolosin et al., 1993) can provide the potential route for the release of HCO_3^- into the posterior chamber.

Surprisingly, no net HCO_3^- transport was observed in bovine CE (To et al., 2001) and one of the CA inhibitors acetazolamide was found to reduce net Cl^- secretion rather than HCO_3^- transport. Based on these findings, To et al. (2001) proposed that HCO_3^- may mediate AHF indirectly via the regulation of Cl^- transport.

1.3.3. Cl^- transport

Transepithelial Cl^- transport across CE has been considered to be of vital importance in AHF (Civan, 2003). The presence of Cl^- transport has been supported by several concomitant findings. A Cl^--dependent Isc across CBE has been detected in toad (Watanabe and Saito, 1978), cat (Holland, 1970), ox (Do and To, 2000), rabbit (Kishida et al., 1981) and pig (Kong et al., 2006), while a net Cl^- secretion across CE from the blood side to the aqueous side has also been noticed in toad (Saito and Watanabe, 1979), cat (Holland and Gipson, 1970), ox (Do and To, 2000), rabbit (Kishida et al., 1982; Crook et al., 2000) and pig (Kong et al., 2006). In addition, the Isc, as well as net Cl^- secretion of CE are significantly reduced by several chloride or anion transporter inhibitors and channel blockers (Do and To, 2000; Kong et al., 2006). The Cl^- transport cross CE involves three steps and they are reviewed below.

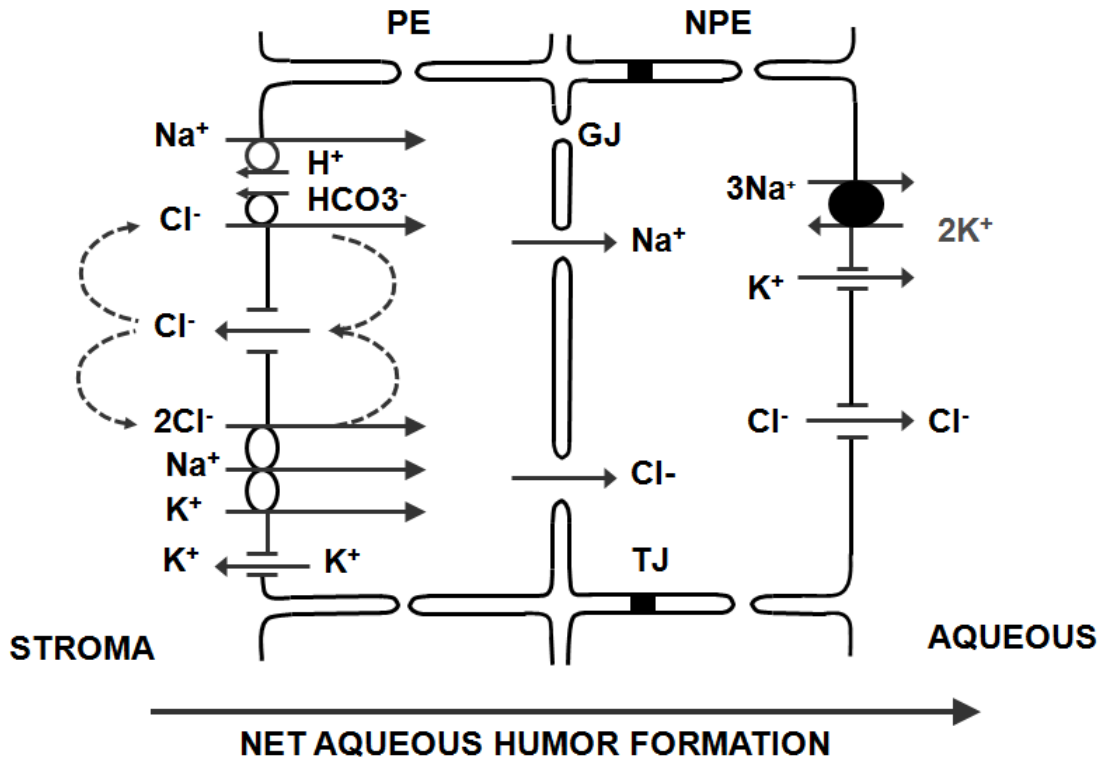

Fig 1.1 The consensus model of Cl^- transport across CE. TJ, tight junctions; GJ, gap junctions.

1.3.3.1 Cl^- uptake by PE cells

Based on the remarkably higher intracellular Cl^- concentration ($[Cl^-]_i$) in CE than that expected from electrochemical equilibrium, an active mechanism was suggested for the Cl^- uptake by PE cells (Green et al., 1985; Wiederholt and Zadunaisky, 1986; Bowler et al., 1996). Furosemide significantly inhibited the Cl^- uptake and reduced the intracellular Cl^- activity in the isolated CE of shark (Wiederholt and Zadunaisky, 1986). The coupling uptakes of radiolabelled ^{22}Na and ^{36}Cl were found in the cultured PE cells of ox (Helbig et al., 1989a). Based on

these observations, there are two major pathways prosposed for the Cl^- uptake by PE cells (Wiederholt et al., 1991): (1) Na^+-K^+-$2Cl^-$ cotransporter (NKCC), and (2) paired Cl^-/HCO_3^- (AE) and Na^+/H^+ (NHE) antiports. Both pathways have been shown to be active in the PE by several studies (Crook et al., 2000; Do and To, 2000; To et al., 2001; Shahidullah et al., 2003; Kong et al., 2006).

(A) Na^+-K^+-$2Cl^-$ cotransporter

NKCC belongs to a kind of membrane protein capable of simultaneous transport of Na^+, K^+ and Cl^- in an electroneutral way. Immunolabeling studies have localized the NKCC to the basolateral membrane of PE cells of pars plicata (Crook et al., 2000; Dunn et al., 2001). The intracellular Cl^- activity in shark CE was decreased by inhibiting the NKCC activity with furosemide (Wiederholt and Zadunaisky, 1986). A selective NKCC blocker, bumetanide, also markedly inhibited the ^{22}Na and ^{36}Cl uptakes in culture PE cells (Helbig et al., 1989a) and the Na^+, K^+ and Cl^- -dependent shrinkage in native PE cells (Edelman et al., 1994) in ox. The importance of NKCC in Cl^- secretion and AHF has been manifested by several Ussing chamber studies. Blockade of NKCC with bumetanide inhibited Isc as well as net Cl^- secretion of CE in different species including ox (Do and To, 2000), rabbit (Crook et al., 2000), and pig (Kong et al., 2006). In addition, the *in*

vitro fluid flow (FF) across porcine CE (Law et al., 2009) and the AH production of bovine perfusing eye (Shahidullah et al., 2003) were reduced by bumetanide application.

(B) Cl^-/HCO_3^- and Na^+/H^+ antiports

The AE/NHE antiports have also been demonstrated to play a vital part in the uptake of Cl^- by PE cells (Helbig et al., 1989a). The $[Cl^-]_i$ of both PE and NPE cells was increased in the HCO_3^--rich solution and decreased by the CA inhibitor acetazolamide (McLaughlin et al., 1998, Macknight et al., 2000). Moreover, both AE and NHE exchangers were reported to participate in key cellular events in bovine PE cells, including the ^{22}Na and $^{36}Cl^-$ uptake (Helbig et al., 1989a), ^{22}Na and fluid uptake, and pH_i regulation (Counillon et al., 2000).

By immunostaining investigation in cultured bovine PE cells and reverse transcriptase polymerase chain reaction study of human ciliary body, AE has been identified as AE2 isoform (Counillon et al., 2000). The NHE has displayed pharmacological feature of NHE-1 isoform (Counillon et al., 2000). Na^+ and Cl^- are transported into PE cells by the double exchanger in exchange for H^+ and HCO_3^- converted from water and CO_2, which was catalyzed by CA. The functional roles of different CA isoforms have been characterized. Cytosolic CAII

accelerates the transport of HCO_3^- and H^+ to PE cells (Sterling et al., 2001; Li et al., 2002), while membrane-bound CAIV is mainly involved in the conversion of H^+ and HCO_3^- into water and CO_2 (Wu et al., 1998).

In rabbit CE, the antiports were suggested to be the dominant uptake mechanism for Cl^- (McLaughlin et al., 1998). However, Neither net Cl^- secretion across bovine and porcine CE (Do and To., 2000; Kong et al., 2006), nor FF (Law et al., 2009) across porcine CE were reduced by AE inhibitor 4,4'-diisothiocyanatostilbene-2,2'-disulfonic acid (DIDS), suggesting that in ox and pig, AE may play a minor role in Cl^- transport and AHF.

1.3.3.2 Cl^- transfer from PE to NPE cells

Cl^- transport from PE to NPE cells is through intercellular gap junctions. In CE, gap junctions either located between the bilayer or between neighboring cells within a layer for intercellular communication (Raviola and Raviola, 1978). Through intercellular gap junctions, PE and NPE cells are coupled together and function as a syncytium (Krupin and Civan, 1996). The notion of PE and NPE working as a syncytium is supported by several observations, including

biochemical approach (Coca-Prados et al., 1992; Wolosin et al., 1997b; Coffey et al., 2002), structural study (Raviola and Raviola, 1978), and functional investigation (Green et al., 1985; Wiederholt and Zadunaisky, 1986; Edelman et al., 1994; Oh et al., 1994; Bowler et al., 1996; Stelling and Jacob, 1997; Do and To, 2000; McLaughlin et al., 2004; Kong et al., 2006).

Blockade of gap junctions with heptanol dramatically inhibited both Isc (Wolosin et al., 1997a; Do and To, 2000; Kong et al., 2006) and Cl^- secretion (Do and To, 2000; Kong et al., 2006) across CE. In addition, heptanol also reduced about 80% of FF across porcine CE (Law et al., 2009). These results indicated a very pivotal role of gap junction in the Cl^- transport and AHF. The molecular identities of connexin (Cx) have not been fully identified yet. Cx43 was the first connexin identified in these gap junctions (Coca-Prados et al. (1992). Later, both Cx40 and Cx43 were detected at the interface between PE and NPE cells, while Cx26 and Cx31 were localized between fellow NPE cells in rat CE (Coffey et al., 2002).

1.3.3.3 Cl^- release by NPE into AH

Under physiological conditions, Cl^- secretion by NPE into AH is believed to be the rate-limiting step of AHF (Civan et al., 1997) by virtue of the following experimental observations:

1. the $[Cl^-]_i$ is remarkably higher than that expected from electrochemical equilibrium, suggesting the Cl^- uptake from the stroma by PE cells is not rate-limiting (Wiederholt and Zadunaisky, 1986; Bowler et al., 1996);

2. PE and NPE cells share similar intracellular potentials and ionic contents, indicating a free ion transfer between the PE and NPE cells through gap junctions (Wiederholt and Zadunaisky, 1986; Bowler et al., 1996);

3. Under basal conditions, the K^+ channels and Na^+, K^+-ATPase at NPE cells are highly active, suggesting that they are not rate-limiting (Yantorno et al., 1992).

Administration of Cl^- channel blockers significantly reduced net Cl^- secretion across CE in ox (Do and To, 2000) and pig (Kong et al, 2006). Moreover, *in vitro* FF across porcine CE (Law et al, 2009) and AHF of bovine CE (Shahidullah et al., 2003) were also dramatically inhibited by Cl^- channel blockers. All these observations provide strong evidences for the vital importance of Cl^- channels in AHF.

The Cl^- channels identities at NPE cells have not been clearly identified. Both pICln and ClC-3 were thought to be possible candidates. The Cl^- channel regulator pICln used to be considered as the major Cl^- channel based on several observations. The pICln was detected in the NPE cells of human (Anguita et al., 1995), rabbit (Wan et al., 1997), and ox (Chen et al., 1999). The antisense down-regulation of pICln reduced the swelling-triggered Cl^- current in native bovine NPE cells (Chen et al., 1999), indicating the vital role of pICln in maintaining the swelling-triggered Cl^- current. However, Sanchez-Torres et al. (1999) found that in NPE cells, the major location of pICln was in the cytoplasm. In addition, they failed to notice any change in the expression or translocation of pICln from the cytoplasm into the plasma membrane after hypotonic swelling. Therefore, pICln is not likely to be the dominant Cl^- channel responsible for Cl^- secretion at the NPE (Sanchez-Torres et al. 1999).

The transcripts and protein expression of ClC-3 were reported in human NPE cells previously (Coca-Prados et al., 1996). The evidences for ClC-3 as the dominant Cl^- channel at the NPE have been demonstrated by several studies. The inhibition of Cl^- channel activities by protein kinase C (PKC) in NPE cells (Civan et al., 1994; Coca-Prados et al., 1995; Coca-Prados et al., 1996) indicated a ClC-3 associated

Cl^- current which is known to be sensitive to PKC (Kawasaki et al., 1994). In NPE cells, antisense oligonucleotides also down-regulated both the ClC-3 message and the swelling-activated Cl^- channels (Wang et al., 2000). Moreover, the Cl^- currents in cultured rabbit (Vessey et al., 2004) and native bovine (Do et al., 2005) NPE cells were both found to be inhibited by specific antibody of ClC-3. However, the predominance of ClC-3 in transepithelial Cl^- transport of CE is questioned by several studies. In NPE cells, ClC-3 was found to be primarily distributed within the nucleus instead of the plasma membrane, and it only partially accounted for the Cl^- current (Wang et al., 2000). Therefore, the identity of major Cl^- channels remains elusive and awaits further investigation.

The stimulation of Cl^- channel activity by hypotonic swelling has been extensively demonstrated in NPE cells (Yantorno et al., 1992; Zhang and Jacob, 1997; Shi et al., 1999; Carre et al., 2000; Do et al., 2006). The potential role of the swelling-activated Cl^- channels in facilitating AHF has been suggested by Do et al (2006). In their study, the Isc across bovine CE was increased by activating the swelling-activated Cl^- channels in NPE cells, showing a commensurate time-course with the regulatory volume decrease (RVD) of NPE cells. However, under basal isotonic condition, except for a human NPE cell line (Coca-Prados et

al., 1995), the swelling-activated Cl^- channels were found to be inactive in both native bovine NPE cells (Wang et al., 2000) and cultured rabbit NPE cells (Shi et al., 2002). Therefore, the exact role and contribution of the swelling-activated Cl^- channels to basal AH secretion is uncertain.

1.3.3.4 Regulation of Cl^- transport

(A) Cyclic 3', 5'-adenosine monophosphate (cAMP)

The role of cAMP in modulating Isc across ciliary body/epithelium (CBE) has been extensively studied. In rabbit, Cl^- secretion by the CE was enhanced by isoproterenol which was linked to an elevated cAMP level (Crook et al., 2000). Similar stimulation of the Isc by a cAMP analog (8-Br-cAMP) was detected in isolated porcine CBE as well, which also triggered a transient increase of net Cl^- transport (Ni et al., 2006). However, in bovine CBE, the net Cl^- secretion was reduced rather than enhanced by 8-Br-cAMP (Do et al., 2004a). Despite the conflicting results, these data suggested an important role of cAMP in regulating transepithelial Cl^- transport across CBE.

The exact molecular targets that are modulated by cAMP have also been intensely investigated. The activity of Na^+, K^+-ATPase was reported to be down-regulated by cAMP (Delamere and King, 1992). In ox, the maxi-Cl^- channels located at PE cells was activated by cAMP, facilitating the Cl^- reabsorption from PE cells thereby inhibiting AH secretion (Do et al., 2004b). Moreover, the NKCC at the PE cells (Crook et al., 2000; Hochgesand et al., 2001) and gap junctions (Do et al., 2004a) were reported to be regulated by cAMP as well. Activation of the NPE Cl^- channels was also observed after the application of cAMP in several species including dog (Chen et al., 1994), rabbit (Chen and Sears, 1997) and ox (Edelman et al., 1995).

(B) Nitric oxide (NO) and cyclic 3', 5'-guanosine monophosphate (cGMP)

NO is a vital second messenger involving in various physiological processes (Hobbs et al., 1999), which acts by elevating the intracellular cGMP level by activating guanylate cyclase (sGC) (Moro et al., 1996). The localization and functional presence of Nitric oxide synthase (NOS) has been demonstrated in porcine (Haufschild et al., 1996; Meyer et al., 1999) and bovine (Geyer et al., 1997) ciliary processes.

In an arterially perfused porcine eye, 8-pCPT-cGMP (a cGMP analog), L-arginine (a precursor of NO) and sodium nitroprusside (SNP, a NO donor) were demonstrated to reduce AHF and IOP (Shahidullah et al., 2005). This NO-cGMP pathway was reported to mediating Cl^- transport across CE in several studies. Transient increase of the Isc induced by NO donors and cGMP was observed in porcine CBE (Wu et al., 2004), and the protein kinase G (PKG) pathway was thought to be involved as the downstream signals. Similar responses were observed by Kong et al. (2005), yet two concomitant but distinct mechanisms were proposed: the stimulation of Isc and Cl^- transport may be attributed to the NO-cGMP pathway; while the cytochrome P-450 pathway may contribute to the concomitant inhibition of Isc and Cl^- secretion. In addition, Na^+, K^+-ATPase activity was shown to be down-regulated by NO in bovine ciliary process (Ellis et al., 2001) and porcine NPE cells (Shahidullah and Delamere, 2006). This inhibition of Na^+, K^+-ATPase may indirectly reduce Cl^- secretion across CE.

(C) Adenosine receptors (AR)

The presence of adenosine in AH has been detected in rabbit, ox and pig (Howard et al., 1998; Crosson and Petrovich, 1999). Several AR subtypes have been

identified in the ciliary process. In rat ciliary processes, the A1, A2A and A2B AR subtypes were identified (Kvanta et al., 1997), while the A3 subtype was detected in human NPE cells and rabbit ciliary processes (Mitchell et al., 1999). Both A3ARs knockout mouse and application of A3ARs antagonists could decrease the IOP (Avila et al., 2002), indicating a critical role of A3ARs in modulating IOP.

Adenosine was reported to stimulate the Cl^- channels in rabbit CE, native bovine NPE cells and cultured human NPE cells (Carre et al., 1997). The adenosine-induced stimulation of whole cell Cl^- current was suppressed by selective A3AR antagonists, indicating the adenosine evoked activation of Cl^- channels was modulated by A3ARs (Mitchell et al., 1999; Carre et al., 2000). In cultured human NPE cells, the whole cell Cl^- current could be stimulated by A3AR-selective agonists (Carre et al., 2000), which showed that A3AR may enhance Cl^- secretion and increase AHF. In cultured human NPE cells, the selective A3AR antagonist MRS 1292 also inhibited the adenosine elicited *in vitro* cell shrinkage (Yang et al., 2005), further supporting a regulatory role of A3ARs in Cl^- channel activity.

(D) Calcium (Ca^{2+}) signaling

Calcium could mediate activities of several important transporters in CE. In the cultured human NPE cells, the ouabain-sensitive Na^+, K^+-ATPase, Ca^{2+}-activated K^+ channel and bumetanide-sensitive NKCC were all reported to be up-regulated by elevated intracellular Ca^{2+} level (Mito et al., 1993). Besides, the PE-NPE coupling in intact rabbit CE (Oh et al., 1994) and native bovine ciliary epithelial cells (Stelling and Jacob, 1997) was found to be interrupted by elevated Ca^{2+} concentration as well. In addition, K^+ channels was also activated by increased Ca^{2+} level in electrophysiological studies of PE (Jacob, 1991; Stelling and Jacob, 1996; Ryan et al., 1998) and NPE cells (Helbig et al., 1989d; Barros et al., 1991; Edelman et al., 1995). The activated K^+ current may provide the driving force for Cl^- efflux in other secretory epithelia (Devor et al., 1990; Martin and Shuttelworth, 1994), suggesting an indirect regulatory role of Ca^{2+} in Cl^- transport across CE. Furthermore, in bovine PE cells, Ca^{2+} was involved in the ATP induced stimulation of Cl^- channels (Fleischhauer et al., 2001).

(E) Protein kinase C signaling

PKC is a family of protein kinase enzymes participating in a variety of cellular functions such as cell growth, immune response and muscle contraction.

It has also been proposed to be of vital importance in transepithelial solute transport across CE, via regulating the activities of different vital ion pumps, transporters and channels. In human cultured NPE cells, Na^+, K^+-ATPase was markedly stimulated by Phorbol 12, 13-dibutyrate (PDBu, a potent PKC activator) (Mito and Delamere, 1993). PKC has been reported to modulate the activity of NKCC in various cell types. In rabbit cultured NPE cells (Dong and Delamere, 1994), human cultured NPE cells (Crook et al., 1992; Mito and Delamere, 1993) and human PE cells (Von Brauchitsch and Crook, 1993; Layne et al., 2001), the activity of NKCC was significantly inhibited by PKC activator (Dong and Delamere, 1994; Crook et al., 1992; Mito and Delamere, 1993), while in hamster fibroblast cells, PDBu induced a significant stimulation of NKCC rather than inhibition (Paris and Pouysseyur., 1986), highlighting the heterogeneity in responses to PKC activation in different cell types.

In human cultured NPE cells, RVD was enhanced by PKC inhibitor staurosporine (Civan et al., 1994) which indicated the increase of K^+ and Cl^- release. The results

suggested that inactivation of PKC up-regulated the activities of K^+ and Cl^- channels subserving the RVD response. The involvement of PKC in modulating Cl^- channel activity was evident in several studies. The activities of swelling-activated Cl^- channels were markedly altered by PKC in native bovine NPE cells (Do et al., 2005), cultured rabbit (Shi et al., 2002) and human NPE cells (Coca-Prados et al., 1996; Shi et al., 2003). Hypotonic swelling triggered Cl^- current was potentiated by PKC inhibitors (Coca-Prados et al., 1996; Shi et al., 2002), and was inhibited (Shi et al., 2002; Shi et al., 2003) or significantly delayed (Do et al., 2005) after the introduction of PKC activators. Besides hypotonic stimulated current, the basal Cl^- current could also be stimulated by the PKC inhibitor staurosporine, displaying similar characteristic as the swelling-activated Cl^- current (Civan et al., 1994; Coca-Prados et al., 1995). These observations pointed to the vital role of PKC in regulating NPE Cl^- channels under basal conditions.

1.4 Structure and function of baicalein

The dry root of Scutellaria baicalensis (Scutellaria radix) is one of the most popular medicinal herbs used in several oriental countries such as China and Japan. Clinically, the extracts of Scutellaria radix have been widely used in treating dysentery, hypertension, hyperlipemia and inflammatory diseases. Baicalein, baicalin and wogonin are the major bioactive components that can be isolated from the Scutellaria radix.

1.4.1 Structure of baicalein

Baicalein belongs to the family of flavones, a subcategory of flavonoids. It is an aglycone of baicalin. The structure of baicalein is shown below. Besides the basic structure of flavone (2-phenyl chromone), the key structural feature for baicalein is the 5, 6, 7-trihydroxyl groups, which impart lipophilicity to baicalein.

a b

c.

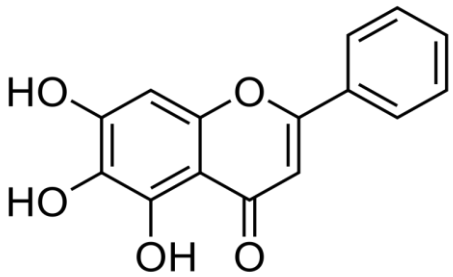

Fig1.2. a. Scutellaria baicalensis; b. Scutellaria radix; c. chemical structure of baicalein

1.4.2 Biological and pharmacological function of baicalein

Baicalein has multiple pharmacological functions such as anti-inflammatory, anti-oxidative, anti-cancer and anti-viral. In this section, the major bioactivities of baicalein are reviewed.

1.4.2.1 Anti-inflammation

Baicalein was reported to possess significant anti-inflammatory activity by a number of *in vitro* studies (Wakabayashi, 1999; Nakamura et al., 2003; Cheng et al., 2007). It has been shown to suppress inflammation in animal models including allergen and IL-13 induced airway inflammation model (Mabalirajan et al., 2013), experimental autoimmune encephalomyelitis (Xu et al., 2013), chemical colitis (Dou et al., 2012), carrageenan-induced inflammation model (Yoo et al., 2009) and a rat model of acute pancreatitis (Li et al., 2009).

Multiple mechanisms have been suggested for the anti-inflammation activity of baicalein. Several mediators are activated during inflammatory process including NO, cytokines, leukotrienes and adhesion molecules (Tunon et al., 2009). Baicalein may exert the anti-inflammatory activity by reducing NO production through the inhibition of various inflammation-related genes, including inducible NO synthase (iNOS), lipoxygenases (LOX) and cyclooxygenases (COX). In microglia, the endotoxin/cytokine induced NO production was reduced by baicalein via inhibiting iNOS gene expression (Chen et al., 2004). Similar down-regulation of iNOS gene expression induced by baicalein was reported in RAW 264.7 cells, which may explain the therapeutic effect of baicalein on sepsis

(Cheng et al., 2007). COX-2 is intensively expressed in cells undergoing inflammatory responses, and its product prostaglandins are also important inflammation associated mediators. Lipopolysaccharides (LPS)-induced COX-2 expression was significantly inhibited by baicalein (Woo et al., 2006). 5-LOX and 12-LOX are usually related to the inflammatory processes and baicalein suppressed the carrageenan-induced inflammation by acting as a 12-LOX inhibitor (Yoo et al., 2009). Moreover, a variety of cytokines usually acting as pro-inflammatory factors in inflammation can also be targeted by baicalein. Decreased productions of IL-1, IL-6, IL-8, IL-18 and TNF-α have been observed after baicalein treatment (Nakamura et al., 2003; Yang et al., 2009).

Several cellular signaling pathways that are impaired or activated by inflammation have been found to be significantly counteracted by baicalein, such as p38 Mitogen-activated protein kinases (MAPK) activation (Stavniichuk et al., 2011), nuclear factor-κB (NF-κB)-mediated MAPKs and AKT activation (Li et al., 2011) and Phosphatidylinositol-4,5-bisphosphate3-kinase (PI3K)/AKT activation (Hwang et al., 2008). These results further substantiate the anti-inflammatory property of baicalein.

1.4.2.2 Antioxidant

The antioxidative effect of baicalein has been well documented in numerous cells and animal models (Hamada et al., 1993; Gao et al., 1995; Gao et al., 1998; Yoshino et al., 1998; Gao et al., 1999; Liu et al., 2012; Moslehi et al., 2012). The anti-oxidative mechanism of baicalein is multifolded, including radical scavenging, metal chelating and the removal of oxidized biomolecules.

Oxidative stress induced by ROS is a culprit of aging and diseases, including cancer, cardiovascular diseases and neurodegenerative diseases. Flavonoids have been considered as a novel class of natural free radical scavengers. The anti-radical activity of baicalein and its protective effects against ROS damages in various tissues have also been described (Shi et al., 1995; Gao et al., 1998; Gao et al., 1999). Free radicals such as DPPH, hydroxyl and alkyl radical (Gao et al., 1998) and lipid peroxyl radicals (Gao et al., 1996; Zhang et al., 2010) were reported to be scavenged by baicalein. Besides, lipid peroxidation was also inhibited by baicalein in mitochondria (Miyahara et al., 1993) and microsomes (Gao et al., 1995). Direct donation of hydrogen atoms, as well as proton loss–electron transfer was thought to be the underlying mechanism for the scavenging property of baicalein (Marković et al., 2011).

Excessive loading of iron and other metal, together with redox metal-induced oxidative stress, can lead to various diseases (Richardson 2006; Wei et al., 2007; Ghosh et al., 2008). Baicalein is capable of chelating iron and inhibiting Fenton reaction (Perez et al., 2009). Besides, baicalein was also found to be a potent inhibitor of xanthine oxidase, which is an important enzyme in producing superoxide anions (Shieh et al., 2000).

In addition, in V79-4 Chinese hamster fibroblast cells, there was activation of DNA repair system and inhibition of H_2O_2 induced DNA damage after baicalein treatment (Zhang et al., 2012).

The structure-activity relationship of flavonoids has been investigated which unravels the key structural features that may account for its antioxidant activity. Apparently, the antioxidant property requires the presence of the 5-hydroxy group in the A-ring, the hydroxyl groups in the B-ring and 2, 3-unsaturation in conjugation with a 4-oxo group in the C-ring. Except for the hydroxyl group in the B-ring, baicalein and baicalin possess almost all of these structural components which make them molecules with strong antioxidant activity (Morel et al., 1994; Brown et al., 1998; Williams et al., 2004).

1.4.2.3 Anticancer

Baicalein was reported to suppress the growth of several cancer cell lines including mouse leukemia cells (L1210) (Ciesielska et al., 2002); human lung squamous carcinoma CH27 cells (Lee et al., 2005); human breast carcinoma cell line (MDA-MB-435) (So et al., 1996), human myeloma cells (Ma et al., 2005) and human glioma cells (Lee et al., 2005). In addition, various mouse tumor models have been employed to further test the anticancer bioactivity of baicalein. Findings in C3H/HeN mice implanted with MBT-2 and nude mice with prostate cancer xenografts also demonstrated the anticancer bioactivity of baicalein (Ikemoto et al., 2004; Bonham et al., 2005). Baicalein is cytotoxic against cancer cells, yet possess very little even no toxicity to normal ones, including epithelial, peripheral blood and myeloid cells. Therefore it is proposed to be an ideal candidate as chemotherapeutic agents. Several potential mechanisms underlying the antitumor/anticancer property of baicalein are reviewed below.

By scavenging ROS

Oxidative stress induced by ROS is considered as the major factor associated with the initiation and evolution of cancer. The association between flavonoids intake and decreased risk of cancer is thought to be attributed to its antioxidative function

(Middleton et al., 2000; Havsteen et al., 2002). In addition, ROS induced mitochondrial dysfunction in experimental pulmonary carcinogenesis was significantly alleviated by baicalein, indicating the chemotherapeutic effect of baicalein through combating ROS (Naveenkumar et al., 2013).

Besides antioxidant activity, baicalein may possess a pro-oxidant effect in its antitumor activity. In human hepatoma cell lines, the cellular glutathione (GSH) content was depleted by baicalein treatment (Change et al., 2002), rendering these tumor cells vulnerable to oxidative damages.

By inhibiting NF-kB

NF-kB is proposed to be a prosurvival factor that stimulates the expressions of several genes (Bcl-2, Mcl-1, IL-6 and Bcl-XL) and promotes proliferation and survival of tumor cells (Suh et al., 2004; Nakano et al., 2006). In myeloma cell lines, NF-kB activity was reduced after baicalein treatment (Ma et al., 2005).

By arresting cell cycle

Baicalein has been observed to exert its cytostatic effect on tumor cells through arresting cell cycle at key checkpoints. Cell cycle was arrested at the G1 phase by baicalein in prostate cancer cell lines (Chen et al., 2001) and oral cancer cells (Cheng et al., 2012), whereas G0/G1 phase was inhibited in prostate cancer cell

lines. In addition to cell cycle arrest, reduction of Cyclin D1 expression after baicalein treatment was observed as well (Pidgeon et al., 2002; Lee et al., 2005; Leung et al., 2007). Cyclin D1 is responsible for regulating the cell cycle transition from S-phase to G2/M-phase. Direct inhibition of cyclin D1 would result in a decrease of cell population at G2/M-phase.

By inducing apoptosis

Baicalein can trigger apoptosis in many cancer cell lines. The underlying molecular mechanism is largely unknown, but a number of apoptotic signaling pathways may have been targeted by baicalein. They include PI3K/Akt pathway (Zhang et al., 2013), mitochondria-mediated pathway (Li et al., 2012; Zhang et al., 2013), MEK/extracellular signal-regulated kinase (ERK) pathway (Liang et al., 2012), ERK/p38 MAPK pathway (Zhou et al., 2009), ERK and PI3K-Akt signaling pathways (Agarwal et al., 2009) and Ca^{2+} involving caspase-3-dependent pathway (Lee et al., 2008).

1.4.2.4 Anti-virus

Baicalein was found to inhibit HIV-1 infection and replication by acting as a novel integrase inhibitors, inhibiting the retroviral reverse transcriptase activity *in vitro* (Ahn et al., 2001). Recently, the antiviral activity of baicalein against-dengue virus type 2 (Zandi et al., 2012) and Japanese encephalitis virus (Johari et al., 2012) were also reported. These studies showed that both virus replication and adsorption were interrupted by baicalein. Besides, a direct virucidal action induced by baicalein was also observed (Zandi et al., 2012; Johari et al., 2012). Cotin et al. (2012) found that baicalein possessed significant antiviral effect against human cytomegalovirus through inhibiting the immediate early gene expression during early stage of viral cycle.

Highly pathogenic influenza A viruses have attracted extensive attention in the past decades. Interestingly, in the H5N1 influenza A virus-infected cells, baicalein showed novel inhibitory and antiviral activity (Sithisarn et al., 2013). The H5N1 nucleoprotein expression, virus titres and neuraminidase activity were all significantly reduced by baicalein. In addition, viral-induced caspase-3 activation was also prevented by baicalein, indicating that baicalein may exert its antiviral effect through modulation of cellular signaling cascade.

1.4.2.5 Chloride transport

The regulatory role of baicalein in transepithelial Cl^- transport was initially demonstrated by Marshall et al. (1993). In their study, baicalein was found to stimulate Cl^- secretion of opercular epithelium of sea-water killifish. Similar stimulatory effects were found after the application of the nonspecific LOX inhibitor nordihydroguaiaretic acid (NDGA) and LOX metabolites, indicating Cl^- secretion across opercular epithelium was modulated by LOX products. Baicalein induced stimulation of Cl^- secretion may be attributed to the inhibition of 12-LOX. In the past decades, the role of baicalein in modulating transepithelial ion transport across secretory epithelia has received growing attention. Baicalein was reported to exert stimulatory effect on basal Cl^- secretion across rat colonical mucosa (Ko et al., 2002) and human colonic epithelial (T84) cells (Yue et al., 2004). The involvement of a cAMP-dependent pathway was implicated in both studies. In another study in T84 cells, baicalein induced mild but significant inhibition of forskolin-stimulated Cl^- secretion in a dose-dependent manner (Schuier et al., 2005), which is consistent with the observation that baicalein caused about 8% inhibition after forskolin maximally stimulated the Isc (Yue et al., 2004). A cAMP-mediated blockade of cystic fibrosis transmembrane conductance regulator

(CFTR) was proposed to account for this inhibitory action of baicalein (Schuier et al., 2005). In contrast, in rat distal colon, baicalein still induced significant Isc increase even after forskolin was pretreated, suggesting a cAMP-independent pathway, or even a direct stimulation on CFTR may be at work (Ko et al., 2002).

1.4.3 Implications in ocular diseases

Recently, baicalein has gained prominence in preventing and treating several diseases including ocular disorders on account of its multiple bioactivities.

Several evidences from *in vivo* and *in vitro* studies have supported a therapeutic role of baicalein in ocular inflammatory diseases. The anti-inflammatory action of baicalein was observed in the rabbit with experimental uveitis, in which the prostaglandin E2 (PGE2)-elevated aqueous flare was effectively reduced after administration of baicalein (Nagaki et al., 2001; Nagaki et al., 2003). The IL-1β stimulated expressions of pro-inflammatory cytokines (IL-6 and IL-8) were also suppressed by baicalein in culture human retinal pigment epithelium (RPE) cells (Nakamura et al., 2003). Baicalein induced protection from oxidative stress evoked cell death was demonstrated in both human RPE cells (Hanneken et al.,

2006; Liu et al., 2010) and immortalized RGC cell line (Maher and Hanneken, 2005).

Moreover, the inflammatory process in the diabetic rat retina that was represented by microglial activation and Müller cell dysfunction was effectively ameliorated by oral administration of baicalein, which in turn prevented retina from vascular abnormality and neuron loss (Yang et al., 2009).

Retina ischemia was always implicated in various ocular diseases, such as glaucoma, age-related macular degeneration and central retinal artery/vein occlusion (Osborne et al., 2004; Peng et al., 2011; Chen et al., 2012). Baicalein was found to effectively protect the RGC against the iodoacetic acid induced ischemia (Maher and Hanneken, 2008). In addition, in a pressure induced ischemic model, the ischemic retinal damage was effectively blunt by the administration of baicalein. The protective efficacy of baicalein against retinal ischemic damage was attributed to its properties as antioxidant, anti-apoptosis and regulator of tissue remodeling (Chao et al., 2013). Retinal neovascularization was also reported to be retarded by baicalein via specifically inhibiting 12-LOX (Al-Shabrawey et al., 2011). Baicalein may indeed be further developed into a clinical treatment for protecting the retina against ischemia associated ocular disorders.

1.5 Objectives

Baicalein is a natural occurring flavone possessing multiple bioactivities, such as anti-inflammation, antioxidant, anticancer and regulating Cl^- transport. Since Cl^- transport across CE is the major driving force for AHF, baicalein may also regulate AHF through modulation of transepithelial Cl^- transport. In addition to elevated IOP, glaucoma is known to associate with oxidative stress, inflammatory responses and insufficient blood supply. Baicalein, being a multifunctional compound may provide a multi-facet and novel therapeutic approach in glaucoma treatment.

The major goal of current study is to characterize the effects of baicalein on chloride transport, AHF and IOP. Specifically, the main objectives are listed below:

To explore the potential role of baicalein in modulating transepithelial Cl^- transport and *in vitro* fluid secretion across porcine CBE;

To characterize the cellular mechanism underlying the effects induced by baicalein;

To examine the hypotensive effect of baicalein on guinea pig IOP.

Chapter 2 Methods

2.1. Measurement of Isc across porcine CBE

2.1.1. Isolation of porcine CBE

Freshly isolated porcine eyes were collected in the local slaughterhouse and transported to the laboratory on ice. The dissection procedures of porcine CBE were shown in Fig 2.1. First of all, to expose the sclera, extraocular tissues were removed by a razor blade. Four incisions were then made through sclera from the equator to the limbus, with two on the nasal sides and two on the temporal sides. After that, the incisions were extended into the limbal cornea by about 1.5 mm. The central cornea was then trimmed away, leaving behind the limbal region. By holding the residual cornea with a forcep, an incision was made at the anterior angle with a paired curved scissors, and then the sclera was separated from the choroid all the way to the equator. After the superior CBE sector was exposed, the procedure was repeated for the inferior sector. When both CBE sectors were exposed, the initial incision at the limbal region was then extended into the centre of crystalline lens in order to separate the CBE sectors from the eyeball. Prior to

the saparation, vitreous attached to CBE was gently removed. The isolated CBE was then bathed in a petri dish containing Normal Ringer solution (NRR).

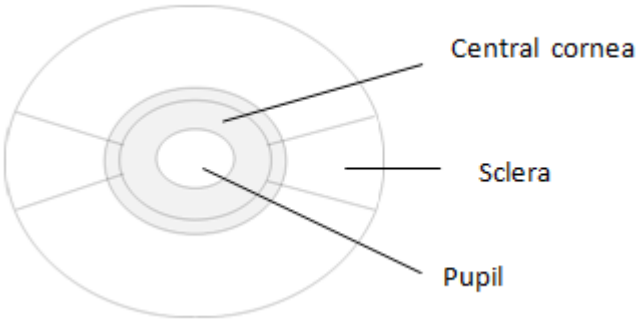

1. Four cuts were made through sclera, and central cornea was removed.

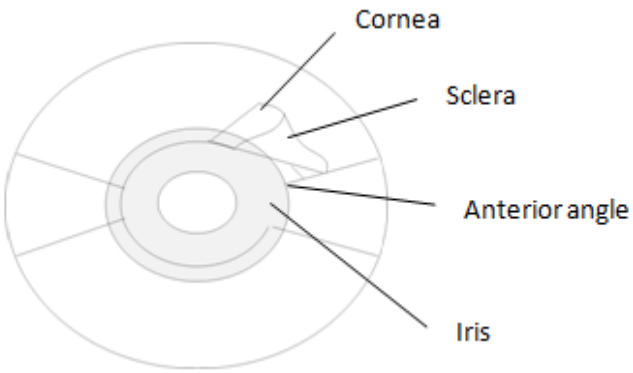

2. A tangential incision was made at anterior angle, and sclera was detached from choroid.

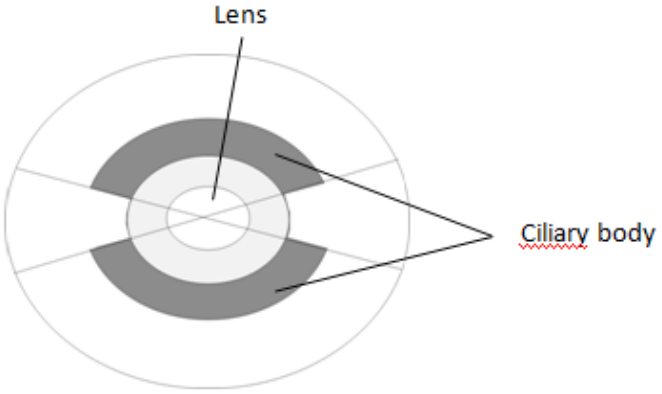

3. The superior and inferior CBE sectors were exposed, and the incisions at the limbal region were extended into the centre of lens.

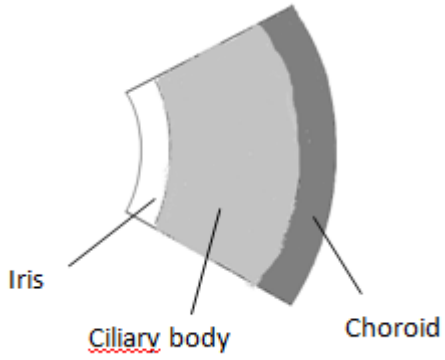

4. One sector of the exercised CBE

Fig2.1. The dissection procedures of porcine CBE

2.1.2. The Modified Ussing-Zerahn–Type Chamber

The open re-circulating chamber (ORC) (Kong et al., 2006) was used in our experiments, and the schematic diagram of ORC chamber is illustrated in Fig.2.1.

A

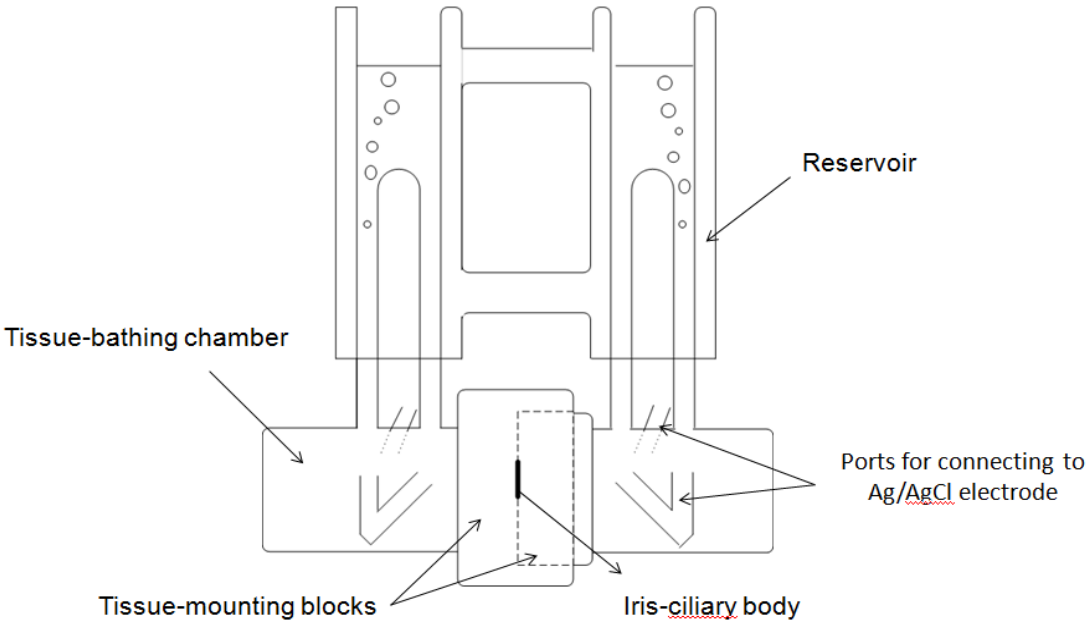
Reservoir
Tissue-bathing chamber
Ports for connecting to Ag/AgCl electrode
Tissue-mounting blocks
Iris-ciliary body

B

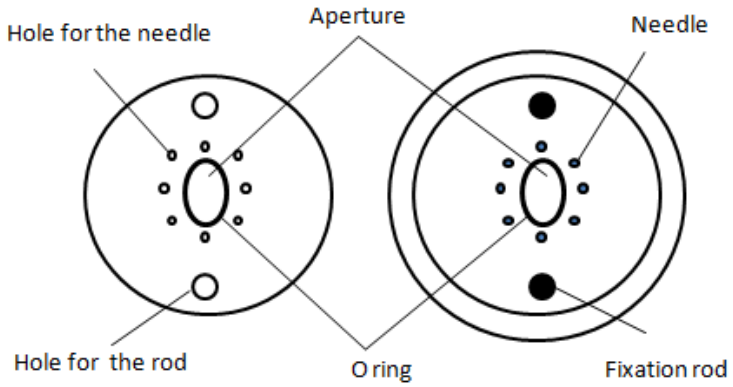
Hole for the needle
Aperture
Needle
Hole for the rod
O ring
Fixation rod

C

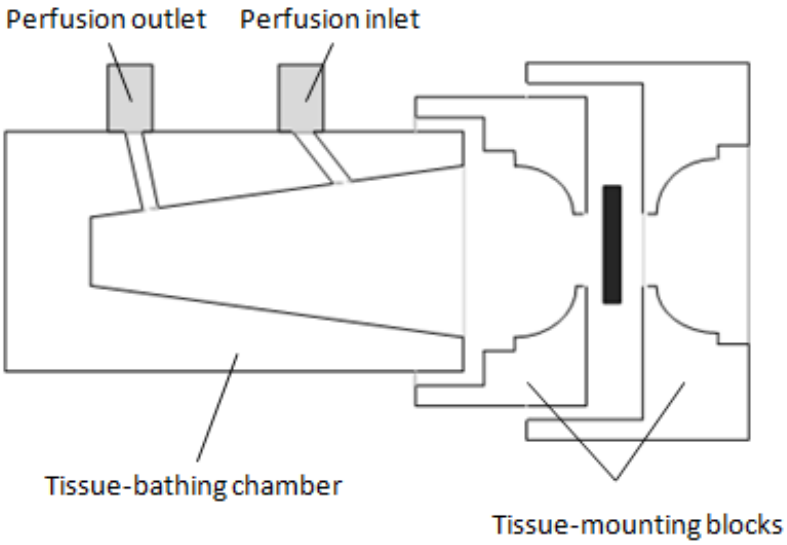

D

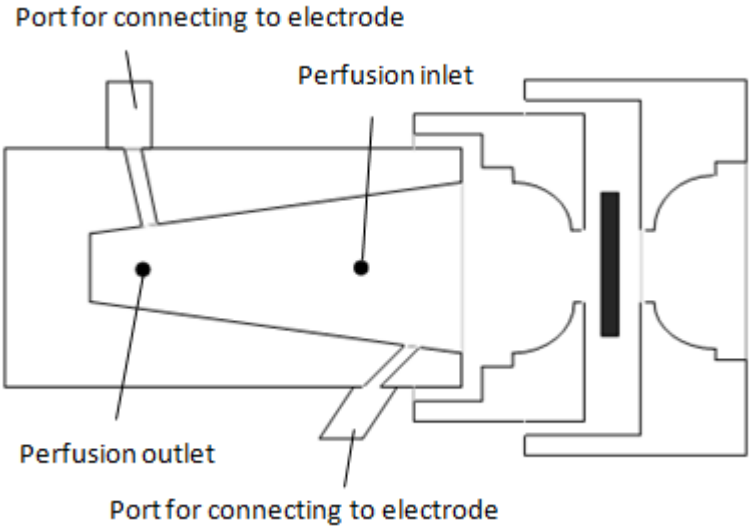

Fig.2.2. The structure of ORC chamber. (A) A schematic diagram illustrating the main components of ORC chamber. The chamber-mounting rack has been omitted. (B) The front view of tissue-mounting blocks. (C) The side view of the assembly of tissue-mounting blocks with tissue-bathing chamber, the ports for connecting to electrode has been omitted. (D) The top view of the assembly of tissue-mounting blocks with tissue-bathing chamber.

As shown in Fig2.2 (B), the tissue-mounting blocks consist of a large block and a small one. In the centre of the two blocks, slotted aperture was made to accommodate and fix the preparation. With an O ring in place, the area of the aperture is about 0.1 cm^2. The two blocks are conjugated with each other. They were assembled by inserting the two stainless metal rods in the 6 o'clock and 12 o'clock position of the large block into the conjugated holes in the small block.

The tissue-bathing chamber was made in pairs. As shown in Fig2.2(C)&(D), on the top of each chamber, two ports were machined for connecting to the re-circulating bath. On the opposite sides, there were another two ports made for the connection to the current-clamp electrode and the potential-sensing electrode respectively. When assembling the chambers, the bathing chamber was inserted into the mounting blocks by an O ring placed on the trough around the opening.

After the assembly of the tissue-mounting blocks and the tissue-bathing chambers, the whole part was placed on the stainless steel rods of the mounting rack via the grooves at the bottom of the bathing chambers. The two screws in the upper part of the rack were gently tightened into the holes at the back of the bathing chambers for securing the whole chamber. And finally, the screws, the holes and the apertures were aligned horizontally.

The glass reservoir was filled with bathing solution and the top was opened to air for replacing buffer and drug adminstration. Two inlets were machined into the reservoirs for the bubbling of gases.

2.1.3. Tissue mounting

The silicone rings of the chambers were coated with silicone grease (Dow Corning Corporations, USA) to form a better seal and to cushion the preparation**.** The CBE sector was placed on the mounting stage of the small block, with the aqueous side facing upward, and only the pars plicata area was exposed to the aperture (0.10 cm^2). The large mounting block was placed on top of it subsequently. The two half-chambers were then assembled together with the tissue bathing chambers. The whole assembled chamber was then positioned onto the mounting rack. Finally, the chamber was connected to the reservoir, potential-sensing bridge and current-clamp electrodes through PVC tubes. The bathing solution (20 mL NRR) was added into each reservoir. Gases (5% CO_2 and 95% O_2) were continuously bubbled through the reservoir.

2.1.4. The transepithelial electrical parameters measurement

The dual voltage current clamp unit (DVC-1000; World Precision Instruments, Sarasota, FL, USA) was used to moniter the transepithelial electrical parameters. The signal outputs were fed into the Powerlab data acquisition system (ADinstrument, Dunedin, New Zealand).

The spontaneous transepithelial PD was measured with one paired Ag/AgCl electrodes (EKV; World Precision Instruments) containing polyacrylamide gel (3%) and NaCl (154 mM). The electrical drift of the electrodes can be nullified by the potential-sensing bridge between them. Another pair of electrodes at the back was used to pass an external current (5 μA). The blank resistance of bathing solution was predetermined and compensated by the "Fluid resistance compensation" mode in the absence of tissue. The tissue resistance (Rt) was calculated by the Ohm's law:

$Rt = (\Delta PD/\Delta I)*A$

ΔPD represents the change of PD induced by the applied current

ΔI represents the magnitude of the applied current

A represents the surface area of the chamber aperture

The Isc can also be obtained by the Ohm's law:

Isc= PD/Rt.

The experimental interventions such as bathing anion replacements or addition of drugs were applied after the electrical parameters were stable for at least 15 minutes, and the effects were continuously monitored until all parameters were stabilized. All the experiments were conducted in room temperature (22-24℃) .

2.1.5. Bathing Solution and pharmacological agents

The bathing solution was NRR comprising (mM): NaCl 113.0, KCl 4.56, $NaHCO_3$ 21.0, $MgSO_4$ 0.6, D-glucose 7.5, reduced glutathione 1.0, Na_2HPO_4 1.0, HEPES 10.0, and $CaCl_2$ 1.4. The pH was adjusted to 7.4 with NaOH/HCl. In the Cl^- replacement experiments, Cl^- was replaced with equal quantity of gluconate. The NRR and low Cl^- solutions were equilibrated with gases (5% CO_2 and 95% O_2) for 15 minutes before use.

All pharmacological agents were bought from Sigma-Aldrich, Inc. (St. Louis. MO, USA). Baicalein, baicalin, chrysin, bumetanide (BMT), furosemide (FSM), niflumic acid (NFA), diphenylamine-2-carboxylate (DPC), NDGA, staurosporine and calphostin C were dissolved in dimethyl sulfoxide (DMSO), and the final

concentration didn't exceed 0.1%. H-89 was dissolved in DDH_2O (final concentration of DDH_2O=0.1%).

2.1.6. Statistical analysis

All data are expressed as MEAN±SEM. GraphPad Prism (San Diego, CA, USA) was used for statistical analysis. The comparisons between baseline values and drug-treated values were performed with Paired Student's *t*-tests, or repeated measures ANOVA followed by Tukey's post hoc test. The comparisons among three or more groups were performed with one-way ANOVA, followed by Tukey's post hoc test. The significance was set as $p<0.05$.

2.2. Measurement of FF across porcine CBE

2.2.1. Isolation of porcine CBE

Freshly isolated porcine eyes were collected in the local slaughter house and transported to laboratory on ice. The procedures for the dissection of porcine CBE were the same as described by Law et al. (2009). Extraocular tissues were removed first. Then a cut was made through the cornea and the central cornea was removed, leaving behind about 2 mm around the limbal region. An incision was made on the residual cornea and extended into TM around the anterior angle. The sclera was then separated from the choroid at the anterior angle and all the way to the equator. After the ciliary body was completely exposed, the intact ring of porcine CBE with the adjoining choroid was cut away from the eyeball and bathed in NRR, with the ciliary processes facing upward. The vitreous humour attached to the ring was gently removed away. After the cross incision was made, the posterior lens capsule was removed around the zonules, and the lens cortex was eventually taken away. The anterior lens capsule remained attached to the CBE and bathed in NRR at room temperature (22-24℃).

2.2.2. FF Chamber

The whole ring of porcine CBE was mounted to the FF chamber, which was a modified Ussing chamber for FF measurement (Law et al., 2009). A schematic diagram is shown in Fig.2.3 illustrating the configuration of FF chamber.

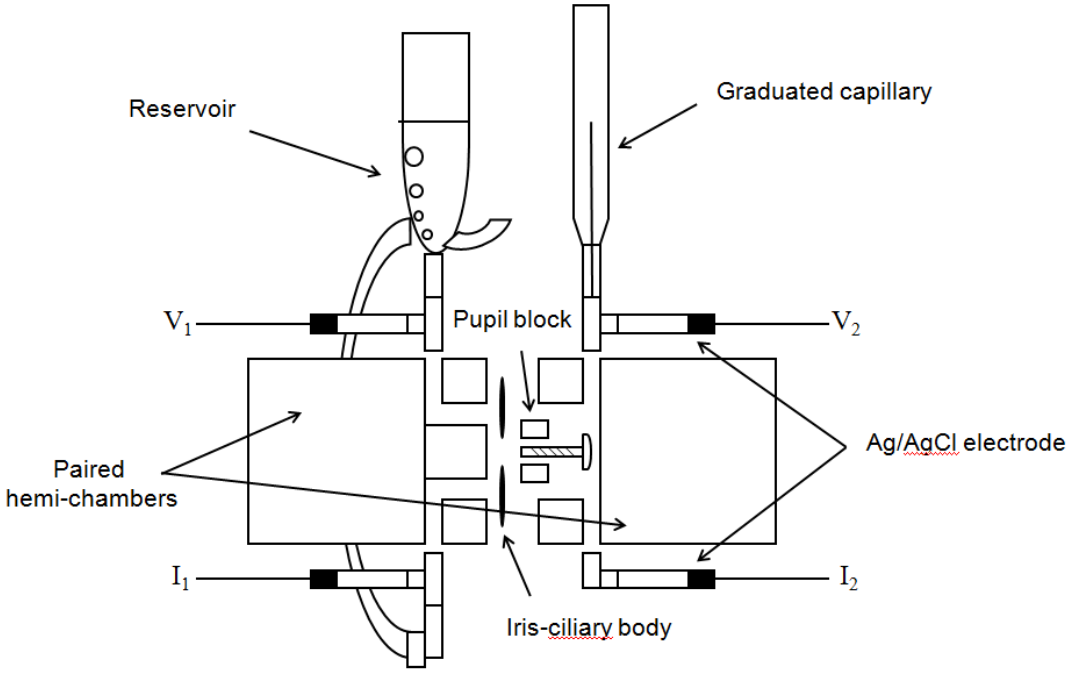

Fig.2.3. A schematic diagram showing the configuration of FF chamber.

V1, V2: the potential-sensing electrodes; I1, I2: the current-clamp electrodes.

The hemi-chamber consists of an outer circular trough with a diameter of 16.0 mm, and an decentred central post with a diameter of 12.5 mm, which is designed to be narrower at the nasal area, and wider at the temporal area to fit the asymmetrical

ciliary processes. A small circular Lucite block (pupil block), with four pins and an O-ring was made to match the central post. By screwing the block into the central post, the pupil was occluded and the iris could be secured. The two hemi-chambers were assembled by aligning their outer circular troughs.

Two paired Ag/AgCl electrodes (EKV/EKC; World Precision Instruments) filled with polyacrylamide gel (3%) and NaCl (154 mM) were connected to the chamber, with one for simultaneous recording of PD (V1&V2 in Fig2.2), and the other for applying an external current across the preparation (I1&I2 in Fig2.2) to estimate Rt.

On one side, the bubbling reservoir was connected to the chamber by two 3-way connectors inserted at the top and the bottom of the chamber; on the other side, another 3-way connector was inserted to connect the chamber and the capillary, leaving extra ports for two pairs of electrodes.

2.2.3. Tissue mounting

Prior to the placement of the preparation, the tightly stretched nylon was used to cover the circular Lucite hemi-chamber. The whole ring of the CBE preparation was then transferred onto the chamber with a flat spatula. The preparation was

carefully aligned, with only the ciliary processes (area of 1.28 cm^2) exposed to the chamber cavity. The pupil was then enclosed by the pupil block before the other hemi-chamber was assembled and covered the preparation.

The bathing solution was equilibrated with gases (5% CO_2 and 95% O_2) before delivering into hemi-chambers either through the bubbling reservoir (8 mL) or through the port and connector. The capillary was inserted to the connector after the filling of bath solution. Gases were continuously bubbled through the reservoir at room temperature (22-24℃).

2.2.4. FF Measurement

As demonstrated in previous study by Candia (2005), the fluid transport across CBE was in the the blood to the aqueous direction, which induced a rise in the water level within the capillary if set at the aqueous side of CBE, or a decrease in the water level when set at the blood side. In our experiments, the capillary was placed at the blood side, so a consistent fall in the fluid level was expected under basal condition. To equate the hydrostatic pressure induced by difference in water level between the reservoir and the capillary, the solution in the capillary was replenished and the difference was keep within 5 mm.

After mounting of the preparation, the first 60 minutes was considered as equilibration period. FF was monitored for the following 90 minutes as baseline recording. After the addition of baicalein, FF was recorded for another 120 minutes, and the value within this time period was taken average and treated as baicalein induced response.

2.2.5. Recording of electrical parameters

The PD across CBE was recorded through one paired Ag/AgCl electrodes connected to a voltage-current clamp unit (DVC-1000; World Precision Instruments). The signal recorded was exported to a dual-channel chart recorder (BD-12E; Kipp & Zonen Inc., Saskatoon, Saskatchewan, Canada).

Another pair of Ag/AgCl electrodes were used for applying an external current (10 μA) across the preparation. A current was applied for a few seconds in 30-minute interval through the current-clamp mode of the dual-voltage clamp unit. The blank resistance of the chamber filled with bathing solution was predetermined and compensated by the dual-voltage clamp unit before mounting of the preparation. Rt was calculated by the Ohm's law: $Rt=\Delta PD/\Delta I$

Where ΔPD represents the potential change induced by the applied current and ΔI is the magnitude of the applied current.

2.2.6. Bathing solutions and pharmacological agents

NRR was used as bathing solution and the composition has been described in Chapter 2, Section 2.1.6. Baicalein was purchased from Sigma-Aldrich, Inc. and dissolved in DMSO (Final concentration of DMSO= 0.05%).

2.2.7. Statistical analysis

All data are expressed as MEAN±SEM. GraphPad Prism was used for statistical analysis. The comparison between the baseline values and drug-treated values was performed by Paired Student's *t*-tests. The statistical significance was set as $P<0.05$.

2.3. Measurement of $[Cl^-]_i$ in porcine NPE cells

2.3.1. Cell preparation

Freshly isolated porcine eyes were obtained from the local slaughterhouse. The extraocular tissues were first removed, and the cornea and iris were then trimmed away. The tips of ciliary processes were cut out and rinsed with phosphate-buffered saline (PBS) (Invitrogen-Gibco, Grand Island, NY, USA). Then the tissues were incubated in trypsin (0.25%) at 37℃ for 30 min with agitation. After that, DMEM (Thermo Fisher Scientific, Waltham, MA, USA) with fetal bovine serum (FBS, 10%) (Invitrogen-Gibco) and gentamicin (0.1%, Invitrogen-Gibco) was added, and trituration was performed to dissociate the PE and NPE cells. The cells were then pelleted by centrifugation, and resuspended in DMEM with 10% FBS and 0.1% gentamicin for two times. Finally, cells were nurtured at 37℃ in 5% CO_2 for 24 hours to 36 hours before use. Prior to each experiment, the cells were rinsed twice with PBS.

2.3.2. Measurement of $[Cl^-]_i$

N-ethoxycarbonylmethyl-6-methoxyquinolinium bromide (MQAE, Invitrogen, CA, USA) was used as the fluorescence dye for $[Cl^-]_i$ measurement. MQAE fluorescence is quenched by Cl^-, so the fluorescence change inversely with the $[Cl^-]_i$.

Native porcine ciliary epithelial cells were incubated with 10 mM MQAE in NRR for an hour at room temperature (22-24℃). The coverslips with attached cells were then washed twice with NRR before transferred to the perfusion chamber placed on an inverted fluorescent microscope (Nikon, Tokyo, Japan). The cells were superfused by NRR all through the experiment, and each time prior to measurement the cells were allowed to equilibrate in NRR for at least 5 minutes. The MQAE fluorescence was excited at 360 nm, and the emission light at 460± 10 nm was collected through a 400 nm dichroic mirror with a barrier filter (435~485 nm). The fluorescence images were captured with a cooled digital CCD camera (Sensicam qe, PCO, Germany), using the Metafluor Version 5.0r6 software (Universal Imaging Corp, New York, USA) with a sampling interval of 10 s. All of the experiments were conducted at room temperature (22-24℃).

2.3.3. Calibration of MQAE fluorescence

Calibration of MQAE fluorescence against $[Cl^-]_i$ was performed by exposing cells to a series of calibration solutions in the presence of nigericin (K^+/H^+ ionophore, Sigma-Aldrich) and tributyltin (Cl^-/OH^- ionophore, Sigma-Aldrich). With the double ionophores, the Cl^- concentration in the bathing solution ($[Cl^-]_o$) is assumed to be equal with $[Cl^-]_i$. The calibration solution contained (mM): KCl 117.56, $KHCO_3$ 21.0, $MgSO_4$ 0.6, D-glucose 7.5, reduced glutathione 1.0, K_2HPO_4 1.0, HEPES 10.0, and $CaCl_2$ 1.4 (pH 7.4). The variation of $[Cl^-]_o$ was achieved by substitution of Cl^- with NO_3^-, and the sum of $[Cl^-]_o$ and $[NO_3^-]_o$ was always kept at 120 mM.

The procedure for calibration experiment is shown in Fig2.4 (A). In each experiment, cells were sequentially exposed to the calibration solutions containing 0, 20, 40 and 60 mM Cl^- in the presence of 5 μM nigericin and 10 μM tributyltin. At the end, 150 mM Potassium thiocyanate (KSCN) was applied into the bathing solution to quench the MQAE fluorescence. The fluorescence after the application of KSCN was considered as background fluorescence (F_{kscn}), which was always substracted from the fluorescence value at each time point.

The $[Cl^-]_i$ was then calculated using the Stern-Volmer equation:

$F_0/F = 1 + K_{SV}[Cl^-]_i$

F_0 represents the fluorescence when $[Cl^-]_i$ is 0 mM, F represents the fluorescence in the presence of Cl^-, and K_{SV} is the Stern-Volmer constant. K_{SV} is calculated by plotting a linear regression curve of F_0/F against different $[Cl^-]_i$, as shown in Fig2.4(B). All of the fluorescence intensities represented the values after the substraction of F_{kscn}.

A

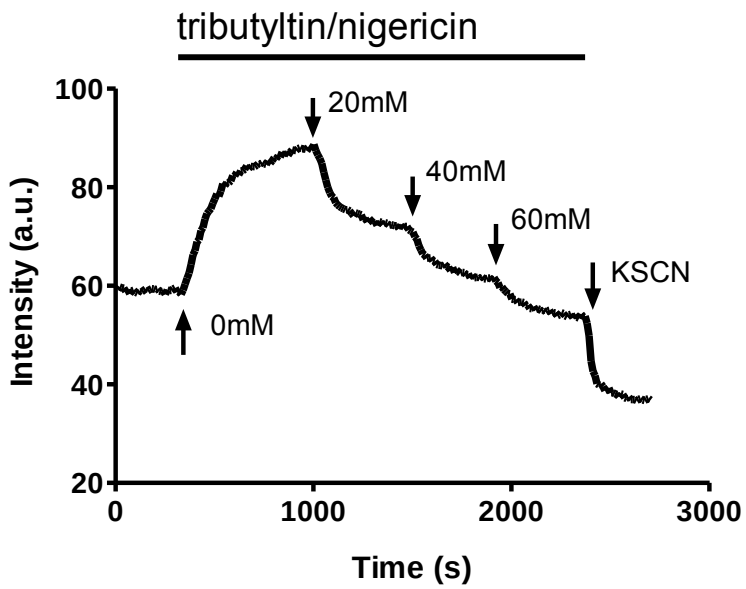

B.

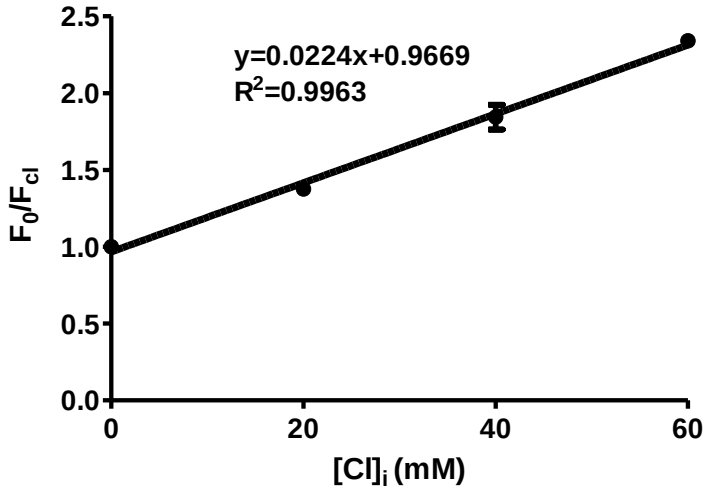

Fig2.4. Calibration of MQAE fluorescence against $[Cl^-]_i$ in primary cultures of porcine NPE cells. The calibration experiments were performed by sequential changing Cl^- concentration in the bathing solution in the presence of nigericin and tributyltin. F_0/F was plotted agains $[Cl^-]_i$ The best-fit linear regression lines were demonstrated. Data were collected from 32 NPE cells of 3 independent dishes.

2.4. Membrane potential measurement in porcine ciliary epithelial cells

2.4.1. Membrane potential measurement in porcine ciliary epithelial cells

An potential-sensitive fluorescent dye, bis (1, 3-dibutylbarbituric acid) trimethine oxonol [DiBAC4(3)] (Invitrogen, CA, USA) was used in this study to measure the membrane potential of native porcine ciliary epithelial cells. DiBAC4(3) is a lipophilic anion dye giving fluorescence when binding to membranes and proteins. Depolarization causes the dye to enter the cytosol and results in an increase of fluorescence intensity; while hyperpolarization extrudes the dye to the cell membrane and causes a decrease of fluorescence within cytosol (Br.auner et al. 1984). DiBAC4(3) has been used to determine membrane potential in various cell types (Brauner et al. 1984; Miao and Joyner, 1994)

The native porcine ciliary epithelial cells were prepared as described in Chapter 2, Section 2.3.1. Cells were then incubated in NRR with 1 μM DiBAC4(3) for 30 minutes at room temperature (22-24 ℃). The coverslips with attached cells were then transferred to a perfusion chamber on the stage of an inverted fluorescent microscope (Nikon, Tokyo, Japan). The perfusion rate of bath solution containing DiBAC4(3) (1 μM) was maintained at 1 mL/min by a perfusion pump.

DiBAC4(3) was excited at 490 nm and the emission light at 510 ± 10 nm was collected by a 505 nm dicroic mirror with a barrier filter (515~550 nm). The fluorescence images were captured with a cooled digital CCD camera (Sensicam qe, PCO, Germany) and acquired by Metafluor Version 5.0r6 software (Universal Imaging, NY, USA.). The sampling interval of the fluorescence was 10 seconds. The background fluorescence was always substracted from the images of cells. All of the experiments were conducted at room temperature (22-24 ℃).

2.4.2. Calibration of the Fluorescence

Calibration of DiBAC4(3) fluorescence against membrane potential was performed by sequentially changing Na^+ concentrations in NRR in the presence of gramicidin. Gramicidin is a monovalent cation ionophore making the plasma membrane equally permeable to both K^+ and Na^+. As illustrated in Fig2.5(A), at the presence of gramicidin (2 μg/mL), extracellular Na^+ concentrations were reduced by isometric choline substitution in a stepwise manner (in mM, 136, 60, 25.6, 9.4, 2), and the sum of Na^+ and choline was always kept to be 136 mM.

The membrane potential was obtained by the equation:

$$59 \log \{([Na^+]_o + [K^+]_o)/([Na^+]_i + [K^+]_i)\}$$

The sum of intracellular concentration of Na^+ and K^+ ($[Na^+]_i+[K^+]_i$) is assumed to be 140 mM. The calculated membrane potential values were then plotted against the log of the fluorescence intensities with different $[Na^+]_o$, and the best-fit linear regression lines for PE and NPE cells were shown in Fig2.5(B).

A.

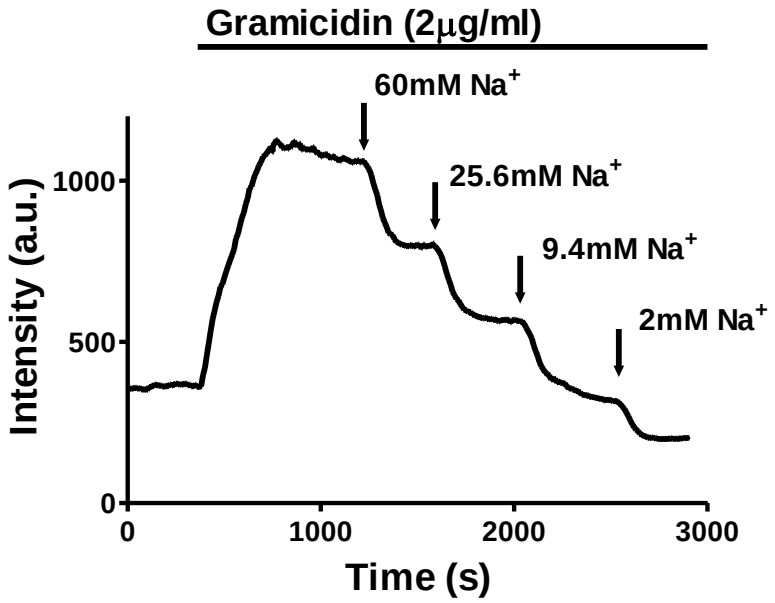

B.

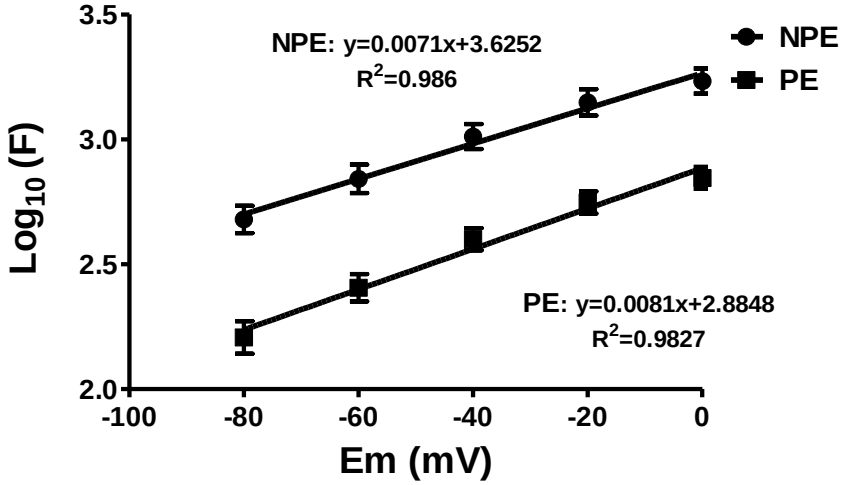

Fig.2.5. Calibration of DiBAC4(3) fluorescence against membrane potential in native porcine PE and NPE cells. The calibration experiments were performed by sequentially reducing Na^+ concentration in the bathing solution $[Na^+]_o$ in the presence of gramicidin.The logs of the fluorescences (F) with different $[Na^+]_o$ were plotted against the calculated membrane potential (Em) respectively. The best-fit linear regression lines were demonstrated. Data were collected from 72 NPE cells and 49 PE cells of 5 independent dishes.

2.4.3. Solutions and pharmacological agents

NRR was used as bathing solution (290 mOsmol/kg H_2O, pH 7.4, composition described in Chapter 2, Section 2.1.6). In the low Na^+ solution, Na^+ was replaced with equal amount of choline; in the low Cl^- solution, Cl^- was replaced with equal amount of gluconate. All pharmacological agents were purchased from Sigma-Aldrich, Inc and dissolved in DMSO.

2.4.4. Statistical analysis

All data are expressed as MEAN±SEM. GraphPad Prism was used for statistical analysis. The comparisons between baseline values and drug-treated values were performed by Paired Student's *t*-tests. The comparisons between two groups were performed by Unpaired Student's *t*-tests. Statistical significance was set as $P<0.05$.

2.5. Whole cell current measurement of native porcine NPE cells

2.5.1. Cell preparation

The native porcine ciliary epithelial cells were prepared as described in Chapter 2, Section 2.3.1. Each time prior to the patch clamp measurements, cells were rinsed twice by PBS before seeding onto the coverslips.

2.5.2. Whole cell current measurement

Micropipettes were prepared from glass capillary tubes (World Precision Instruments, Sarasota, FL, USA) by a micropipette puller (model P-97; Sutter Instruments). The pipettes were then polished by a microforge (MF-830; Narishige, Tokyo, Japan), generating a resistance of 3-6 MΩ after filling with micropipette solution.

Coverslips with attached cells were transferred to a perfusion chamber connecting to Ag/AgCl pellet via a 3 M KCl agar bridge on the stage of an inverted microscope. Whole-cell currents were measured with Axopatch 200B patch clamps (Axon Instruments, Foster City, CA, USA) coupled to an external Bessel filter (Model 990C; Frequency Devices, Haverhill, MA, USA). The voltage

protocol is described as followed. The holding potential was 0 mV, and the command voltages were cycled from -90 to +90 mV in 20-mV steps, and each command potential lasted for 300 ms. Upward current deflections represented outward currents, and vice versa. Data were obtained with a digital interface (Digidata 1440; Axon Instruments) and analyzed by Clampex 10.2 (Axon Instruments). Series resistance and cell capacitance were displayed from the transient cancellation settings of the amplifier. The series resistance was around 15 megaohms and was always compensated. All the experiments were conducted at room temperature (22–24 ℃).

2.5.3. Solutions and pharmacological agents

For whole-cell recording, micropipette solution contained (in mM): 25 NaCl, 110 aspartic acid, 120 *N*-methyl-Dglucamine base (NMDG), 0.38 $CaCl_2$, 12 HEPES, 1.0 EGTA, 1.0 MgATP, and 0.01 GTP (290 mOsmol/kg H_2O, pH 7.4). The Cl^- concentration in micropipette solution was increased by addition of NMDGCl, maintaining the sum of NMDG to be 120 mM (290 mOsmol/kg H_2O, pH 7.4).

Isotonic bathing solution contained (in mM): 116 NaCl, 6 HEPES, 6 NaHEPES, 1.8 $CaCl_2$, 1.2 $MgCl_2$, 5 glucose, 67 mannitol (290 mOsmol/kg H_2O, pH 7.4). The

hypotonic solution was prepared by omitting the mannitol from the solution (240 mOsmol/kg H_2O, pH 7.4).

All chemical reagents were obtained from Sigma-Aldrich, Inc. Baicalein, NFA, 5-nitro-2-(3-phenylpropylamino)-benzoic acid (NPPB), staurosporine and calphostin C were dissolved in DMSO (maximum concentration, 0.05%).

2.5.4. Statistical analysis

All data are expressed as MEAN±SEM. GraphPad Prism was used for statistical analysis. The comparisons between baseline values and drug-treated values were performed by Paired Student's *t*-tests, or repeated measures ANOVA followed by Tukey's post hoc test. Comparisons among three or more groups were conducted with one-way ANOVA, followed by Tukey's post hoc test. Statistical significance was considered as $P<0.05$.

2.6. Western-blot analysis

2.6.1. Cellular extract preparation

The native porcine ciliary epithelial cells were prepared as described in Chapter 2, Section 2.3.1. After grown to sub-confluency in four-well plates (~0.4 M cells/plate) in DMEM (Thermo Fisher Scientific) / 10% FBS / 0.1% gentamicin, cells were incubated with 300 nM phorbol 12-myristate 13-acetate (PMA) (Sigma-Alrich) for 15, 30 and 60 minutes, or treated with 50 and 100 μM baicalein (Sigma-Alrich) for 5 minutes. Cells without any treatment were considered as control group. After that, cells were rinsed twice with ice-cold PBS before the lysis buffer (100 μL/well) was added. Cells were then scraped into the buffer and gently agitated on ice for 10 minutes. Cell lysates were centrifuged for 20 minutes at 1, 2000 rpm, 4 ℃. The supernatant was collected.

Lysis buffer: Radio Immuno Precipitation Assay buffer (RIPA buffer**)** [150 mM sodium chloride, 1.0% Triton X-100, 0.5% sodium deoxycholate, 0.1% sodium dodecyl sulphate (SDS), 50 mM Tris, pH 8.0] with One Complete, Mini protease inhibitor cocktail tablet (Complete, Roche Applied Science, Switzerland) and one phosphatase inhibitor Ccocktail tablet (PhosSTOP, Roche Applied Science) in 10 mL buffer.

2.6.2. Protein quantification

Bradford protein assay (BioRad, San Diego, CA, USA) was used to determine the concentration of protein in the supernatant. The method is a colorimetric assay which utilizes the blue complex formed by an improved Coomassie blue G reagent and the protein present in solution. The intensity of the blue complex is positively related to the concentration of protein in the sample. By comparison to the standard curve made by bovine serum albumin (BSA) (Sigma-Alrich), the concentration of protein was determined. The absorbance was measured by a UV/VIS Spectrophotometer SP-300 Plus (Optima, Japan) at 595 nm.

2.6.3. Gel electrophoresis

The sample mixed with loading buffer was heated at 95℃ for 5 minutes. Presteined Protein markers (Fermentas PageRuler Protein Ladder Plus, Canada) and samples were loaded in a 10% SDS-polyacrylamide gel. The gel electrophoresis was performed at constant voltage (80 mV) for around 180 minutes. The progress of electrophoresis can also be demonstrated by the protein markers.

Loading buffer: 0.3 M Tris, 10% SDS, 50% v/v glycerol, 3.6 M beta-mercaptoethanol and 0.5% bromophenol blue.

2.6.4. Transfer of protein to PVDF membrane

After gel electrophoresis, the electroblotting was performed to transfer the proteins to the polyvinylidene difluoride (PVDF) membrane (Immuno-Blot PVDF membrane, BioRad, San Diego, CA, USA). The gel, PVDF membrane, filter papers and sponges were clamped together by a cassette and placed in a Mini Trans-Blot® Electrophoretic Transfer Cell (BioRad) filling with cool transfer buffer. At 4 ℃, transfer was conducted at 57 mV for 120 minutes.

Transfer buffer: 25 mM Tris, 192 mM glycine, 20% v/v methanol, pH 8.3

2.6.5. Blocking

The non-specific binding of PVDF membrane was blocked by 5% non fat dry milk (Carnation non fat dry milk, Nestle, Switzerland) in TBST. The blocking was performed at room temperature (22-24 ℃) for an hour with agitation.

TBST: Tris-buffered solutions (0.1 M Tris-HCL, pH 8.0, 0.5 M NaCl) with 0.05% Tween-20

2.6.6. Antibodies incubation

The membranes were incubated with diluted primary antibodies overnight at 4 ℃ with shaking. After incubation, the membranes were rinsed with TBST for 15 minutes and repeated for 3 times. Then the membranes were incubated with HRP-conjugated secondary antibodies for an hour at room temperature. After that, the membranes were rinsed again with TBST for 15 minutes and repeated for three times.

Target Protein	Primary Antibody	Dilution	Secondary Antibody	Dilution
Phospho-PKC	Phospho-PKC (pan) (Zeta Thr410) rabbit mAb (Cell Signaling Technology, Beverly, MA, USA)	1:1000 in 5% BSA TBST	Goat anti-rabbit IgG-HRP (Invitrogen, CA, USA)	1:5000 in 5% non fat dry milk TBST
GAPDH	Anti-GAPDH mouse mAb (Calbiochem, San Diego, CA, USA)	1:5000 in 5% non fat dry Milk TBST	HRP-Goat anti-mouse IgG (H+L) (Invitrogen, CA, USA)	1:10000 in 5% non fat dry milk TBST

Table 2.1. The antibodies used in the experiments

2.6.7. Development of immunoblots

Enhanced chemiluminescent (ECL) was used in this study for the detection of proteins. In the existence of peroxide buffer, the oxidation of luminal is catalyzed by HRP and generates a reagent that emits light. The intensity of emission is proportional to the amount of this HRP-catalyzed reaction. HRP forms complex with protein on the membrane and the intensity of signal is positively correlated to the amount of protein. Equal volumes of luminol solution and peroxide buffer

from Pierce SuperSignal® West Pico Chemiluminescent substrate (ThermoFisher Scientific, Waltham, MA, USA) were mixed together as working solution. The membranes were incubated with the working solution for 5 minutes at room temperature before being transferred to a plastic wrap. Air bubbles trapped between the membranes and plastic wrap were removed. A CCD camera (Lumi-Imager, Roche Applied Science) was used to capture the signal. The exposure time ranged from 8 seconds to 2 minutes according to the signal strength. The intensities of signals were analyzed by the software Image J (National Institutes of Health, USA).

2.7. IOP measurement

2.7.1. Animal

Thirteen Albino Guinea pigs aged 2-3 months old, weighing from 900 g to 1100 g, were used in all experiments. Seven guinea pigs (3 female, 4 male) were randomly allocated to the topical administration group, and the rest six animals (2 female, 4 male) were allocated to the intravitreal injection group. Animals were kept in a room with a 12-hour light/dark cycle and water and food were provided *ad libitum*. All animals were taken care and handled in compliance with the ARVO Statement for the Use of Animals in Ophthalmic and Vision Research and the local regulations from the Animal Subjects Research Ethnic Subcommittee (ASEC) of Hong Kong Polytechnic University.

2.7.2. IOP measurement with TonoLab

The TonoLab (Colonial Medical Supply, Franconia, NH, USA) was used in IOP measurement. Guinea pigs were gently restrained by hand during the measurement. The “rat” mode was specially chosen for all the measurements. IOP value at each time point was obtained by taking the average of at least three machine-generated

mean IOP readings, which were automatically calculated from 5 consecutive valid readings for each session.

2.7.3. Procedures for topical administration group

To prepare 0.3% baicalein suspension, baicalein (Sigma-Alrich) was dissolved in 10% Hydroxypropyl beta-cyclodextrin (HP-*β*-CD) (Wako Pure Chemical Industries, Osaka, Japan) that diluted in PBS. Benzalkonium chloride (BAC) (Sigma-Alrich) was then added into the baicalein suspension to facilitate the corneal penetration of baicalein, and the final concentration of BAC was 0.015%. The vehicle control was prepared by omitting baicalein from the solution (10% HP-*β*-CD in PBS with 0.015% BAC). Before use, this baicalein suspension was ultra-sonicated for at least 10 minutes.

For topical administration of drugs and IOP measurement, neither general nor topical anesthesia was used. The experimental eyes of seven guinea pigs were instilled with one 20-μL drop of baicalein (0.3%), and the contralaretal eyes were instilled with one 20-μL drop of vehicle solution as control. Each time after the instillation, the drugs and control solutions were kept on the cornea for at least 5 minutes. The administrations were performed hourly for 3 consecutive hours. The

IOP was measured before the initial instillation and hourly thereafter for 4 consecutive hours. All experiments were conducted from 2 pm to 6 pm for each day.

2.7.4. Procedures for intavitreal injection group

Baicalein was freshly prepared immediately before each injection. Baicalein was dissolved in DMSO and then further diluted with sterile PBS to yield the concentration of 2 mM. The vehicle control was prepared by omitting baicalein from the solution (10% DMSO in PBS). Prior to administration, both the baicalein-containing solution and vehicle solution were filtered through sterile syringe with a 0.2 μM cellulose acetate, nonpyrogenic syringe filter (DISMIC-13CP; Advantec, Japan).

After baseline IOP was measured with tonolab, guinea pigs were anesthetized by intramuscular administration of 20 mg/kg ketamine. With a Hamilton syringe and a 30-gauge needle, 13 μL of baicalein (2 mM) was injected into one eye of six anesthetized guinea pigs, and an equal volume of vehicle solution was injected into the contraleteral eyes. To avoid causing mechanical injury to ciliary body and crystalline lens, the injection was performed at 2 mm posterior to the limbus,

directly pointing towards the centre of vitrous chamber. The total volume of the vitrous body in guinea pig was assumed to be around 250 µL (Taskintuna et al., 1997), therefore, the resultant intravitreal concentration of baicalein was around 100 µM after the injection. IOP was measured before intravitreal injection and at 1, 2, 3 and 5 hours thereafter. All experiments were conducted from 2 pm to 7 pm for each day.

2.7.5. Statistical analysis

All data are expressed as MEAN±SEM. GraphPad Prism was used for statistical analysis. Comparisons were made by two-way ANOVA, followed by Bonferroni post tests. $P<0.05$ was taken as statistically significant.

Chapter 3 Results

3.1. Effect of baicalein on Isc across porcine CBE

3.1.1 Effect of baicalein on Isc across porcine CBE

Stromal application of baicalein (100 and 300 μM) did not induce any significant change of Isc (n=5, P>0.05), while application of baicalein on aqueous side elicited significant reduction of Isc in a dose-dependent manner. At the concentration of 50, 100, 300 μM, addition of baicalein on aqueous side reduced the baseline Isc by 24 ±2% (n=6, P<0.01), 51 ±4 % (n=10, P<0.01) and 65 ±7% (n=6, P<0.01) respectively. The effects of baicalein (ST and AQ) on Isc across porcine CBE were summarized in Fig3.1-3.2 and Table 3.1-3.2. The time course of the response was illustrated in Fig.3.3. After the addition of baicalein (AQ), Isc began to decrease within 5 minutes, and reached new steady state at around 60 minutes.

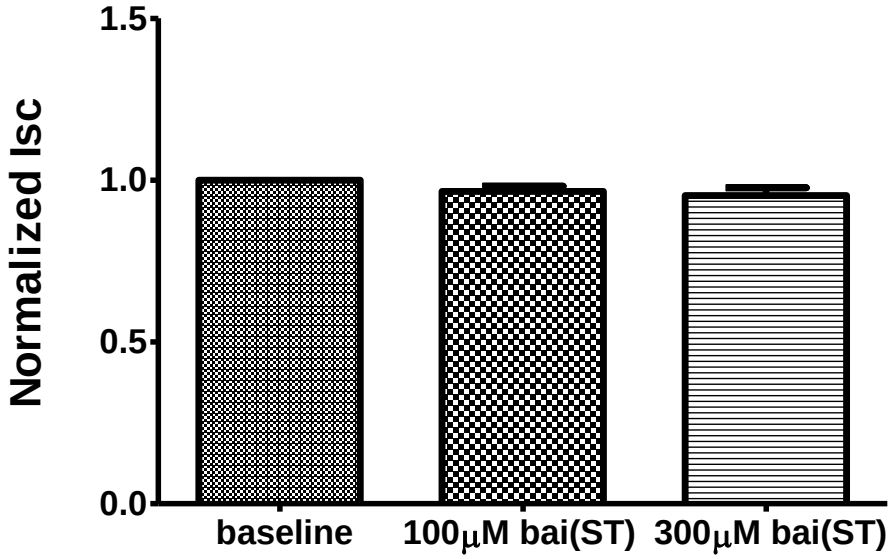

Fig.3.1. Effects of baicalein (100 and 300 μM, ST) on Isc across porcine CBE. Results were normalized to baseline value and given as MEAN±SEM, n=5. P>0.05, compared by repeated measures ANOVA.

	Baseline	100 μM bai(ST)	300 μM bai(ST)
PD(mV)	-0.89±0.12	-0.87±0.12	-0.85±0.10
Isc(μAcm^{-2})	-12.76±2.56	-12.34±2.48	-11.95±2.15
R(Ωcm^2)	75±6	75±6	75±6

Table.3.1. Effect of baicalein (100 and 300 μM, ST) on the transepithelial electrical parameters across porcine CBE. Results are given as MEAN±SEM, n=5. ST: stromal side.

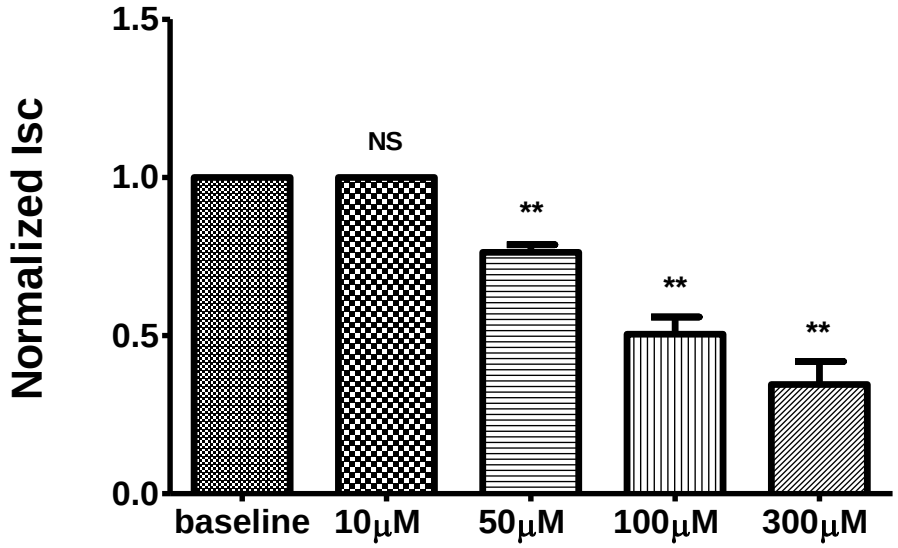

Fig.3.2. Effects of baicalein (10, 50, 100 and 300 μM, AQ) on Isc across porcine CBE. Results were normalized to baseline value and given as MEAN±SEM. NS P>0.05; ** P<0.01 compared with baseline value (One-way ANOVA, followed by Tukey multiple comparison test).

	Baseline	10μM bai(AQ)	50μM bai(AQ)	100μM bai(AQ)	300μM bai(AQ)
PD(mV)	-1.28	-1.28	-0.97	-0.67	-0.47
	±0.12	±0.12	±0.11	±0.11	±0.12
Isc(μAcm^{-2})	-19.32	-19.32	-15.17	-9.90	-6.93
	±1.74	±1.74	±1.19	±1.54	±1.78
R(Ωcm^2)	67±2	67±2	67±2	68±2	68±3

Table.3.2. Effect of baicalein (10, 50, 100 and 300 μM, AQ) on the transepithelial electrical parameters across porcine CBE. Results are given as MEAN±SEM. AQ: aqueous side.

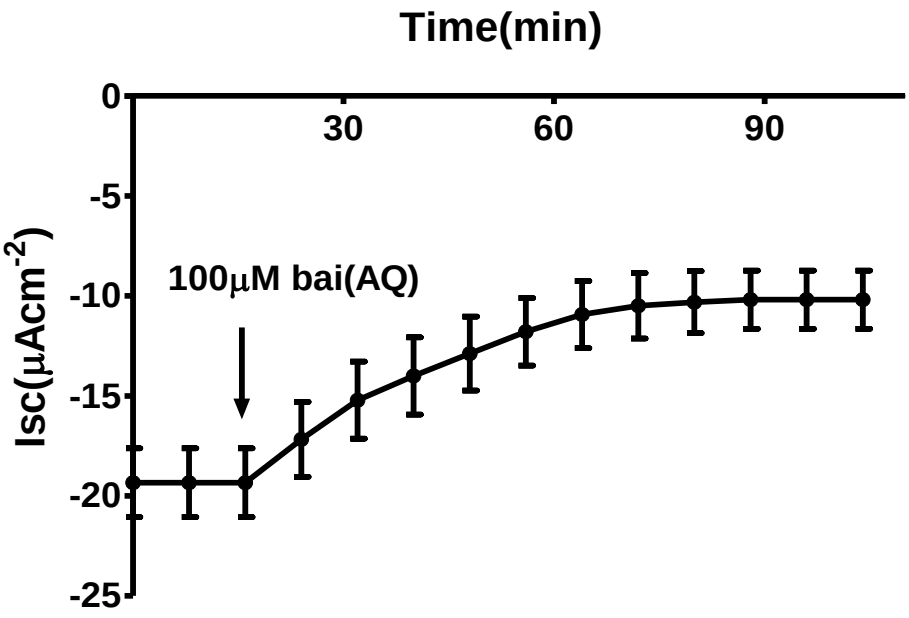

Fig.3.3. The time course of the Isc response of isolated porcine CBE induced by baicalein (100 μM, AQ). Results were given as MEAN±SEM, n=10. The time of drug addition is indicated by the arrow. AQ: aqueous side.

3.1.2 Effect of baicalin on Isc across porcine CBE

Baicalin is a flavone and is also one of the major active components found in Scutellaria baicalensis. Moreover, it is the glucuronide of baicalein. To find out if it exerts similar function in porcine CBE as baicalein, the effect of baicalin on Isc across porcine CBE was studied. Stromal application of baicalin (100 and 300 μM, n=4) and aqueous addition of 100 μM baicalin (n=4) did not induce any significant change of Isc ($P>0.05$), while 300 μM baicalin (AQ) elicited significant reduction of Isc by 22 ± 5% (n=9, $P<0.01$). The effects of baicalin (ST and AQ) on Isc are summarized in Fig 3.4-3.5 and Table 3.3-3.4.

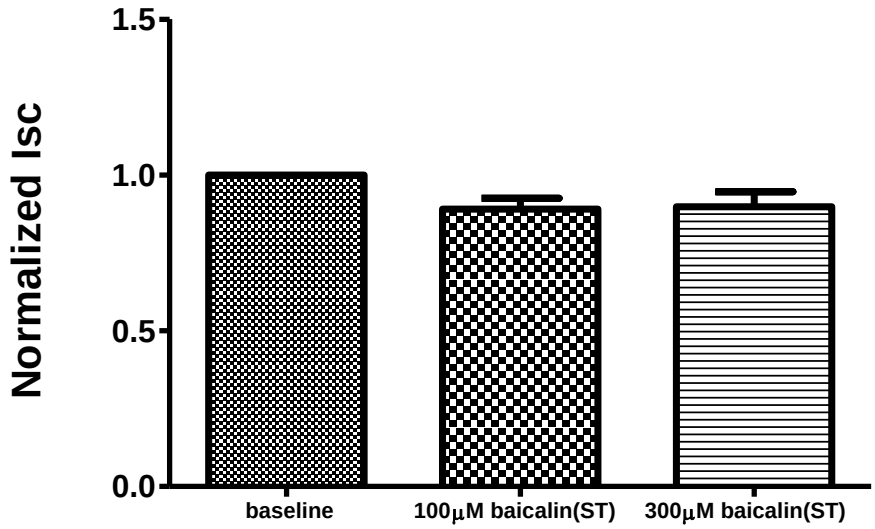

Fig.3.4. Effects of baicalin (100 and 300 μM, ST) on Isc across porcine CBE. Results are normalized to baseline value and given as MEAN±SEM, n=4. ST: stromal side. $P>0.05$, compared by repeated measures ANOVA.

	Baseline	100 μM baicalin (ST)	300 μM baicalin (ST)
PD(mV)	-0.66 ±0.11	-0.60 ±0.12	-0.61 ±0.12
Isc(μAcm^{-2})	-8.80 ±2.06	-8.03 ±2.12	-8.17 ±2.24
R(Ωcm^2)	79 ±5	79 ±5	79 ±5

Table.3.3. Effect of baicalin (100 and 300 μM, ST) on the transepithelial electrical parameters across porcine CBE. Results are given as MEAN ±SEM, n=4. ST: stromal side.

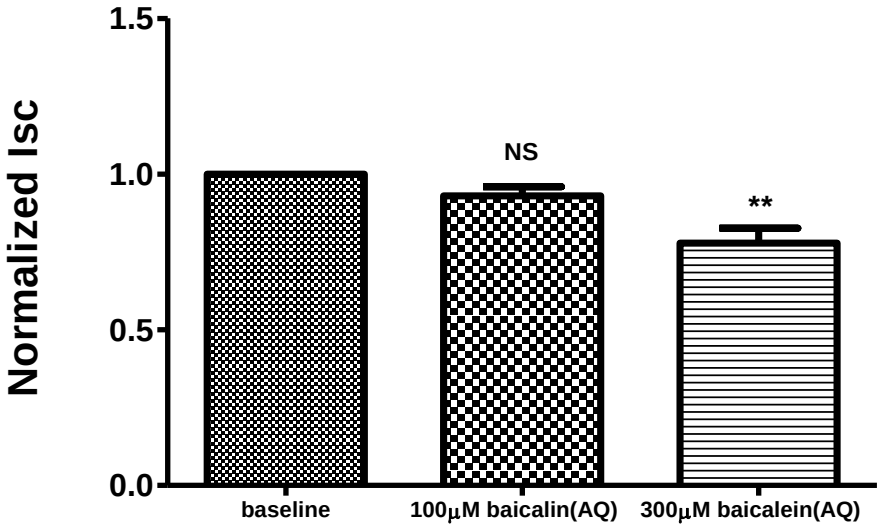

Fig.3.5. Effects of baicalin (100 and 300 μM, AQ) on Isc across porcine CBE. Results are normalized to baseline value and given as MEAN ±SEM. AQ: aqueous side. NS P>0.05; ** P<0.01, compared with baseline value (Repeated measures ANOVA, followed by Tukey multiple comparison test).

	Baseline	100 μM baicalin (AQ)	300 μM baicalin (AQ)
PD(mV)	-0.83 ±0.09	-0.74 ±0.09	-0.67 ±0.09
Isc(μAcm^{-2})	-12.67 ±1.60	-11.78 ±1.26	-10.41 ±1.68
R(Ωcm^2)	69 ±5	69 ±5	69 ±5

Table.3.4. Effect of baicalin (100 and 300 μM, AQ) on the transepithelial electrical parameters across porcine CBE. Results are given as MEAN ±SEM. AQ: aqueous side.

3.1.3 Effect of chrysin on Isc across porcine CBE

Chrysin is a naturally occurring flavone, possessing very similar structure with baicalein. It was studied to investigate if there is structure-function relationship that is similar to that of baicalein. Stromal application of chrysin (100 and 300 μM, n=4) and aqueous addition of 100 μM chrysin (n=6) did not induce any significant change of Isc (P>0.05), while 300 μM chrysin (AQ) elicited significant decrease of Isc by 19 ± 4% (n=8, P<0.01). The effects of chrysin (ST and AQ) on Isc are summarized in Fig 3.6-3.7 and Table 3.5-3. 6.

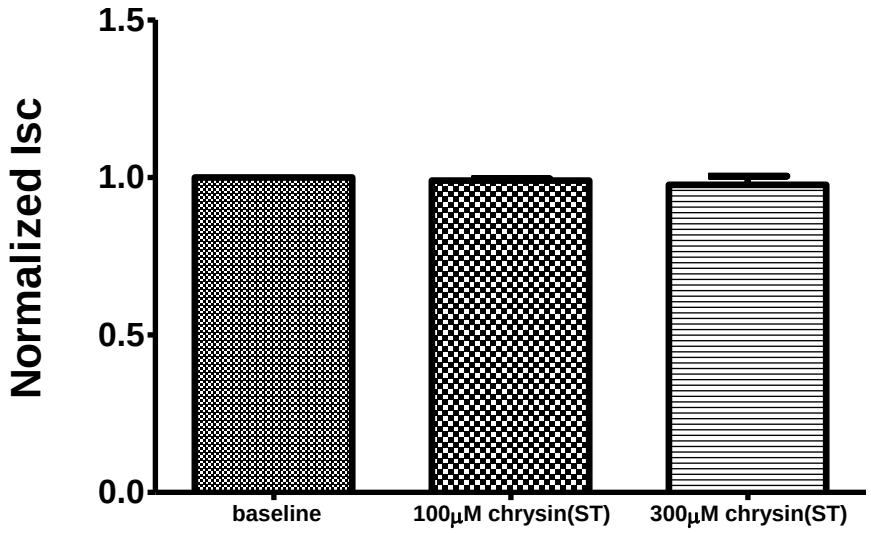

Fig.3.6. Effects of chrysin (100 and 300 μM, ST) on Isc across porcine CBE. Results are normalized to baseline value and given as MEAN ±SEM, n=4. ST: stromal side. P>0.05, compared by repeated measures ANOVA.

	Baseline	100 μM chrysin (ST)	300 μM chrysin (ST)
PD(mV)	-0.78 ±0.11	-0.78 ±0.11	-0.76 ±0.10
Isc(μAcm^{-2})	-9.02 ±0.52	-8.93 ±0.53	-8.76 ±0.37
R(Ωcm^2)	85 ±8	85 ±8	85 ±8

Table.3.5. Effect of chrysin (100 and 300 μM, ST) on the transepithelial electrical parameters across porcine CBE. Results are given as MEAN ±SEM. ST: stromal side.

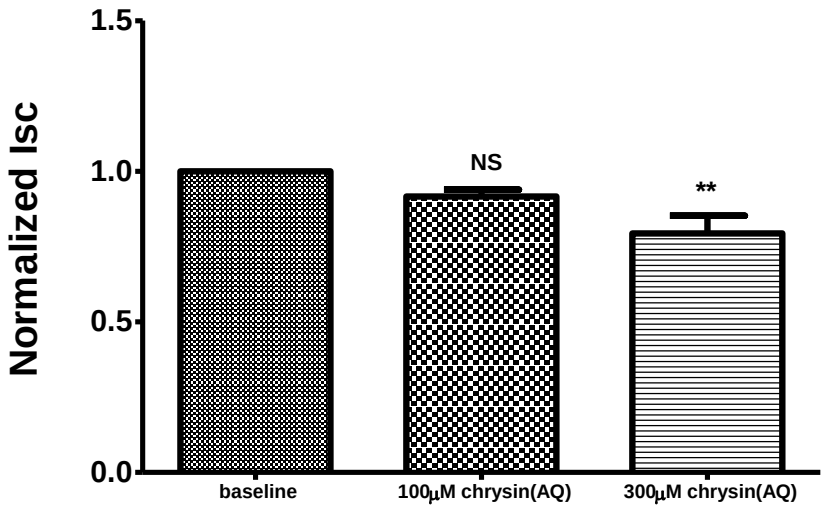

Fig.3.7. Effects of chrysin (100 and 300 μM, AQ) on Isc across porcine CBE. Results are normalized to baseline value and given as MEAN ±SEM. AQ: aqueous side. NS P>0.05; ** P<0.01, compared with baseline value (Repeated measures ANOVA, followed by Tukey multiple comparison test).

	Baseline	100 μM chrysin (AQ)	300 μM chrysin (AQ)
PD(mV)	-0.53 ±0.03	-0.46 ±0.06	-0.42 ±0.04
Isc(μAcm^{-2})	-7.50 ±0.54	-6.35 ±0.38	-6.09 ±0.58
R(Ωcm^2)	72 ±3	72 ±3	71 ±3

Table.3.6. Effects of chrysin (100 and 300 μM, AQ) on the transepithelial electrical parameters across porcine CBE. Results are given as MEAN ±SEM. AQ: aqueous side.

3.1.4 Effect of Cl^- substitution on Isc response induced by baicalein

After bilateral Cl^- replacement by gluconate, a transient hyperpolarization followed by depolarization of Isc was noticed, and at the new steady state, the Isc was almost abolished. Application of baicalein (100 μM, AQ) afterwards could not induce any further decrease of Isc (n=6, P>0.05), which indicated baicalein's effect was on chloride transport. The effect of Cl^- substitution on the Isc response induced by baicalein was summarized in Fig.3.9 and Table 3.8, and the time course is shown in Fig.3.8.

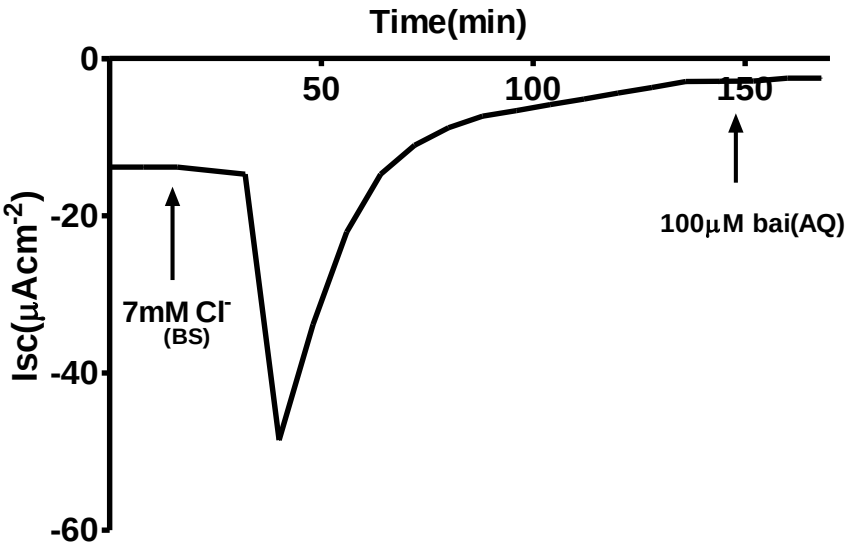

Fig.3.8. The time course of the Isc response of isolated porcine CBE induced by sequential addition of 7 mM Cl^- (BS) and baicalein (100 μM, AQ). BS: bilateral sides. The time of drug addition was indicated by the arrow.

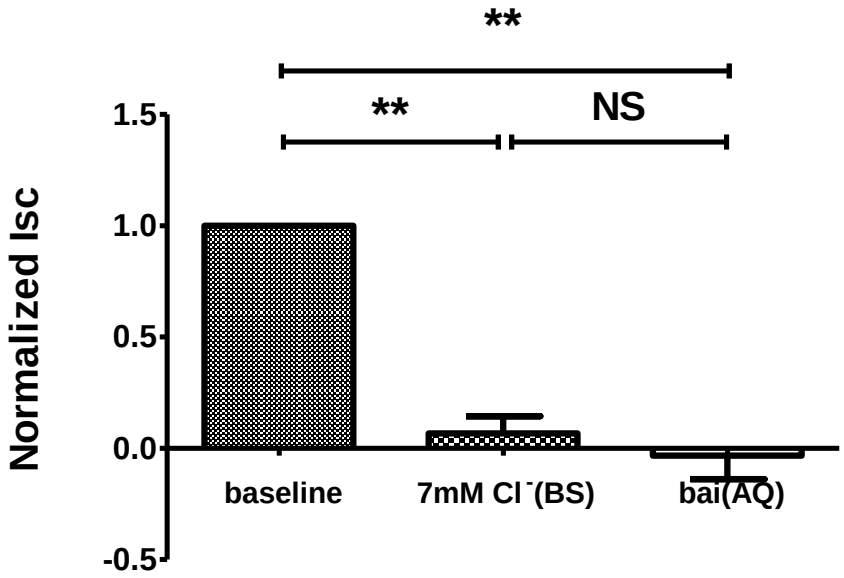

Fig.3.9. Effect of sequential addition of 7 mM Cl^- (BS) and baicalein (100 μM, AQ) on Isc across porcine CBE. Results were normalized to baseline value and given as MEAN±SEM, n=6.

NS P>0.05; ** P<0.01 (Repeated measures ANOVA, followed by Tukey multiple comparison test).

	Baseline	7mM Cl^- (BS)	100μM bai (AQ)
PD(mV)	-0.76±0.03	-0.08±0.07	0.00±0.09
Isc(μAcm^{-2})	-13.80±0.89	-1.05±1.13	0.37±1.48
R(Ωcm^2)	66±3	73±6	73±6

Table.3.7. Effect of sequential addition of 7 mM Cl^- (BS) and baicalein (100 μM, AQ) on the transepithelial electrical parameters across porcine CBE. Results are given as MEAN±SEM, n=6. BS: bilateral sides; AQ: aqueous side.

3.1.5 Effects of NKCC inhibitors on the Isc response induced by baicalein

Furosemide (FSM) and bumetanide (BMT) are loop diuretics widely used as NKCC inhibitors. They were employed in the experiments to investigate the role of NKCC in the inhibitory effect of baicalein on Isc across porcine CBE.

BMT (100 μM, BS) depolarized Isc by 54 ± 3%, and addition of baicalein (100 μM, AQ) afterwards caused a further reduction of Isc by 23 ± 3% (n=7, $P<0.01$). FSM (100 μM, AQ) caused significant reduction of baseline Isc by 45 ± 9% (n=5, $P<0.01$), but the effect of baicalein (100 μM, AQ) was almost abolished after the pretreatment (n=5). The effects of BMT and FSM on the Isc response induced by baicalein were summarized in Fig.3.11 & Table.3.8 and Fig.3.13 & Table.3.9 respectively; the time courses are shown in the Fig.3.10 and Fig.3.12 respectively.

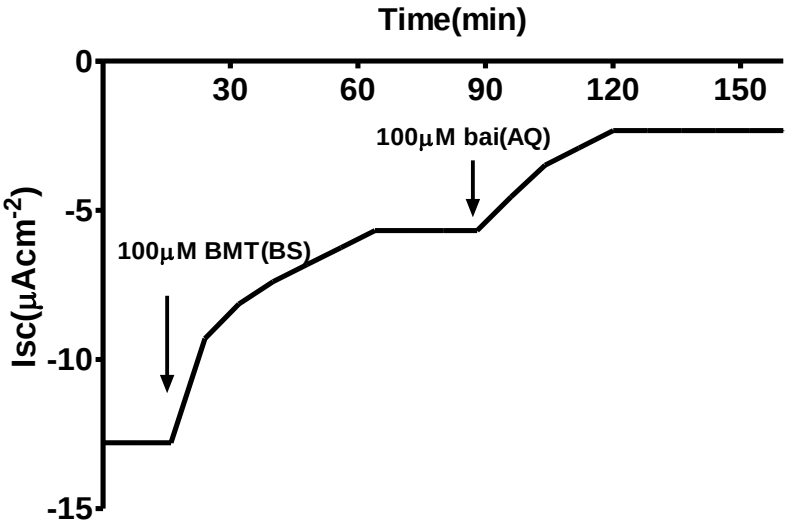

Fig.3.10. The time course of the Isc response of isolated porcine CBE after sequential addition of BMT (100 μM, BS) and baicalein (100 μM, AQ). The time of drug addition was indicated by the arrow. BS: bilateral sides; AQ: aqueous side.

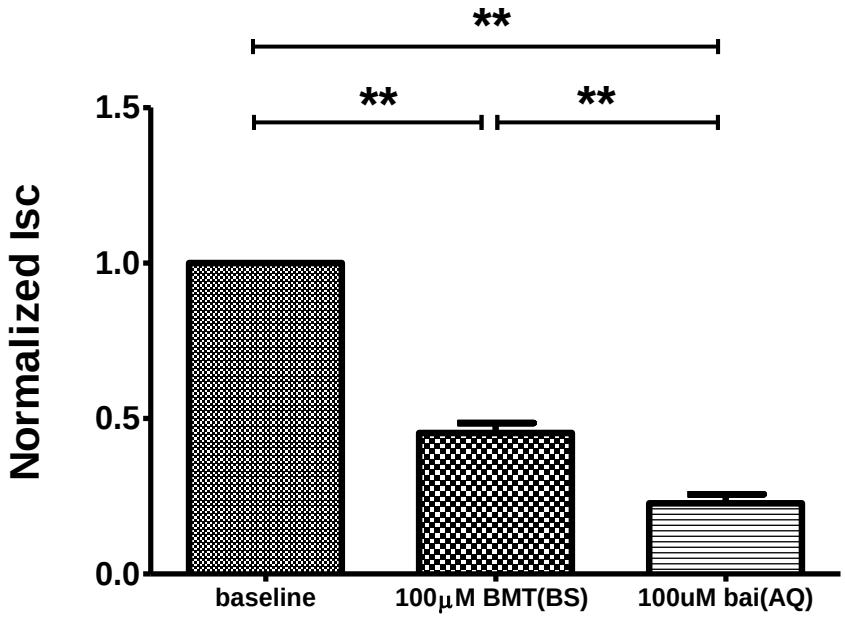

Fig.3.11. Effect of sequential addition of BMT (100 μM, BS) and baicalein (100 μM, AQ) on Isc across porcine CBE. Results were normalized to baseline value and given as MEAN±SEM, n=7. BS: bilateral sides; AQ: aqueous side. ** P<0.01 (Repeated measures ANOVA, followed by Tukey multiple comparison test).

	Baseline	100 μM BMT (BS)	100 μM bai (AQ)
PD(mV)	-1.00 ±0.05	-0.46 ±0.03	-0.24 ±0.04
Isc(μAcm^{-2})	-17.40 ±1.90	-7.82 ±0.87	-4.26 ±0.96
R(Ωcm^2)	60 ±5	61 ±5	61 ±5

Table3.8. Effect of sequential addition of BMT (100 μM, BS) and baicalein (100 μM, AQ) on the transepithelial electrical parameters across porcine CBE. Results are given as MEAN ±SEM, n=7. BS: bilateral sides; AQ: aqueous side.

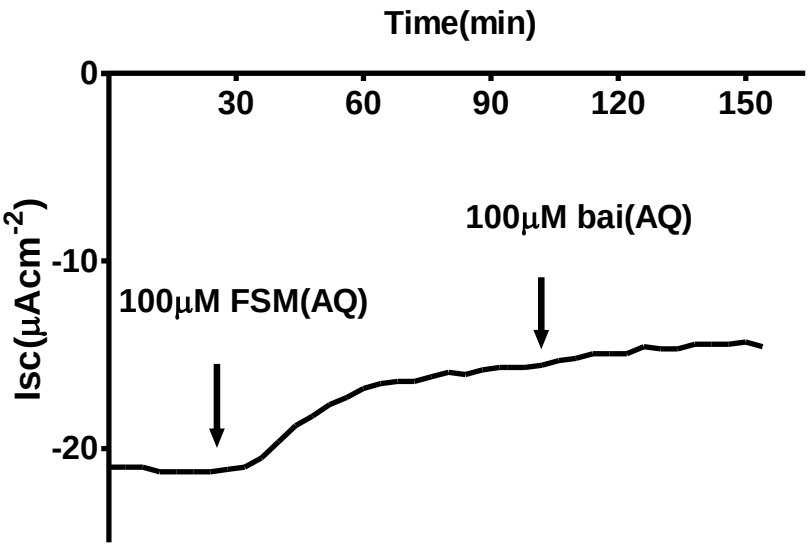

Fig.3.12. The time course of the Isc response of isolated porcine CBE induced by sequential addition of FSM (100 μM, AQ) and baicalein (100 μM, AQ). The time of drug addition was indicated by the arrow. AQ: aqueous side.

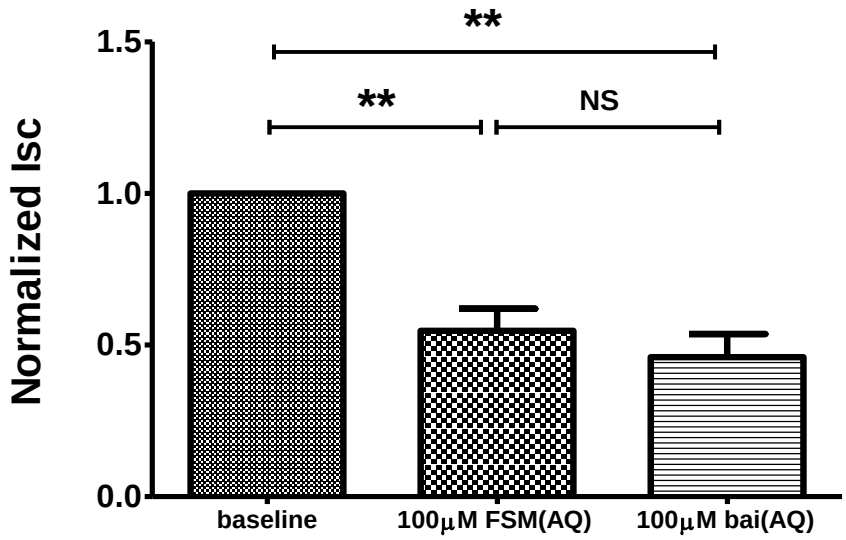

Fig.3.13. Effect of sequential addition of FSM (100 μM, AQ) and baicalein (100 μM, AQ) on Isc across porcine CBE. Results were normalized to baseline value and given as MEAN±SEM, n=5. AQ: aqueous side. NS $p>0.05$; ** $P<0.01$ (Repeated measures ANOVA, followed by Tukey multiple comparison test).

	Baseline	100μM FSM (AQ)	100μM bai (AQ)
PD(mV)	-0.99±0.15	-0.57±0.07	-0.49±0.07
Isc(μAcm^{-2})	-19.20±6.62	-10.26±1.79	-8.49±1.61
R(Ωcm^2)	58±5	57±6	55±6

Table3.9. Effect of sequential addition of FSM (100 μM, AQ) and baicalein (100 μM, AQ) on the transepithelial electrical parameters across porcine CBE. Results are given as MEAN±SEM, n=5. AQ: aqueous side.

3.1.6 Effects of chloride channel blockers on the Isc responses induced by baicalein

DPC and NFA are widely used chloride channel inhibitors. To investigate the role of chloride channel in baicalein evoked response, the preparations were pretreated with DPC and NFA before application of baicalein. Both DPC (500 μM, AQ) and NFA (1 mM, AQ) almost completely abolished the Isc ($P<0.01$) and at time appeared to even reverse the polarity of the preparations. After the pretreatments, baicalein failed to elicit any further reduction of Isc (n=5 for NFA pretreatment and n=5 for DPC pretreatment, $P>0.05$). The effects of DPC and NFA on baicalein-induced Isc response are summarized in Fig.3.15&Table.3.10 and Fig.3.17& Table.3.11 respectively, and the time courses of their effects are shown in Fig.3.14 and Fig.3.16 respectively.

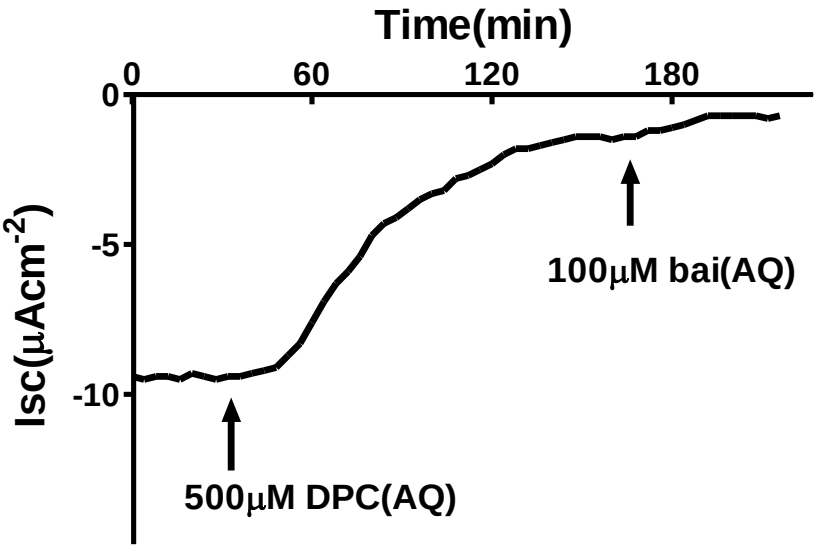

Fig.3.14. The time course of the Isc response of isolated porcine CBE after sequential addition of DPC (500 μM, AQ) and baicalein (100 μM, AQ). The time of drug addition was indicated by the arrow. AQ: aqueous side.

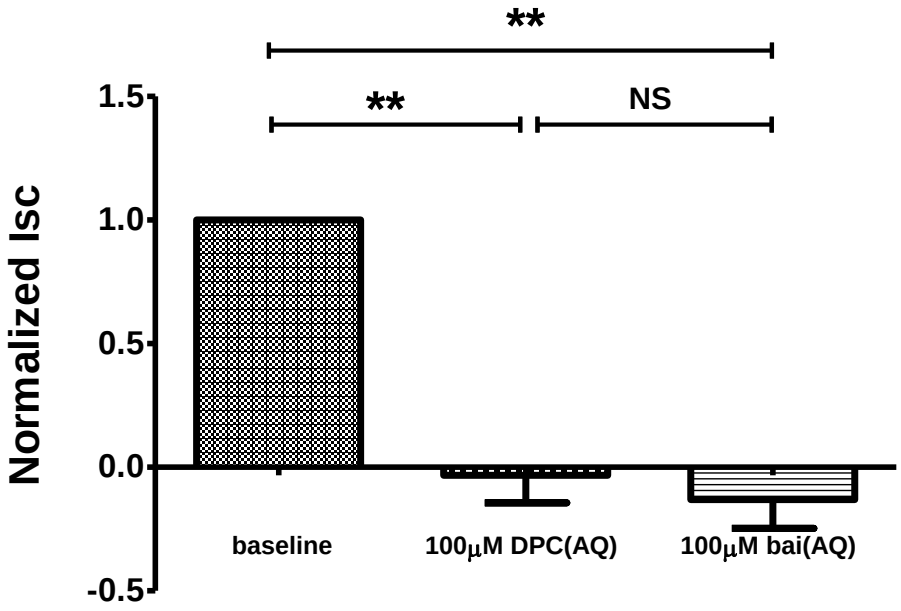

Fig.3.15. Effects of sequential addition of DPC (500 μM, AQ) and baicalein (100 μM, AQ) on Isc across porcine CBE. Results were normalized to baseline value and given as MEAN±SEM, n=5. AQ: aqueous side. NS $P>0.05$; ** $P<0.01$ (Repeated measures ANOVA, followed by Tukey multiple comparison test).

	Baseline	500 μM DPC (AQ)	100 μM bai (AQ)
PD(mV)	-0.74 ±0.11	-0.02 ±0.06	-0.04 ±0.06
Isc(μAcm^{-2})	-7.62 ±0.48	0.06 ±0.78	0.77 ±0.78
R(Ωcm^2)	95 ±10	95 ±9	91 ±10

Table.3.10. Effect of sequential addition of DPC (500 μM, AQ) and baicalein (100 μM, AQ) on the transepithelial electrical parameters across porcine CBE. Results are given as MEAN ±SEM, n=5. AQ: aqueous side.

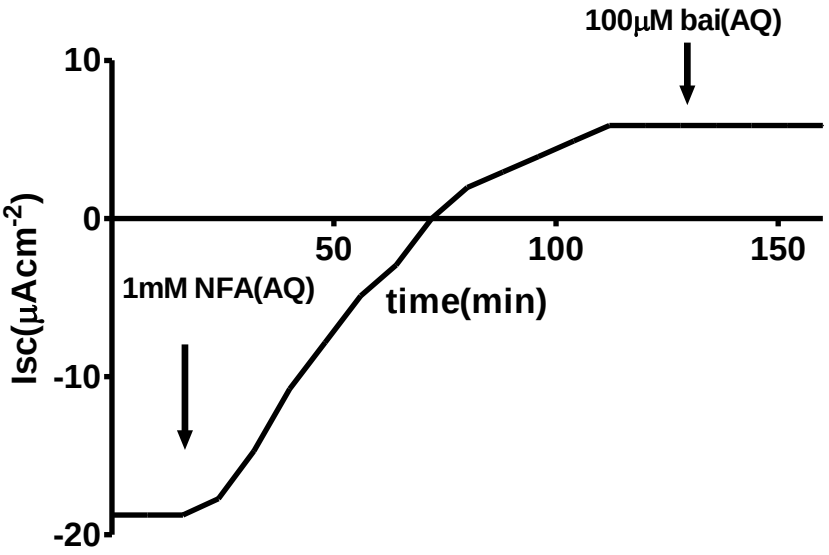

Fig3.16. The time course of the Isc response of isolated porcine CBE induced by sequential addition of NFA (1 mM, AQ) and baicalein (100 μM, AQ). The time of drug addition was indicated by the arrow. AQ: aqueous side.

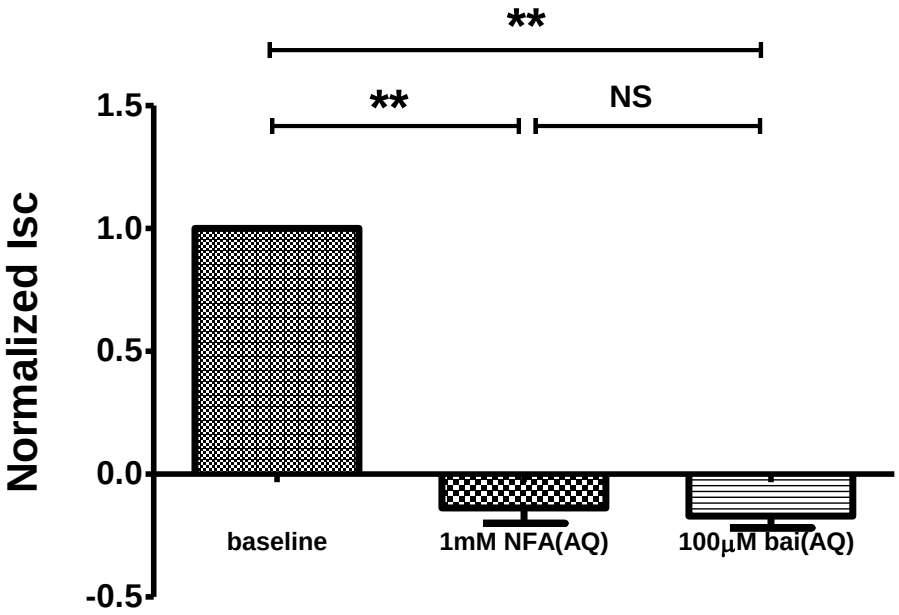

Fig.3.17. Effect of sequential addition of NFA (1 mM, AQ) and baicalein (100 μM, AQ) on Isc across porcine CBE. Results were normalized to baseline value and given as MEAN±SEM, n=5. AQ: aqueous side. NS $P>0.05$; ** $P<0.01$ (Repeated measures ANOVA, followed by Tukey multiple comparison test).

	Baseline	500 μM NFA (AQ)	100 μM bai (AQ)
PD(mV)	-1.08±0.10	0.13±0.07	0.17±0.05
Isc(μAcm^{-2})	-17.32±1.07	2.57±1.22	3.07±1.00
R(Ωcm^2)	64±8	64±8	64±8

Table.3.11. Effect of sequential addition of NFA (1 mM, AQ) and baicalein (100 μM, AQ) on the transepithelial electrical parameters across porcine CBE. Results are given as MEAN±SEM, n=5. AQ: aqueous side.

3.1.7 Effect of LOX inhibitor on the Isc response induced by baicalein

Baicalein is also known to be a potent and specific 12-LOX inhibitor. To test whether baicalein exerted its effect on Isc through this pathway, a LOX inhibitor NDGA was used. NDGA is a non-specific LOX inhibitor, which could down-regulate the activities of 5-LOX, 12-LOX and 15-LOX. If LOXs were involved, NDGA should have inhibitory effect on both baseline Isc and baicalein induced inhibition afterwards. However, the results did not substantiate this hypothesis.

NDGA (100 μM, AQ) elicited significant reduction of baseline Isc by 54 ± 9% (n=5, $P<0.01$), but in the presence of NDGA, baicalein (100 μM, AQ) still caused further decrease of Isc by 36 ± 6% (n=5, $P<0.01$). The findings indicated that the inhibitory property of baicalein in LOX activity may not be the culprit in inhibiting the Isc. The time course and the effect of NDGA on baicalein-induced Isc response are shown in Fig.3.18, Fig.3.19 and Table.3.12.

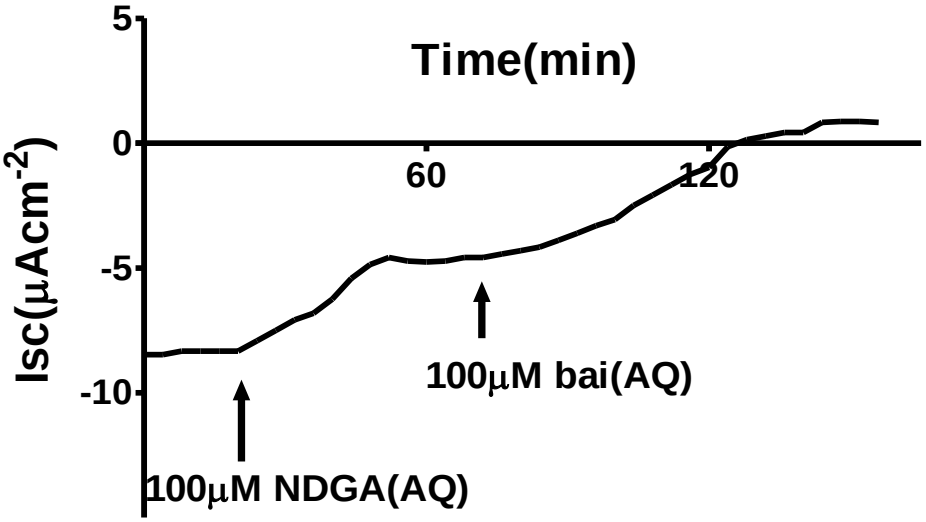

Fig.3.18. The time course of the Isc response of isolated porcine CBE after sequential addition of NDGA (100 μM, AQ) and baicalein (100 μM, AQ). The time of drug addition was indicated by the arrow. AQ: aqueous side.

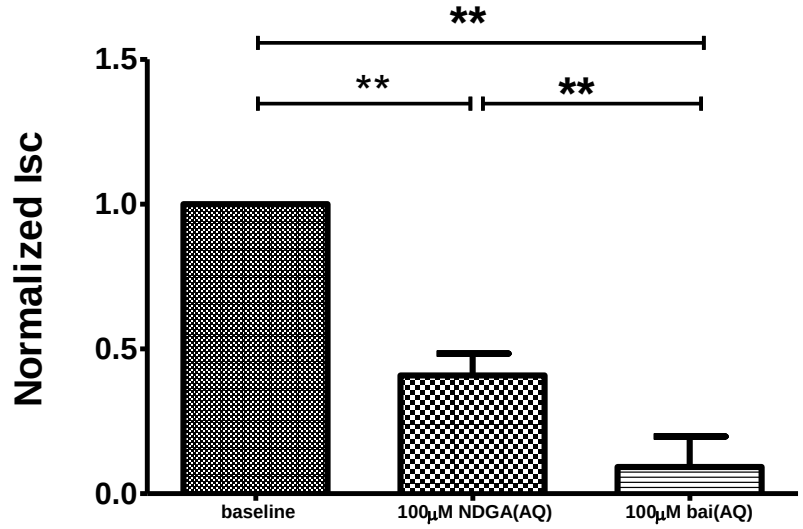

Fig.3.19. Effect of sequential addition of NDGA (100 μM, AQ) and baicalein (100 μM, AQ) on Isc across porcine CBE. Results were normalized to baseline value and given as MEAN±SEM, n=5. AQ: aqueous side. NS $p>0.05$; ** $P<0.01$ (Repeated measures ANOVA, followed by Tukey multiple comparison test).

	Baseline	100 µM NDGA (AQ)	100 µM bai (AQ)
PD(mV)	-0.69 ±0.04	-0.33 ±0.09	-0.08 ±0.09
Isc(μAcm^{-2})	-11.75 ±1.25	-5.12 ±1.55	-1.52 ±1.53
R(Ωcm^2)	66 ±3	66 ±4	70 ±4

Table.3.12. Effect of sequential addition of NDGA (100 µM, AQ) and baicalein (100 µM, AQ) on the transepithelial electrical parameters across porcine CBE. Results are given as MEAN ±SEM, n=5. AQ: aqueous side.

3.1.8 Effects of protein kinase inhibitors on the Isc response induced by baicalein

H89 is a common PKA inhibitor, while calphostin C and staurosporine are common PKC inhibitors. These inhibitors were used to test the possible involvement of PKA and PKC in the baicalein induced inhibition of Isc.

There was no significant change of Isc across porcine CBE after incubation of H89 (10 μM, AQ) for 30 minutes (n=5, P>0.05). Addition of baicalein (100 μM, AQ) thereafter still caused 65 ±8% reduction of Isc (n=5, P<0.01), indicating PKA did not participate in baicalein's effect. The effect of H89 on baicalein-induced Isc response is shown in Fig.3.20-3.21 and Table 3.13.

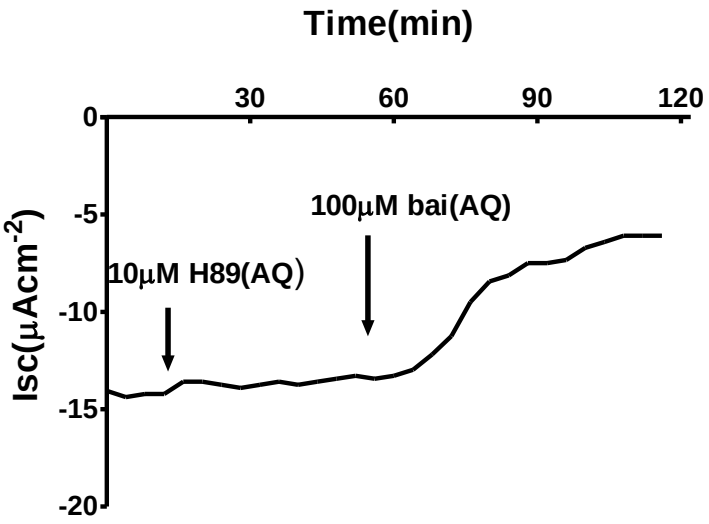

Fig.3.20. The time course of the Isc response of isolated porcine CBE after sequential addition of H89 (10 μM, AQ) and baicalein (100 μM, AQ). The time of drug addition was indicated by the arrow. AQ: aqueous side.

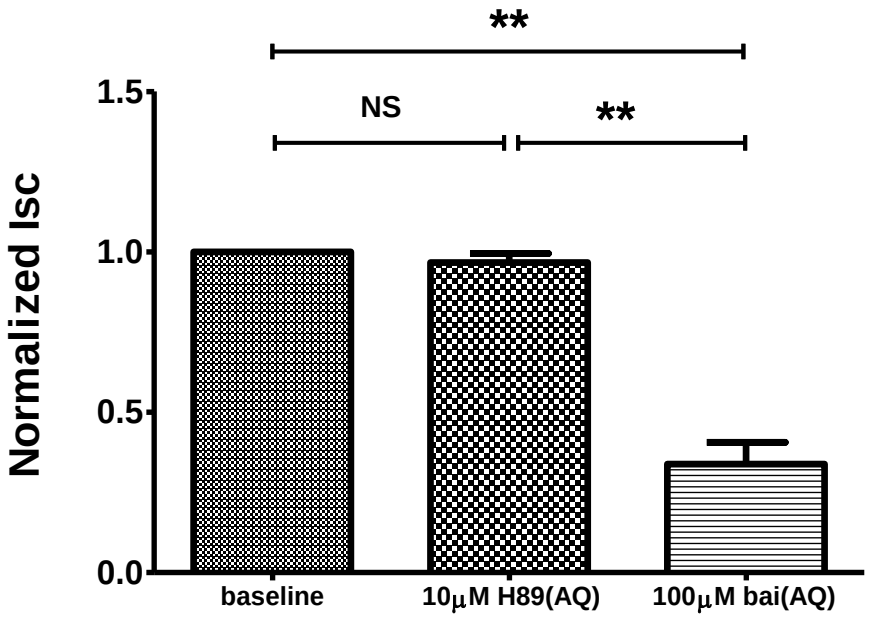

Fig3.21 Effect of sequential addition of H89 (10 μM, AQ) and baicalein (100 μM, AQ) on Isc across porcine CBE. Results were normalized to baseline value and given as MEAN±SEM, n=5. AQ: aqueous side. NS $p>0.05$; ** $P<0.01$ (Repeated measures ANOVA, followed by Tukey multiple comparison test).

	Baseline	10μM H89 (AQ)	100μM bai (AQ)
PD(mV)	-0.67±0.06	-0.64±0.06	-0.24±0.07
Isc(μAcm^{-2})	-11.51±0.78	-11.2±1.03	-3.96±1.08
R(Ωcm^2)	58±3	58±2	58±3

Table3.13. Effect of sequential addition of H89 (10 μM, AQ) and baicalein (100 μM, AQ) on the transepithelial electrical parameters across porcine CBE. Results are given as MEAN±SEM, n=5. AQ: aqueous side.

Pretreatment of both calphostin C (0.3 μM, AQ) and staurosporine (0.3 μM, AQ) for 30 minutes induced no significant change on baseline Isc ($P>0.05$). After the pretreatment, calphostin C significantly reduced baicalein induced Isc inhibition to 20 ± 3% ($n=6$, $P<0.01$), while staurosporine almost completely blocked it ($n=6$). The results revealed that PKC pathway was likely involved in the inhibitory effect of baicalein. The effect of calphostin C on baicalein-induced Isc response is shown in Fig.3.22, Fig.3.23 and Table.3.14; the effect of staurosporine on baicalein-induced Isc response is shown in Fig.3.24, Fig.3.25 and Table.3.15.

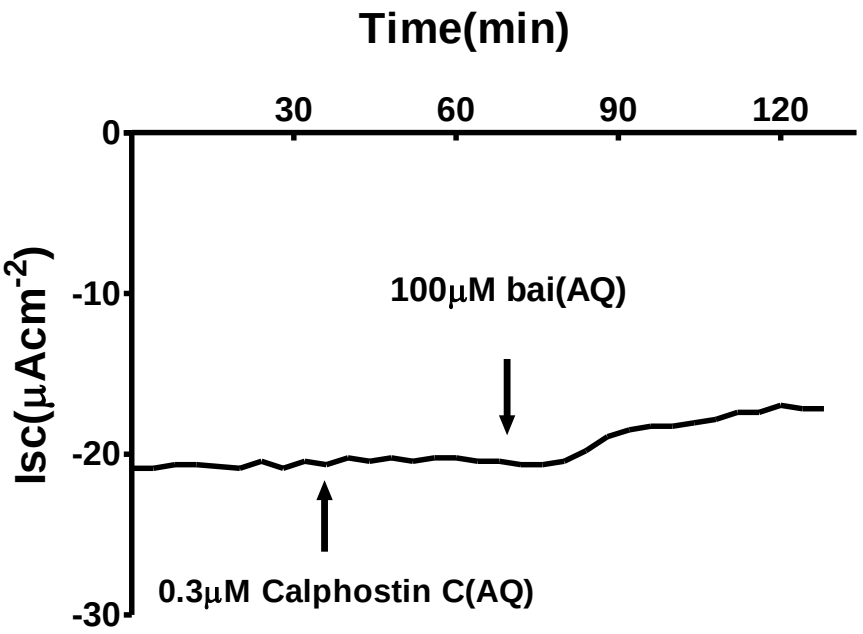

Fig.3.22. The time course of the Isc response of isolated porcine CBE after sequential addition of calphostin C (0.3 μM, AQ) and baicalein (100 μM, AQ). The time of drug addition was indicated by the arrow. AQ: aqueous side.

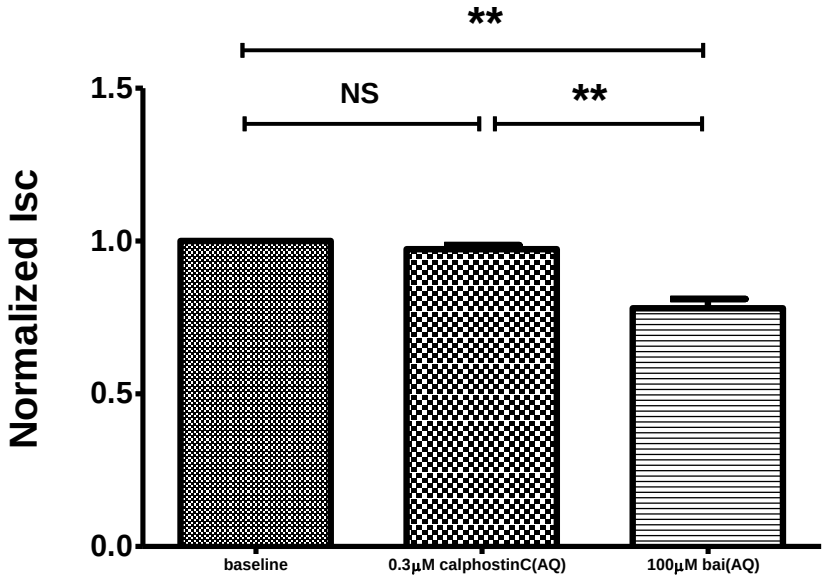

Fig.3.23. Effect of sequential addition of calphostin C (0.3 μM, AQ) and baicalein (100 μM, AQ) on Isc across porcine CBE. Results were normalized to baseline value and given as MEAN±SEM, n=6. AQ: aqueous side. NS $p>0.05$; ** $P<0.01$ (Repeated measures ANOVA, followed by Tukey multiple comparison test).

	Baseline	0.3 μM calphostinC (AQ)	100 μM bai (AQ)
PD(mV)	-0.76 ±0.06	-0.73 ±0.06	-0.58 ±0.04
Isc(μAcm^{-2})	-13.02 ±1.52	-12.66 ±1.45	-10.18 ±1.34
R(Ωcm^2)	66 ±8	66 ±8	66 ±8

Table.3.14. Effect of sequential addition of calphostin C (0.3 μM, AQ) and baicalein (100 μM, AQ) on the transepithelial electrical parameters across porcine CBE. Results are given as MEAN±SEM, n=6. AQ: aqueous side.

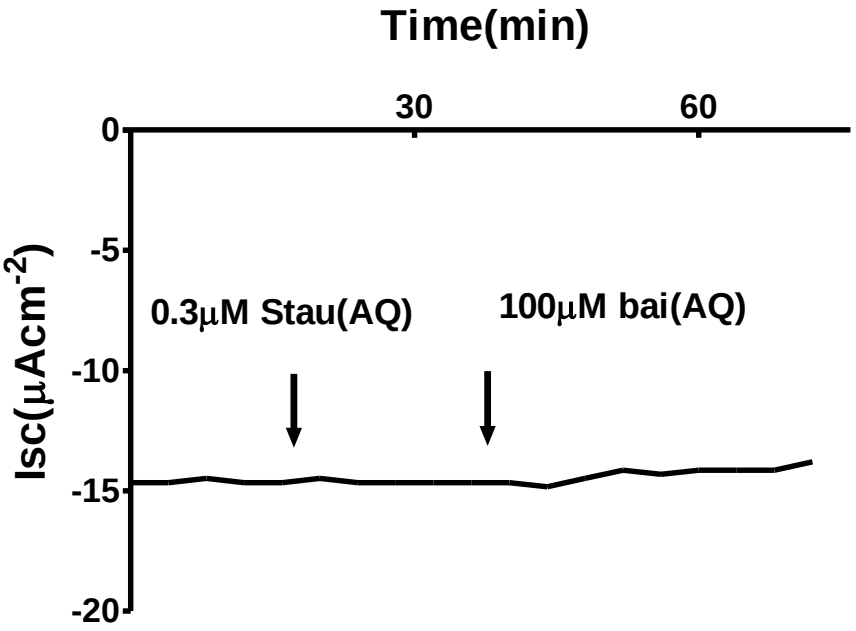

Fig.3.24. The time course of the Isc response of isolated porcine CBE after sequential addition of staurosporine (0.3 μM, AQ) and baicalein (100 μM, AQ). The time of drug addition was indicated by the arrow. AQ: aqueous side.

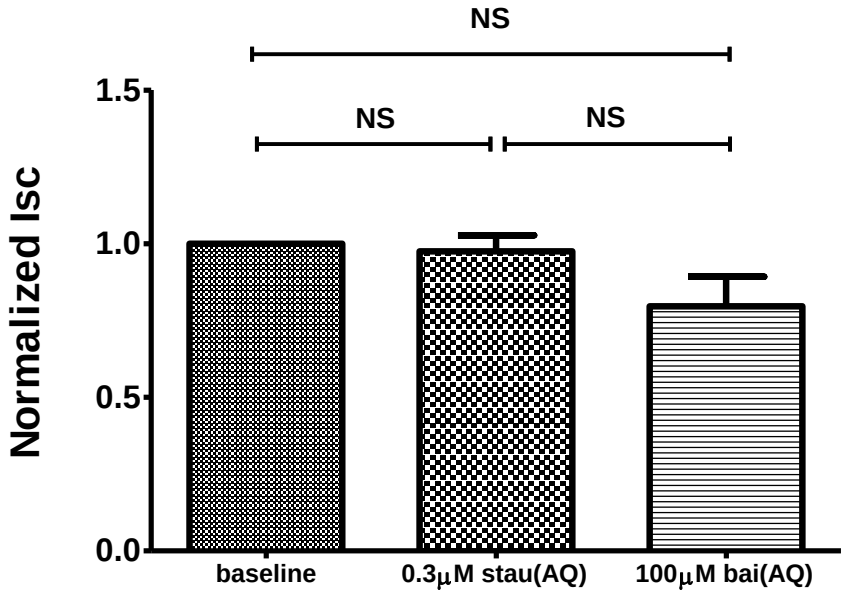

Fig.3.25. Effect of sequential addition of staurosporine (0.3 μM, AQ) and baicalein (100 μM, AQ) on Isc across porcine CBE. Results were normalized to baseline value and given as MEAN±SEM, n=6. AQ: aqueous side. NS $p>0.05$ (Repeated measures ANOVA).

	Baseline	0.3 µM staurosporine (AQ)	100 µM bai (AQ)
PD(mV)	-0.84 ±0.14	-0.82 ±0.16	-0.68 ±0.20
Isc(μAcm^{-2})	-12.57 ±1.12	-12.30 ±1.40	-10.02 ±1.55
R(Ωcm^2)	69 ±13	67 ±13	65 ±10

Table.3.15. Effect of sequential addition of staurosporine (0.3 µM, AQ) and baicalein (100 µM, AQ) on the transepithelial electrical parameters across porcine CBE. Results are given as MEAN ±SEM, n=6. AQ: aqueous side.

3.2 Effect of baicalein on FF across porcine CBE

Chloride release from NPE cells to AH is generally considered as the rate-limiting step in AHF (Civan et al., 1997). NFA-sensitive chloride channels have been proposed to play a vital role in Cl^- efflux (Kong et al., 2006) and AHF (Law et al., 2009) of porcine CBE. Baicalein inhibited Isc across porcine CE probably by acting as an inhibitor of chloride channels sensitive to both NFA and DPC. As a result, significant inhibitory effect on FF was expected with baicalein. Therefore, the effect of baicalein on FF rate across porcine CBE was investigated.

In the present study, the baseline FF rate was 2.75 ± 0.17 μL/h per preparation, which was similar to that of previous study (Law et al., 2009). Application of baicalein (100 μM) on the aqueous side markedly reduced the FF rate by $31 \pm 5\%$ ($n=6$, $P<0.01$). At the same time, PD was also significantly depolarized after the addition of baicalein ($P<0.01$). The effect of baicalein on FF rate was summarized in Table.3.16, and time course of the responses on FF and PD are shown in the Fig.3.26.

Experiment	FF Rate		Change (%)
	Baseline	Drug-treated	
1	2.83	2.50	-11.8
2	3.33	2.38	-28.8
3	3.17	2.44	-23.0
4	2.50	1.63	-35.0
5	2.17	1.38	-36.5
6	2.50	1.19	-52.5
Mean	2.75	1.93**	-31.3
SEM	0.17	0.20	5.2

Table.3.16. Effect of 100 μM baicalein (AQ) on FF across porcine CBE (n = 6). AQ: aqueous side.

**P<0.01, compared with baseline value (Paired student's *t* test).

A

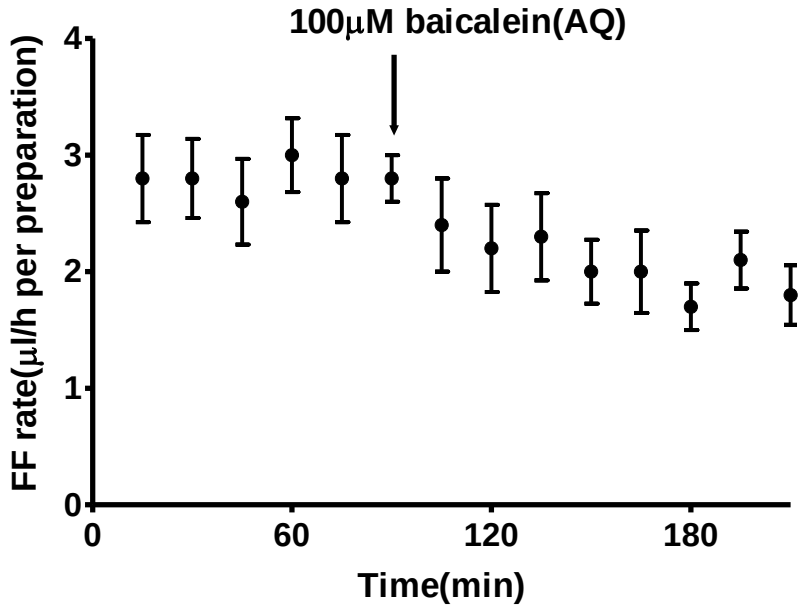

B

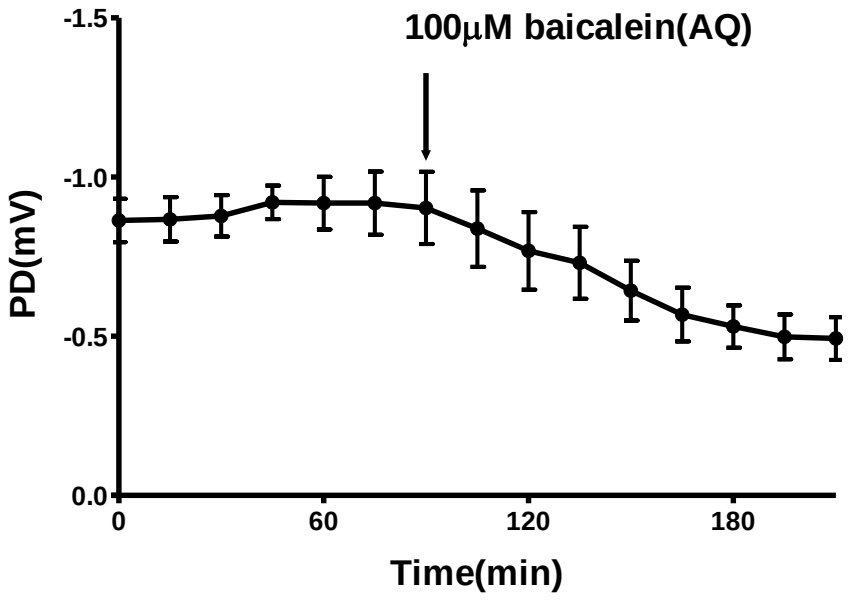

Fig.3.26. Effect of 100 μM baicalein (AQ) on FF and PD across porcine CBE (n=6). AQ: aqueous side. Data points are expressed as MEAN ± SEM. *Arrows:* the point at which baicalein was added to the aqueous-side bath. (A) The calculated FF rate (from blood to aqueous); (B) PD recorded simultaneously with the measurement of FF. The polarity of the PD was consistently negative on the aqueous side relative to the blood side.

To better understand the cellular mechanism by which baicalein inhibited both the Isc and FF across porcine CBE, an electrophysiology study of ionic changes and intracellular potential was carried out.

3.3 Effect of baicalein on $[Cl^-]_i$ of native porcine NPE cells

After loading with MQAE, an intracellular chloride dye, only signals from NPE cells were obtained, while those from PE cells were obstructed by its pigments. The effect of baicalein on $[Cl^-]_i$ of porcine NPE cells was investigated. However, baicalein appeared to interfere with MQAE as they share similar spectra and it acted to quench the fluorescence from MQAE. As illustrated in Fig.3.27, baicalein (100 μM) markedly decreased the fluorescence in NRR, or in Cl^- free and K^+ rich calibration solution, indicating that baicalein interfered with the fluorescence from MQAE.

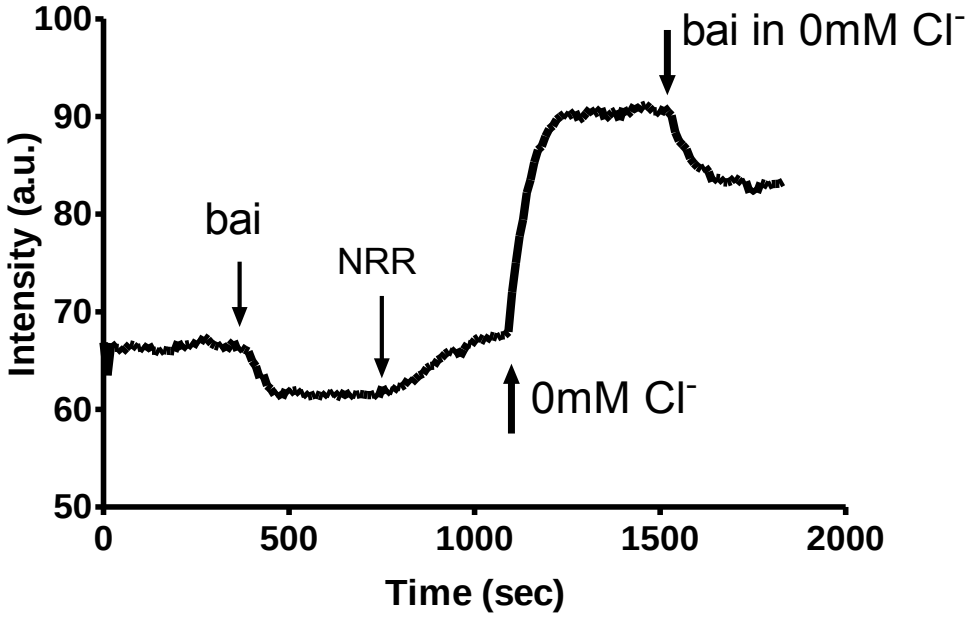

Fig.3.27. A representative trace of baicalein (bai)'s effect on MQAE fluorescence of native porcine NPE cells. NRR: normal Ringer solution; 0mM Cl^-: Cl^- free and K^+ rich solution.

3.4 Effect of baicalein on membrane potential of porcine ciliary epithelial cells

3.4.1. Intracellular electrical properties and transport mechanism of porcine ciliary epithelial cells

The study of membrane potential is an electrophysiological approach that can help reveal cellular transport characteristics of CBE. The membrane potentials of cultured rabbit NPE cells (Green et al., 1985) and human NPE cells (Helbig et al., 1989) have been reported. In this study, the intracellular electrical properties of native porcine NPE and PE cells were characterized.

The membrane potential of single NPE and PE cells were -69 ± 0.87 mV (n=184) and -63 ± 2.08 mV (n=105) respectively, and there was no significant difference between NPE and PE cells. Both NPE and PE cells showed similar electrical responses towards ion substitution, transporter and channel inhibitors; and the magnitudes of effects showed no significant differences between them.

Reducing extracellular Na^+ concentration to 2 mM induced a transient hyperpolarization, followed by a slow depolarization towards but below baseline value.

Replacement of extracellular Cl^- by gluconate caused fast and significant depolarization, followed by hyperpolarization of variable speed.

To test the role of K^+ channel in maintaining membrane potential, a K^+ channel blocker ($BaCl_2$) was used. Addition of $BaCl_2$ (2 mM) into the bath immediately depolarized membrane potential significantly.

Ouabain, a Na^+/K^+-ATPase inhibitor, also induced depolarization of intracellular potential but in a much slower manner.

All three chloride channel blockers, DPC, IAA94 ([(6, 7-dichloro-2-cyclopentyl-2,3-dihydro-2-methyl-1-oxo-1H-inden-5yl)-oxy] acetic acid) and NFA hyperpolarized intracellular potential markedly but to different extent, with NFA showing the maximum hyperpolarization.

The effects of ion substitutions, transporter and channel inhibitors on membrane potential of porcine ciliary epithelial cells were illustrated in the Fig.3.28-3.34 and the data are summarized inTable.3.17.

A

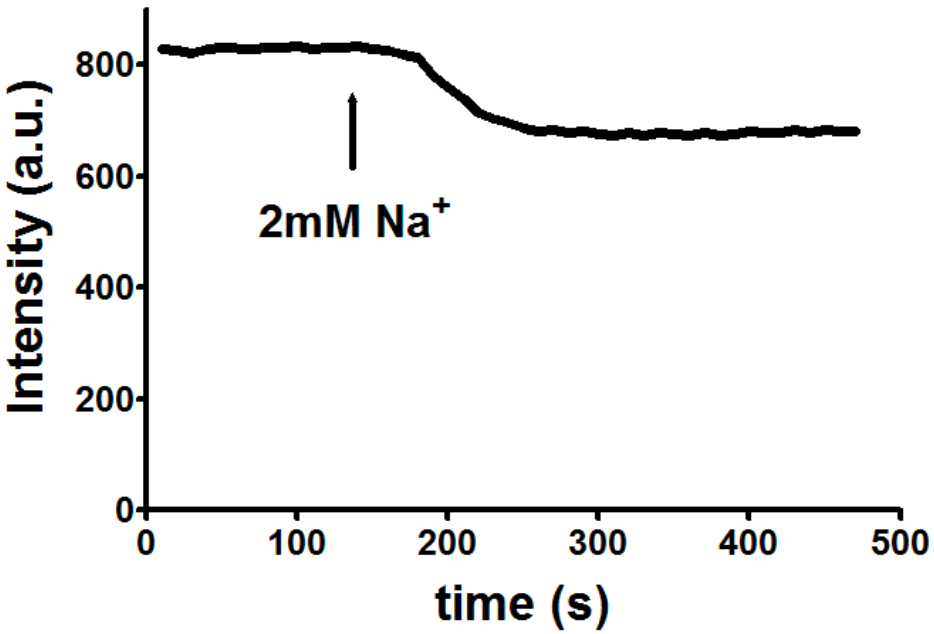

B

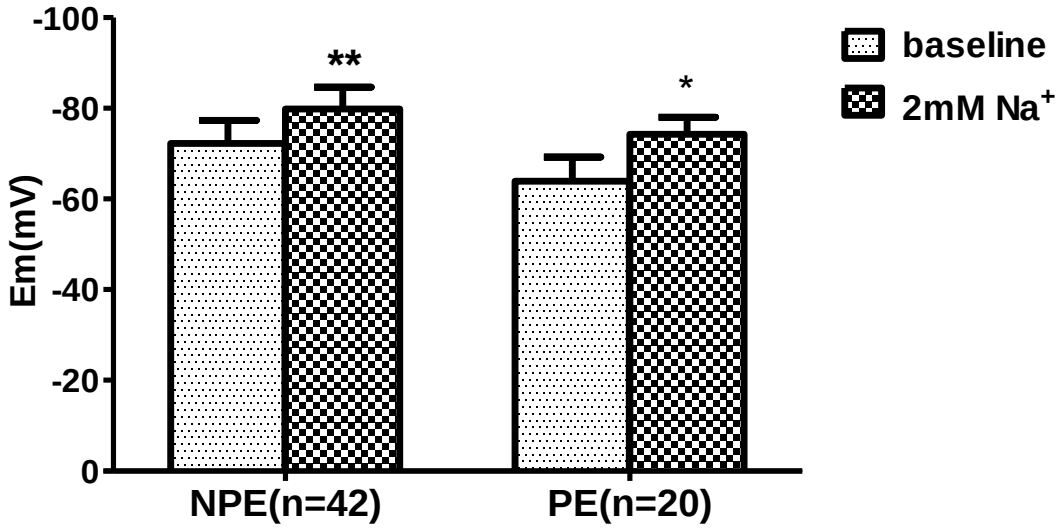

Fig3.28. Effect of 2 mM Na^+ on membrane potential of native porcine NPE and PE cells. (A) The representative trace, the time of ion substitution was indicated by the arrow; (B) The average change. Results were given as MEAN±SEM. **P<0.01, *P<0.05, compared with baseline value (Paired student's *t* test)

A

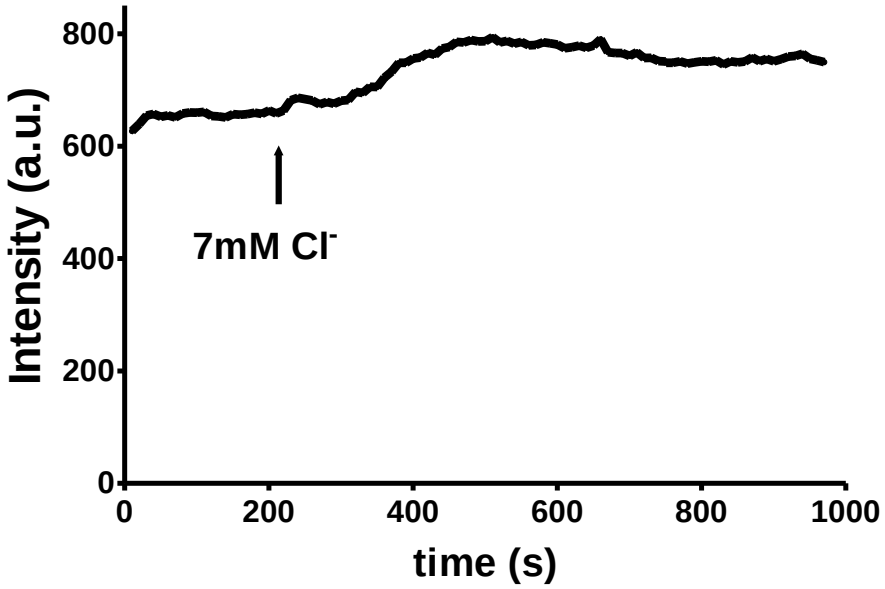

B

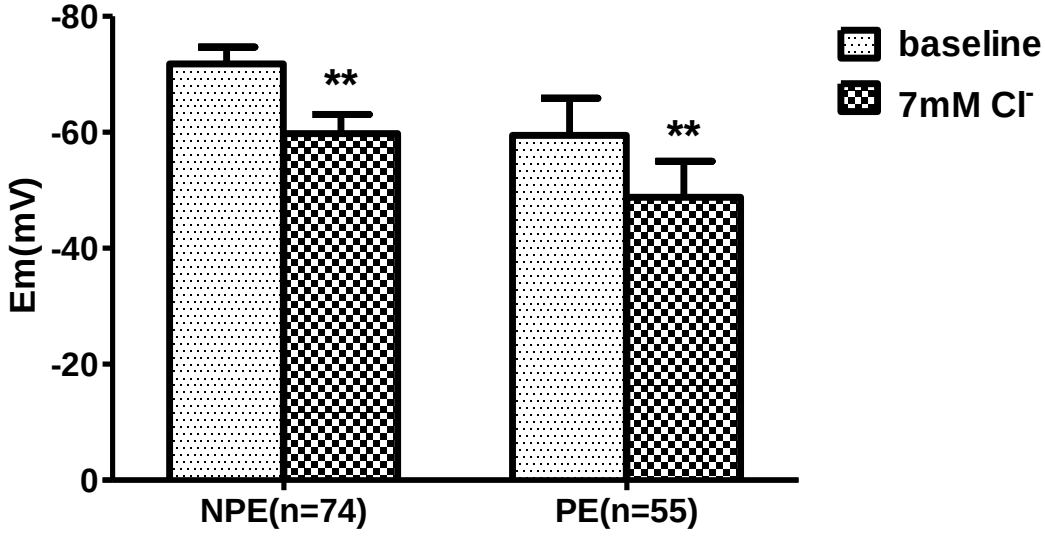

Fig3.29. Effect of 7 mM Cl^- on membrane potential of native porcine NPE and PE cells. (A) The representative trace, the time of ion substitution was indicated by the arrow; (B) The average change. Results were given as MEAN±SEM. **P<0.01, compared with baseline value (Paired student's *t* test)

A

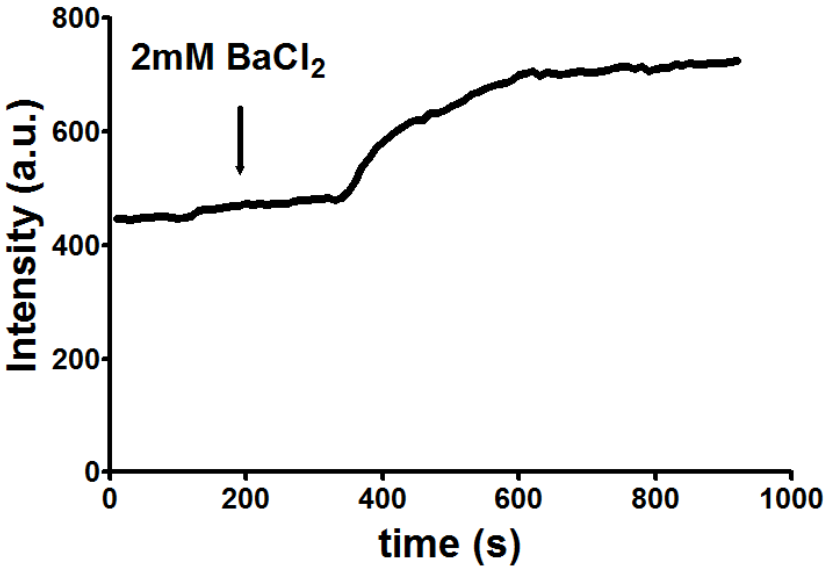

B

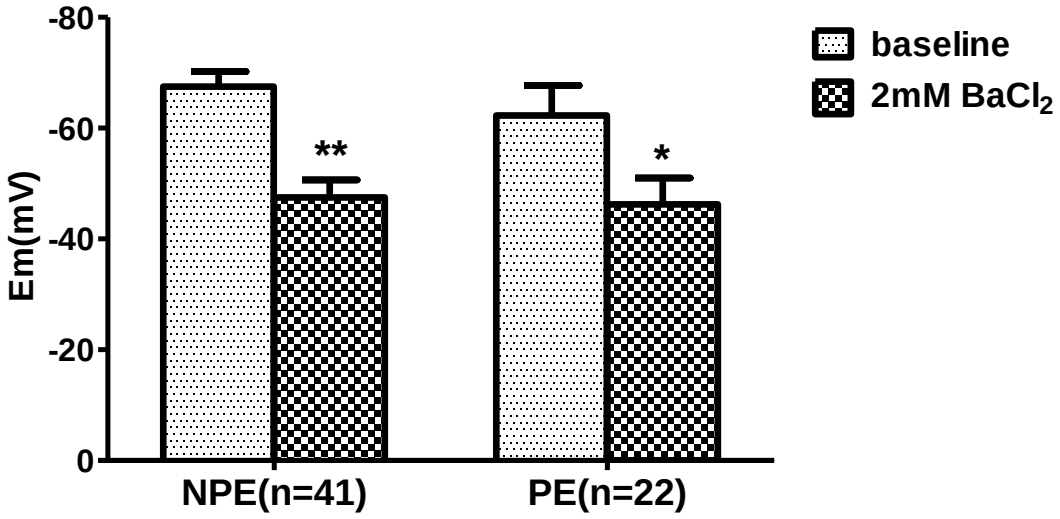

Fig3.30. Effect of 2 mM $BaCl_2$ on membrane potential of native porcine NPE and PE cells. (A) The representative trace, the time of drug addition was indicated by the arrow; (B) The average change. Results were given as MEAN±SEM. **P<0.01, *P<0.05, compared with baseline value (Paired student's *t* test).

A

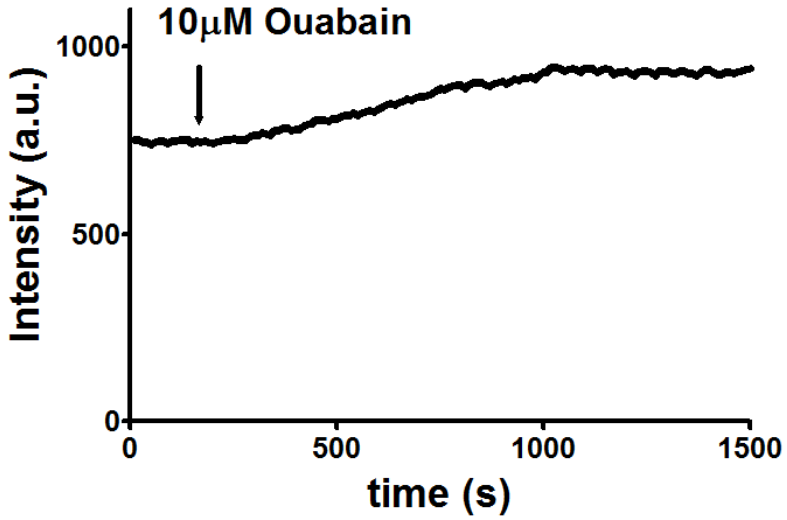

B

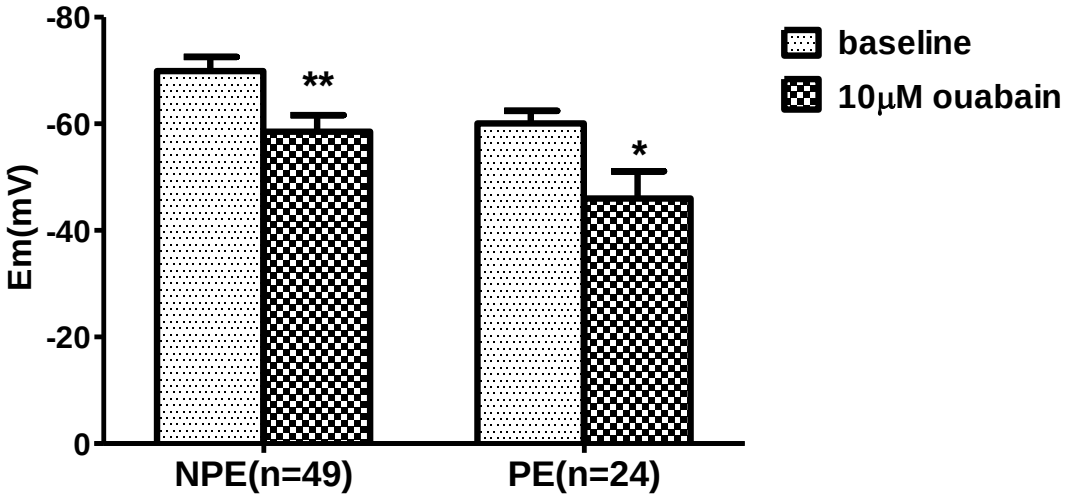

Fig3.31. Effect of 10 μM ouabain on membrane potential of native porcine NPE and PE cells. (A) The representative trace, the time of drug addition was indicated by the arrow; (B) The average change. Results were given as MEAN±SEM. **P<0.01, *P<0.05, compared with baseline value (Paired student's *t* test).

A

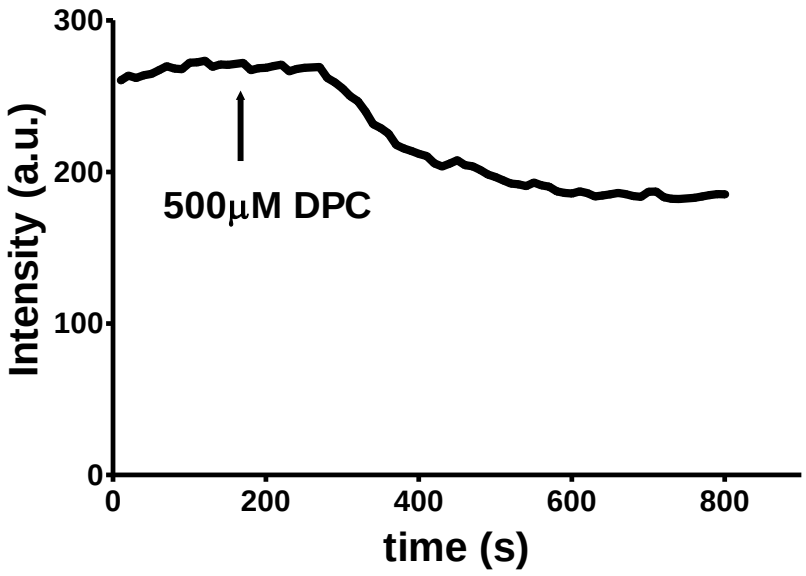

B

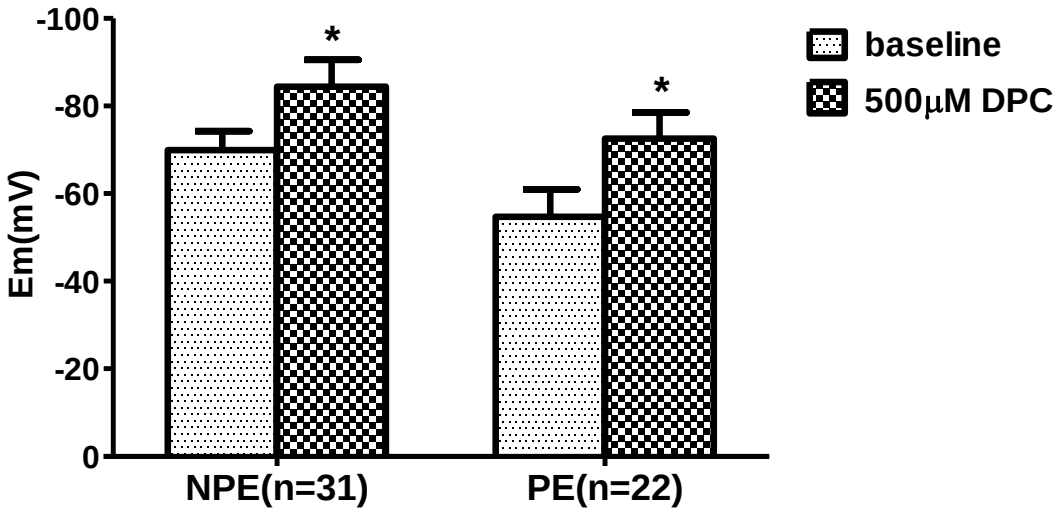

Fig3.32. Effect of 500 μM DPC on membrane potential of native porcine NPE and PE cells. (A) The representative trace, the time of drug addition was indicated by the arrow; (B) The average change. Results were given as MEAN±SEM. *P<0.05, compared with baseline value (Paired student's *t* test).

A

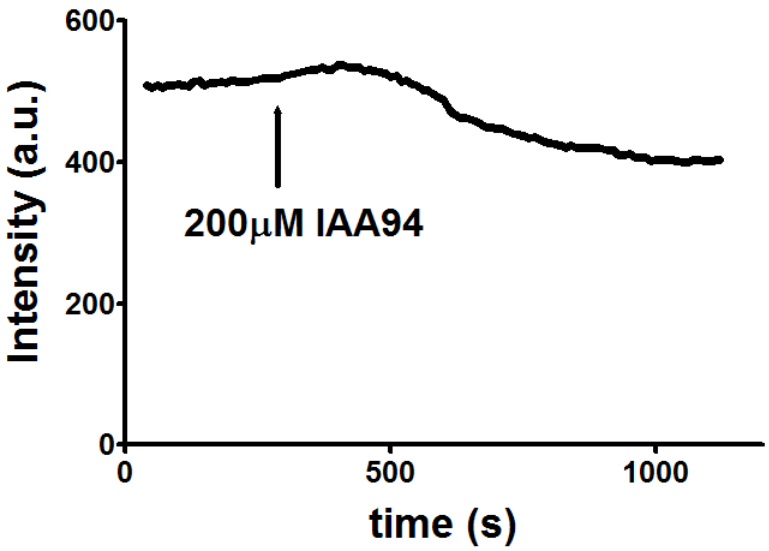

B

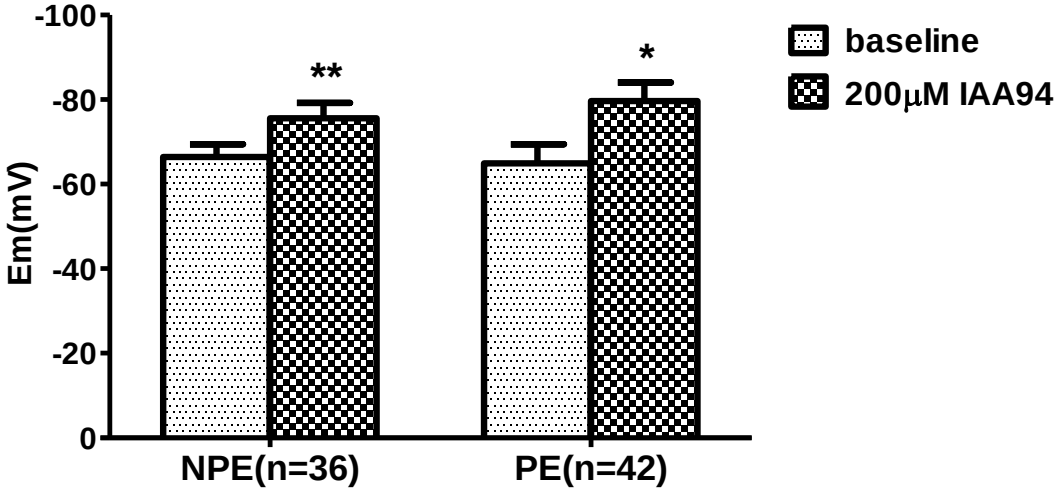

Fig3.33. Effect of 200 μM IAA94 on membrane potential of native porcine NPE and PE cells. (A) The representative trace, the time of drug addition was indicated by the arrow; (B) The average change. Results were given as MEAN±SEM. **P<0.01, *P<0.05, compared with baseline value (Paired student's *t* test).

A

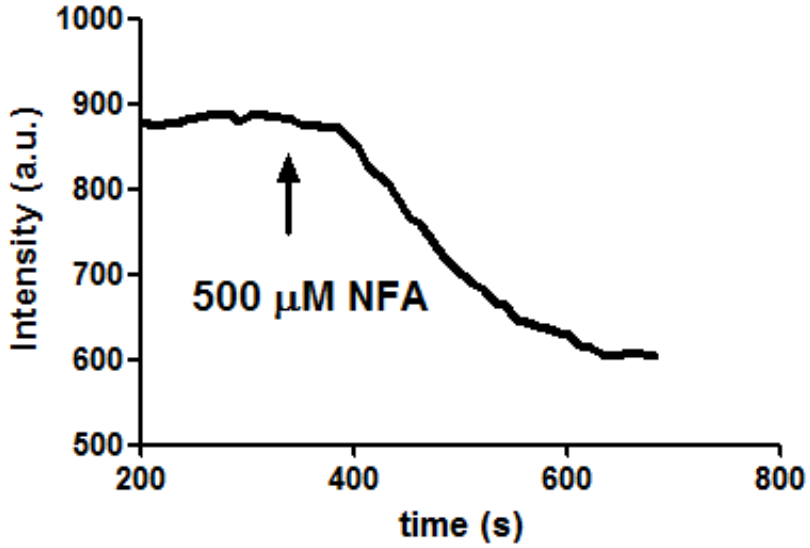

B

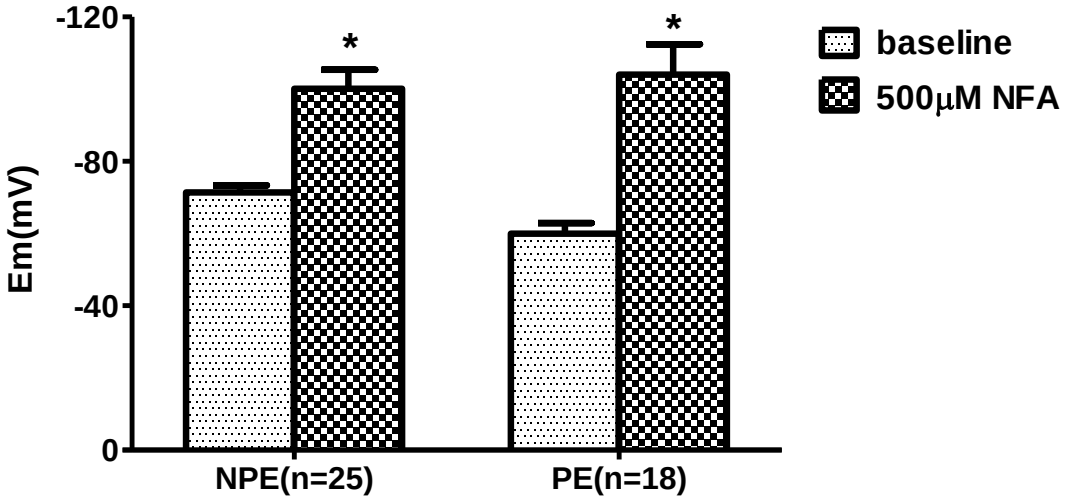

Fig.3.34. Effect of 500 μM NFA on membrane potential of native porcine NPE and PE cells. (A) The representative trace, the time of drug addition was indicated by the arrow; (B) The average change. Results were given as MEAN±SEM. *P<0.05, compared with baseline value (Paired student's *t* test).

Treatment	ΔEm(mV)	
	NPE	PE
2mM Na^+	-07.56 ±0.62	-10.31 ±1.83
$BaCl_2$	+20.00 ±2.48	+16.00 ±4.17
Ouabain	+11.37 ±1.09	+09.70 ±1.80
7mM Cl^-	+14.00 ±0.78	+11.00 ±1.83
DPC	-14.15 ±1.79	-17.24 ±2.39
IAA94	-09.17 ±1.10	-14.00 ±2.80
NFA	-27.00 ±5.39	-34.00 ±3.95

Table3.17 Effects of 2 mM Na^+, $BaCl_2$ (2 mM), 7 mM Cl^-, Ouabain (10 μM), DPC (500 μM), IAA94 (200 μM) and NFA (500 μM) on membrane potential of native porcine NPE and PE cells.

3.4.2. Effects of NFA and baicalein on low Cl^- induced depolarization in native porcine NPE and PE cells

Since baicalein interfered with DiBAC4(3) in the solution without cells, the absolute value of baicalein's effect on plasma membrane potential cannot be quantified directly. In order to decipher its interference, attempts were made to calculate the relative change in potential difference before and after baicalein so as to determine the contribution due to baicalein alone.

After incubation with NFA (500 μM) for 30 minutes, the magnitude of depolarization in NPE and PE caused by low Cl^- replacement was dramatically reduced to 3.17 ± 1.18 mV (n=62) and 2.81 ± 1.00 mV (n=39) respectively. Similarly, pretreatment of baicalein (100 μM) for an hour also significantly inhibited the depolarization to 5.65 ± 0.60 mV in NPE cells (n=121, $P<0.01$), while the inhibition of the depolarization of PE cells was not significant (n=92, $P>0.05$). Both 0.05% and 0.1% DMSO could not induce any significant change over the depolarization caused by 7 mM Cl^- in both NPE and PE cells ($P>0.05$). The effects of DMSO, NFA and baicalein on 7 mM Cl^- induced depolarization in native porcine NPE and PE cells were shown in Fig.3.35 and Fig.3.36 respectively.

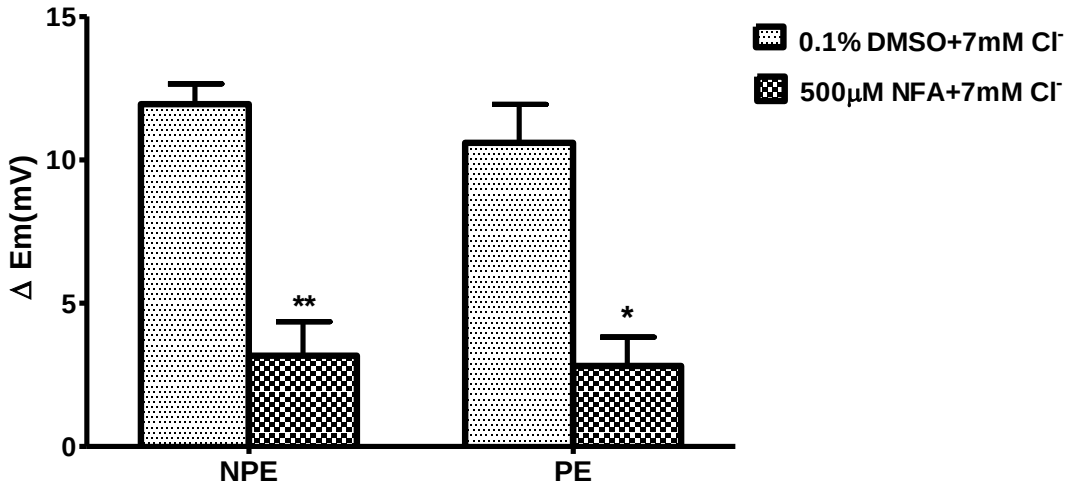

Fig3.35 Effects of pretreatment of 0.1% DMSO (n=54 for NPE, 39 for PE) and 500 μM NFA (n=62 for NPE, 39 for PE) on 7 mM Cl^- induced depolarization of native porcine NPE and PE cells. **P<0.01, *P<0.05, compared with DMSO pretreatment group (Paired student's *t* test).

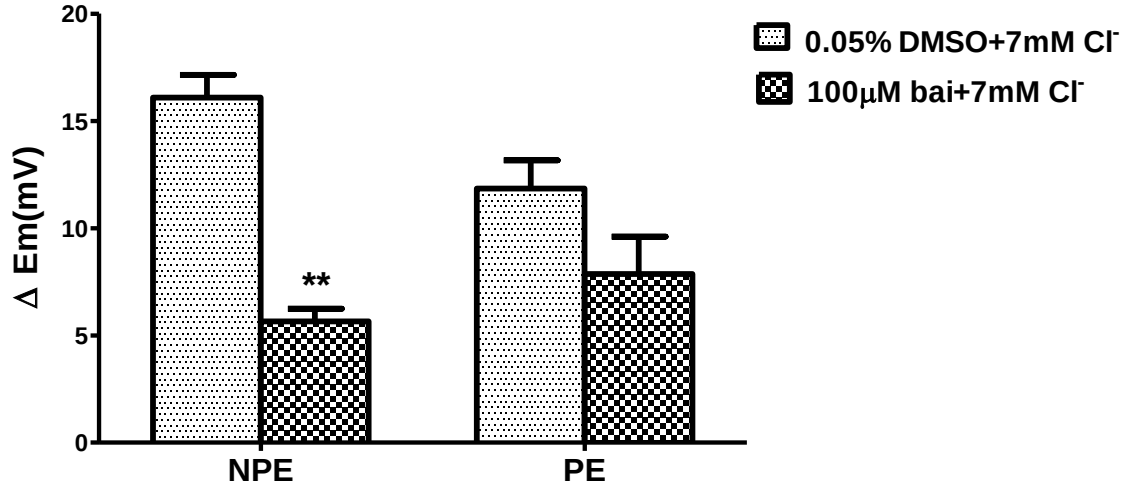

Fig3.36. Effects of pretreatment of 0.05% DMSO (n=121 for NPE, 95 for PE) and 100 μM baicalein (n=121 for NPE, 92 for PE) on 7 mM Cl^- induced depolarization of native porcine NPE and PE cells. **P<0.01, compared with DMSO pretreatment group (Paired student's *t* test).

3.5 Electrophysiological study of baicalein on native porcine NPE cells

3.5.1. Stimulation of swelling-activated whole cell current of native porcine NPE cells

The baseline current of native porcine NPE cell was small in isotonic bathing solution. After challenged with hypotonic solution, a gradual swelling-activated current was observed, which started at 5 minutes and reached a new steady state in around 15 minutes. This current has the characteristics of being outward rectifying, inactivation at large depolarizing potentials and a reversal potential close to -30 mV. These results indicated that the swelling–activated current should primarily be a Cl^- current, which was consistent with the fact that this current could be suppressed by Cl^- channel inhibitors (NFA and NPPB).

After 15 minutes of hypotonic challenge, application of 500 μM NFA to the extracellular bath produced a marked reduction of swelling-activated current in native porcine NPE cells; the outward and inward currents were reduced by 74 ± 3% (from 65.5 ± 15 to 13.3 ± 2 pA/pF) and 67 ± 9% (from -18.9 ± 6 to -7.0 ± 3 pA/pF) respectively (n = 4, P<0.01). Similarly, NPPB (100 μM) inhibited both outward and inward currents by 67 ± 2% (from 76.0 ± 19 to 26.0 ± 7 pA/pF) and

61 ± 2% (from -35.0 ± 9 to -10.1 ± 5 pA/pF) respectively (*n*=4, P<0.01). The effects of NFA and NPPB on swelling-activated whole cell current and the current-voltage relationship are illustrated in Fig.3.37-3.40.

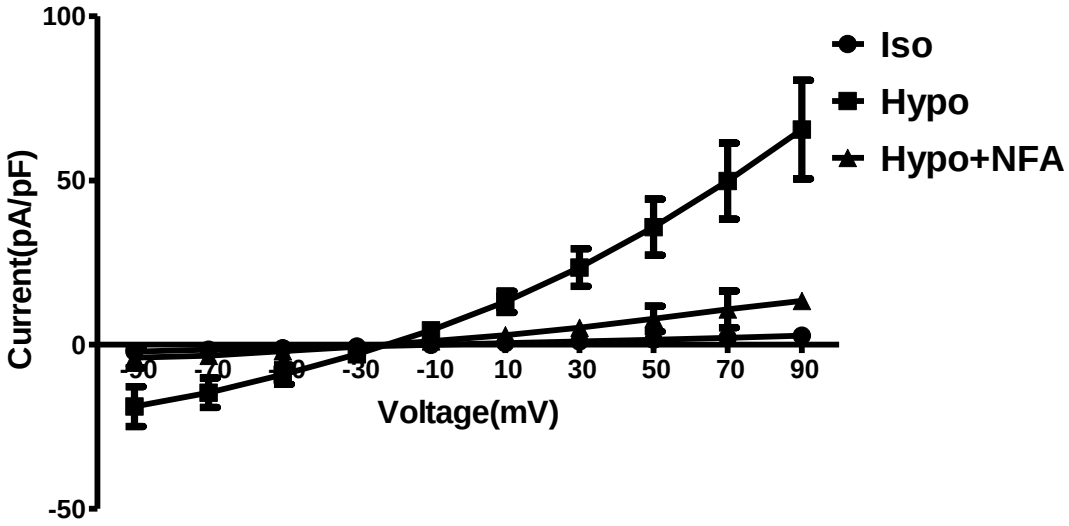

Fig.3.37. Current-voltage relationship demonstrating the activation caused by hypotonic swelling and the inhibition induced by NFA. Iso: isotonic solution; Hypo: hypotonic solution.

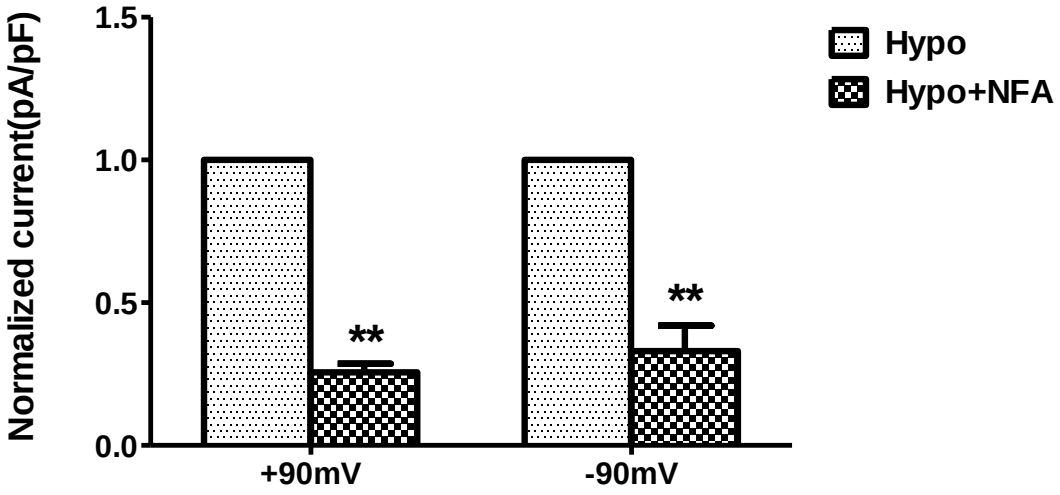

Fig.3.38. Effect of 500 μM NFA on swelling-activated current of porcine NPE cells. Mean whole cell currents were measured at ±90 mV, and normalized to the current after hypotonic swelling for 15 minutes. The results are expressed as MEAN±SEM, n=4. ***P* <0.01, compared with the current after hypotonic swelling for 15 minutes (Paired student's *t* test).

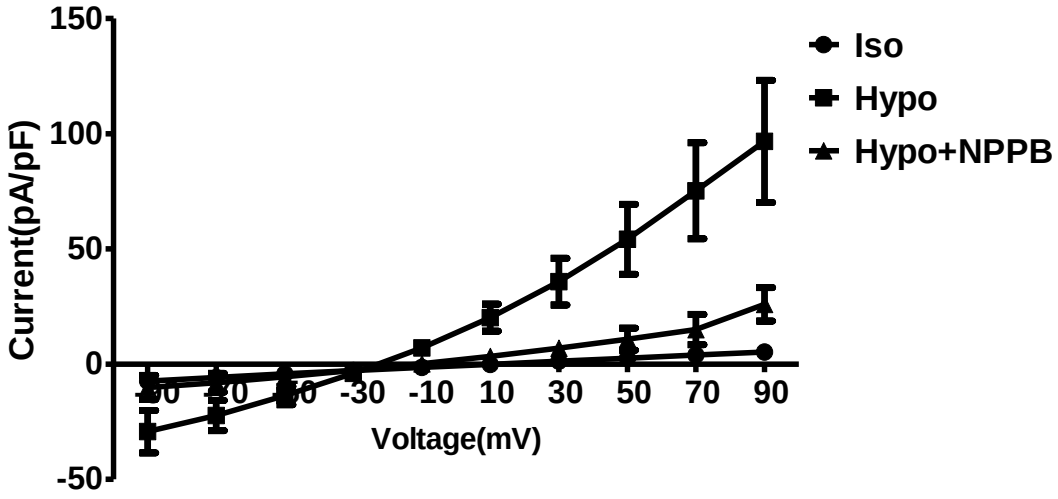

Fig.3.39. Current-voltage relationship demonstrating the activation caused by hypotonic swelling and the inhibition induced by NPPB. Iso: isotonic solution; Hypo: hypotonic solution.

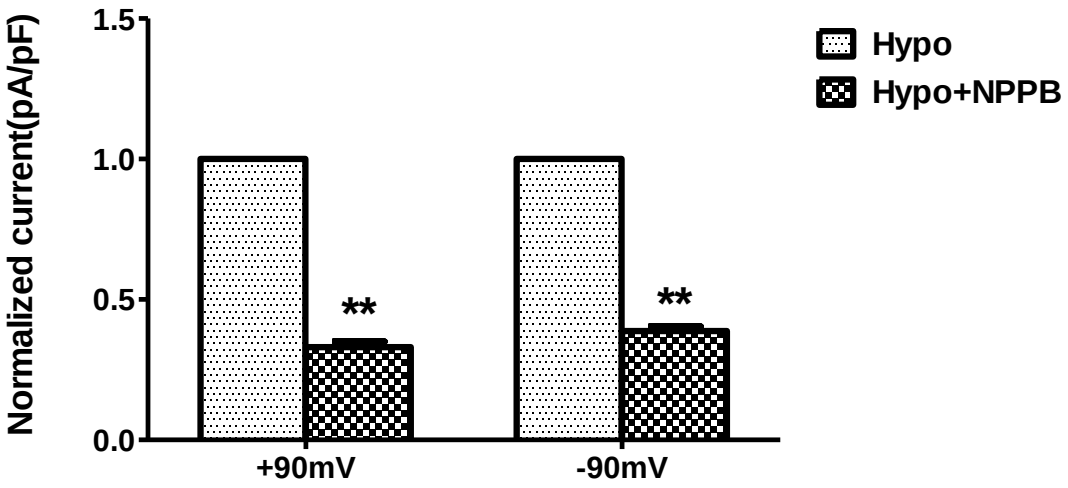

Fig.3.40. Effects of 100 μM NPPB on swelling-activated current of porcine NPE cells. Mean whole cell currents were measured at ±90 mV, and normalized to the current after hypotonic swelling for 15 minutes. The results are expressed as MEAN±SEM, n=4. ***P* <0.01, compared with the current after hypotonic swelling for 15 minutes (Paired student's *t* test).

3.5.2. Effect of baicalein on swelling-activated Cl^- current of native porcine NPE cells

Although the Cl^- channels at NPE cells are of vital importance in AHF, its molecular identity is still not clear. Consistent with previous studies in different species, hypotonic swelling was also found to activate Cl^- current of native porcine NPE cells. Our preliminary results suggested baicalein may have evoked the Isc response through inhibiting some Cl^- channels at NPE cells. To find out if this is the case, swelling-activated Cl^- current was used as the probe for the chloride channels at NPE cells, and the effect of baicalein on swelling-activated Cl^- current of native porcine NPE cells was investigated.

After 15 minutes of hypotonic treatment, application of baicalein (50-200 μM) to the extracellular bath produced fast and significant inhibition of the swelling-activated current. The outward current were inhibited by 53 ± 15% (50 μM, n=6, $P<0.01$), 58 ± 7% (100 μM, n=12, $P<0.01$) and 87 ± 4% (200 μM, n=6, $P<0.01$) respectively, and the inward current were inhibited by 49 ± 14% (50 μM, n=6, $P<0.01$), 55 ± 7% (100 μM, n=12, $P<0.01$) and 85 ± 5% (200 μM, n=6, $P<0.01$) respectively. The current-voltage relationship of swelling-activated current and baicalein's effect are illustrated in Fig.3.41-3.42.

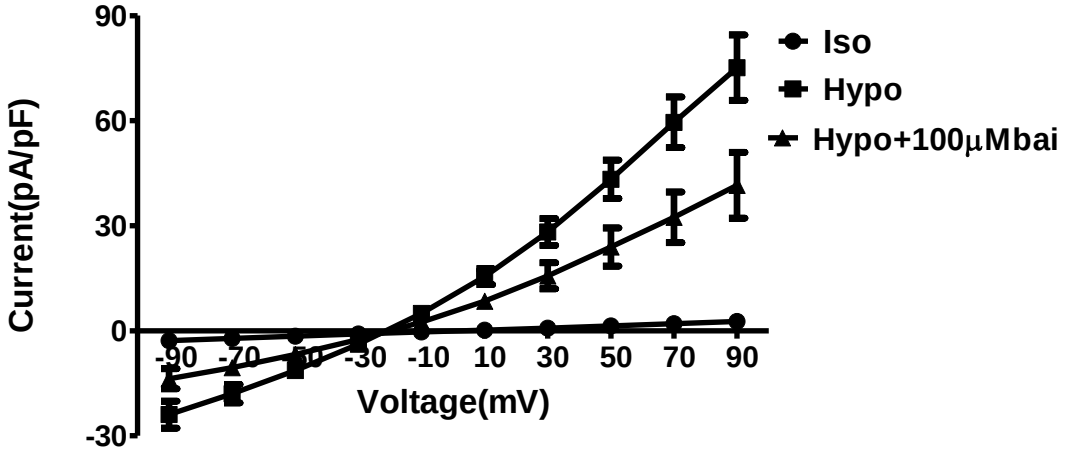

Fig.3.41. Current-voltage relationship demonstrating the activation caused by hypotonic swelling and the inhibition induced by baicalein. Iso, isotonic solution; Hypo, hypotonic solution; bai: baicalein.

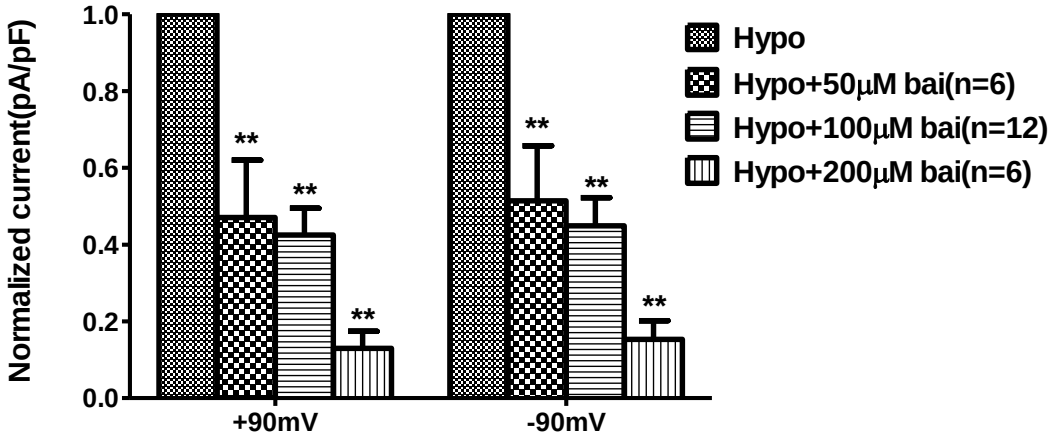

Fig3.42. Dose-dependent effect of baicalein (bai) on swelling-activated current of porcine NPE cells. Mean whole cell currents were measured at ±90 mV, and normalized to the current after hypotonic swelling for 15 minutes. The results are expressed as MEAN±SEM. ***P* <0.01, compared with hypotonic stimulated current (pA/pF) (One-way ANOVA, followed by Tukey multiple comparison test).

To investigate the role of PKC in the baicalein induced inhibition of swelling-activated current, a PKC inhibitor (staurosporine) was used. In the presence of 1 μM staurosporine, hypotonic challenge for 15 minutes significantly stimulated the baseline outward current and inward current to 68.3 ± 11.0 and -25.9 ± 7.9 pA/pF respectively and there was no significant difference between the values of swelling-activated current in the absence and presence of staurosporine. Addition of baicalein (100 μM, n=5) afterwards still inhibited the activated-current by 52% ± 13% for outward current (from 68.3 ± 11 to 34.82 ± 12.8 pA/pF, $P<0.05$) and 51 ± 12% for inward current (-25.9 ± 7.9 to 13.7 ± 6.5 pA/pF, $P<0.05$). The results showed that PKC was not likely involved in baicalein's inhibitory effect over swelling-activated current. The combination effect of staurosporine and baicalein on swelling-stimulated whole cell current of porcine NPE cells is shown in Fig.3.43.

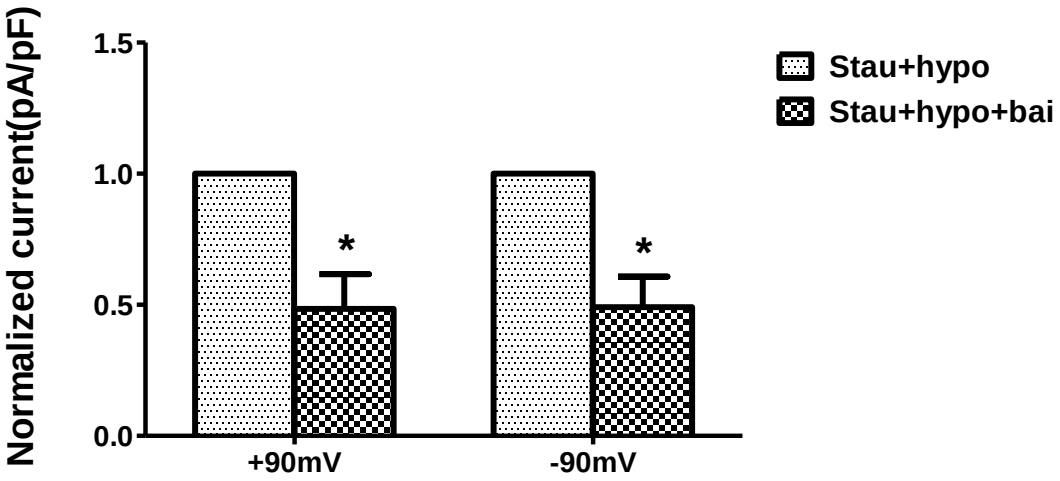

Fig3.43 In the presence of 1 μM staurosporine (stau), effect of 100 μM baicalein (bai) on swelling-activated current of porcine NPE cells. Mean whole cell currents were measured at ±90 mV, and normalized to the current after hypotonic swelling for 15 minutes in the presence of staurosporine (stau). The results are expressed as MEAN±SEM, n=5. **P* <0.05, compared with hypotonic stimulated current in the presence of staurosporine (Paired student's *t* test).

3.5.3. Effect of baicalein on basal whole cell current of native NPE cells with $[Cl^-]_i$ of 100 mM

The PKC inhibitor staurosporine showed no effect on baicalein induced inhibition of swelling-activated Cl^- current of porcine NPE cells. However, it almost abolished baicalein induced inhibition of Isc across porcine CBE (see in Chapter 3, Section 3.1.8). This discrepancy between the effects of staurosporine on baicalein induced responses suggested that other mechanism may explain the baicalein induced Isc response in porcine CBE. Moreover, given the drastic and un-physiological nature of hypotonic swelling, it is plausible to study the effect of baicalein on basal whole cell current of NPE cells under isotonic condition. However, the basal whole cell current of native porcine NPE cells was so small that some inhibition may be too weak to be noticed. Therefore, to enhance the basal current, $[Cl^-]_i$ was increased to 100 mM. With the increased $[Cl^-]_i$, the effect of baicalein on basal whole cell current of NPE cells was examined.

When cytoplasmic Cl^- concentration was increased from 25 mM to 100 mM, the baseline outward current significantly increased to 7.83 ± 2.22 pA/pF ($p<0.05$), while the change of inward current was not significant ($P>0.05$). Application of baicalein (100 μM) significantly suppressed the baseline outward current by 51 ±

7% (from 7.8 ±2 to 3.9 ±1 pA/pF, P<0.01), and the inward current was inhibited by 51 ±17% (from -5.0 ±9 to -2.4 ±1 pA/pF, P<0.05) (n=7), as shown in Fig.3.44.

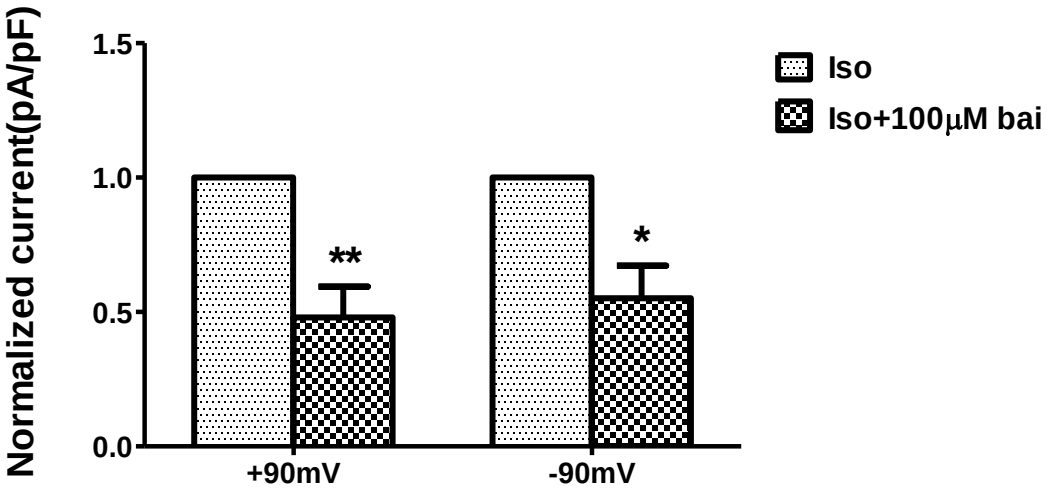

Fig3.44. Effect of 100 μM baicalein (bai) on the basal whole cell current of porcine NPE cells with $[Cl^-]_i$ of 100 mM. Mean whole cell currents were measured at ±90 mV, and normalized to baseline current. The results are expressed as MEAN±SEM, n=7. *P<0.05, ***P* <0.01, compared with baseline current (pA/pF) (Paired student's *t* test).

PKC also seemed not to be involved in the baicalein's action on the baseline current with $[Cl^-]_i$ of 100 mM. Pretreatment of PKC inhibitor staurosporine (1 μM) for 20 minutes could not block baicalein induced inhibition on baseline current. At the presence of staurosporine, baicalein still reduced the outward current and inward current by 45 ±12% (from 3.5 ±1 to 1.6 ±1 pA/pF, P<0.05) and 52 ±11% (from -3.1 ± 0.8 to -1.4 ± 0.3 pA/pF, P<0.05) (n=5) respectively. There was no

significant effect on the inhibitions induced by baicalein with staurosporine (P>0.05 at ±90 mV). The combination effect of staurosporine and baicalein is shown in Fig.3.45.

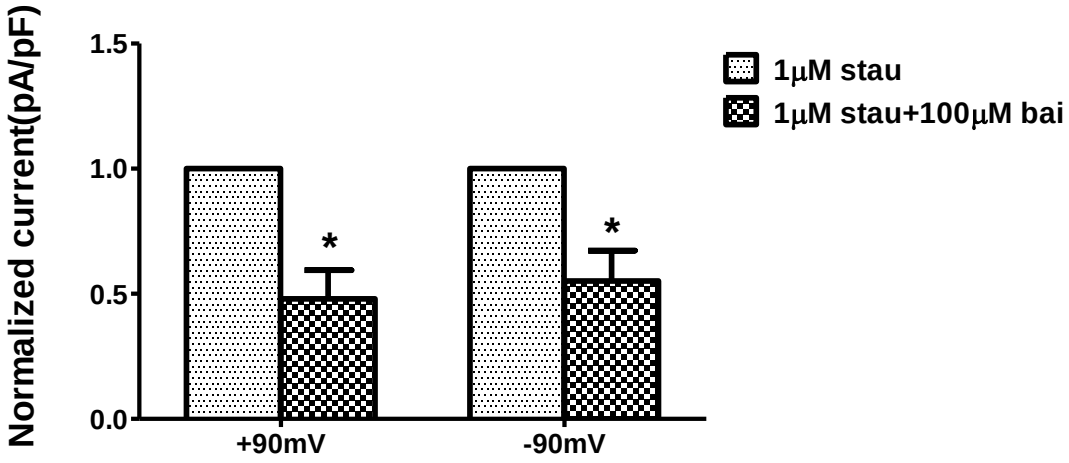

Fig.3.45. In the presence of 1 μM staurosporine (stau), effect of 100 μM baicalein (bai) on the basal whole cell current of porcine NPE cells with $[Cl^-]_i$ of 100 mM. Mean whole cell currents were measured at ±90 mV, and normalized to the steady state current after pretreatment of 1 μM staurosporine for 20 minutes. The results are expressed as MEAN±SEM, n=5. *P<0.05, compared with baseline current (pA/pF) (Paired student's *t* test).

3.5.4. Effects of NFA and baicalein on basal whole cell current of native porcine NPE cells

To characterize the contribution of Cl^- channel to the basal whole cell current, the effect of a Cl^- channel inhibitor NFA was examined. When $[Cl^-]_i$ of NPE cells was 25 mM, the baseline current was very small. NFA (500 μM) significantly reduced the baseline outward current by 40 ±11 % (from 3.2 ±0.5 to 1.8 ±0.5 pA/pF, n=6, P<0.05), while the decrease of inward current was not significant (n=6, P>0.05). The results indicated that even in isotonic solution, some NFA-sensitive chloride channels remained open and contributed to the baseline current. The effect of NFA on baseline current is shown in Fig.3.46.

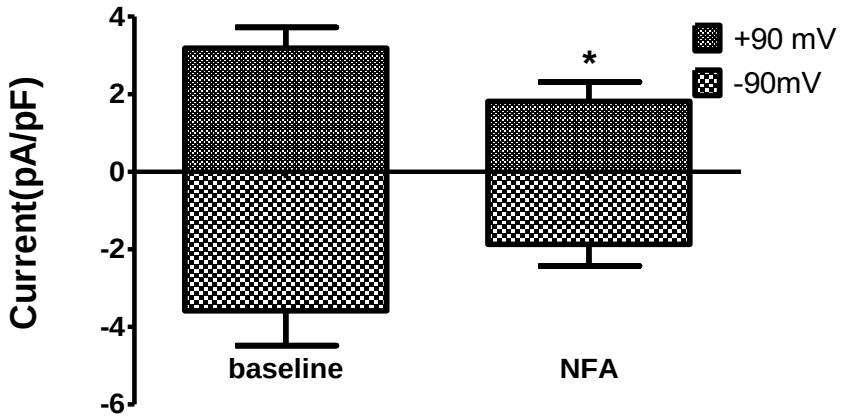

Fig3.46. Effect of 500 μM NFA on basal whole cell current of porcine NPE cells under isotonic condition. Mean whole cell currents were measured at ±90 mV. The results are expressed as MEAN±SEM, n=6. *P<0.05, compared with baseline current (pA/pF) (Paired student's *t* test).

Because of the inhibitory effects of baicalein on baseline Isc of porcine CBE, it is hypothesized that those Cl^- channels that were active in basal physiological condition were potential cellular targets of baicalein. To test this hypothesis, the effect of baicalein on basal whole cell current of native porcine NPE cells was studied.

Application of 100 μM baicalein caused significant inhibition of baseline current. Both outward and inward currents were reduced by 44 ± 17% (from 1.8 ± 0.5 to 0.7 ± 0.1 pA/pF, P<0.05) and 47 ± 9% (from -1.6 ± 0.3 to -0.8 ± 0.2 pA/pF, P<0.05) (n=8) respectively, as shown in Fig 3.47.

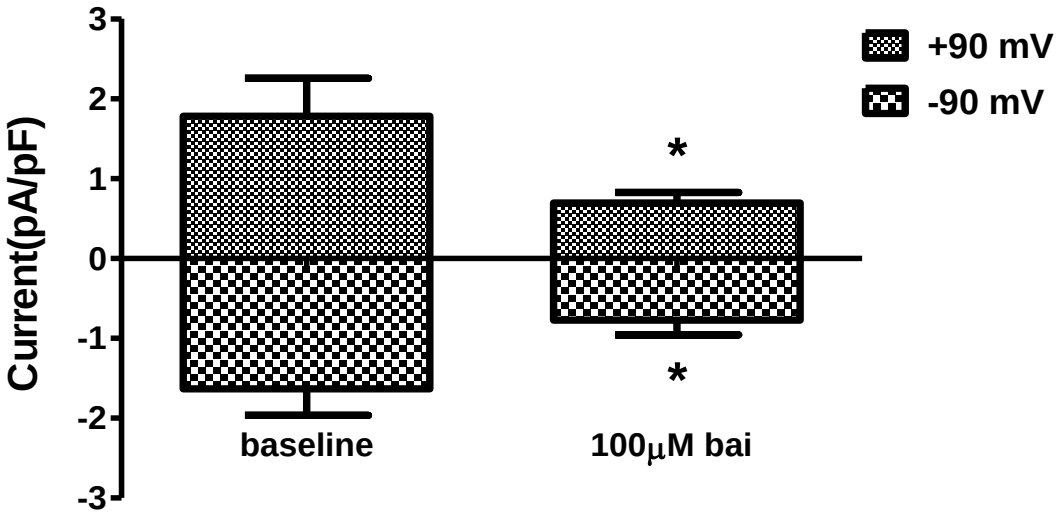

Fig.3.47. Effect of 100 μM baicalein (bai) on basal whole cell current of porcine NPE cells. Mean whole cell currents were measured at ±90 mV. The results are expressed as MEAN±SEM, n=8. *P<0.05, compared with baseline current (pA/pF) (Paired student's *t* test).

Pretreatment of PKC inhibitors staurosporine (0.3 μM, n=6) and calphostin C (0.3 μM, n=5) for 20 minutes caused no significant change in baseline current (P>0.05), but almost completely abolished baicalein evoked inhibition. The findings indicated PKC was very likely involved in the signaling cascade of baicalein's inhibition on baseline current. The effects of staurosporine and calphostin C on baicalein-induced reduction of basal whole cell current in native porcine NPE cells are illustrated in Fig 3.48 and Fig 3.49 respectively.

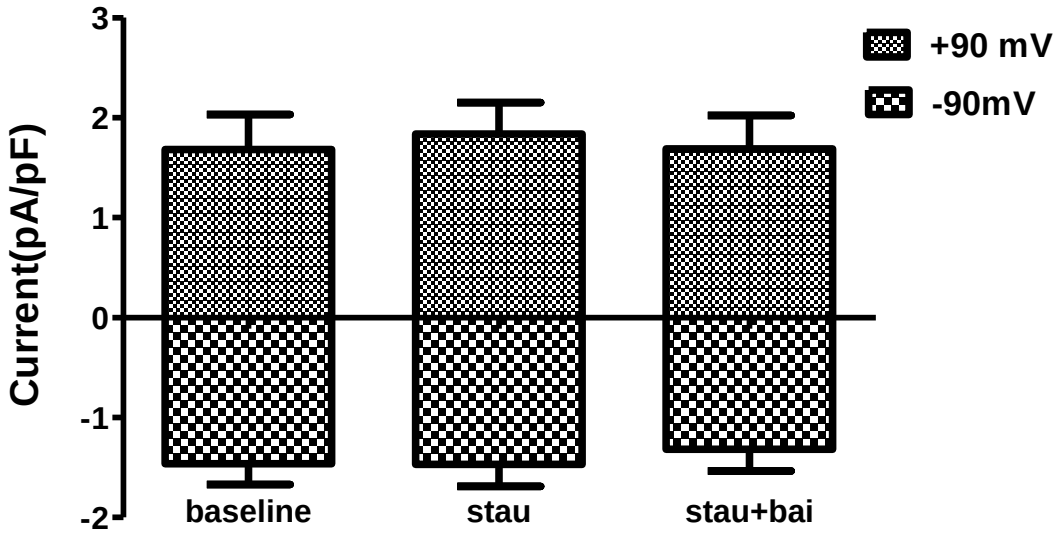

Fig3.48. In the presence of 0.3 μM staurosporine (stau), effect of 100 μM baicalein (bai) on basal whole cell current of porcine NPE cells. Mean whole cell currents were measured at ±90 mV and compared with baseline current (pA/pF) (Repeated measures ANOVA). The results are expressed as MEAN±SEM, n=6.

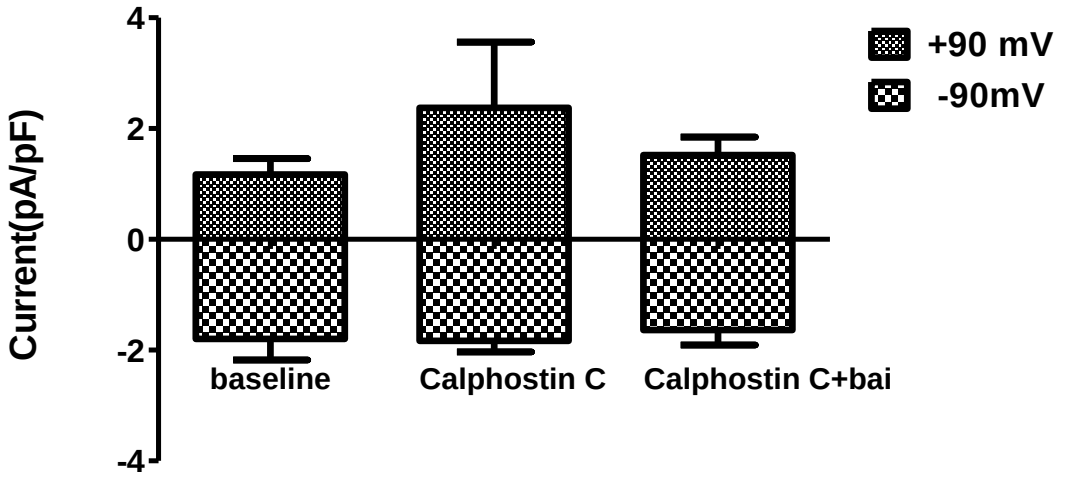

Fig3.49 In the presence of 0.3 μM Calphostin C, effect of 100 μM baicalein (bai) on basal whole cell current of porcine NPE cells. Mean whole cell currents were measured at ±90 mV and compared with baseline current (pA/pF) (Repeated measures ANOVA). The results are expressed as MEAN±SEM, n=5.

3.6 Effect of baicalein on expression of phospho-PKC in native porcine ciliary epithelial cells

From the above results, PKC was found to be likely involved in baicalein induced responses in Isc across porcine CBE as well as basal whole-cell current of native porcine NPE cells. To further study the relationship between baicalein and PKC, the effect of baicalein on phosphorylation of PKC in native porcine ciliary epithelial cells was characterized by western-blot analysis.

A PKC activator PMA significantly increased the expression of phospho-PKC in porcine ciliary epithelial cells. After pretreatment of PMA (300 nM) for 15, 30 and 60 minutes, the expressions were increased by 1.5 ± 0.06 (n=5, $P<0.05$), 1.77 ± 0.13 (n=5, $P<0.01$), 1.78 ± 0.19 folds (n=3, $P<0.01$) respectively, as shown in Fig.3.50.

A

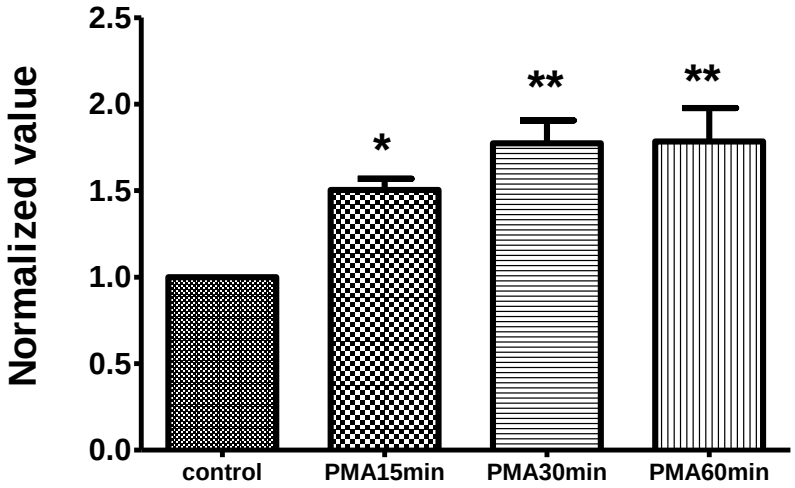

B

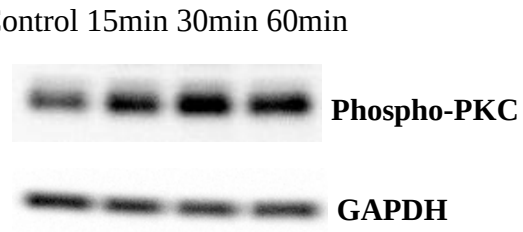

Fig3.50 (A) Effect of PMA on phospho-PKC expressions of native porcine ciliary epithelial cells. The relative band intensity normalized to GAPDH was then normalized to control (expressed as MEAN±SEM). * P<0.05, ** P<0.01, compared with control (One-way ANOVA, followed by Tukey multiple comparison test). (B) Representative image of the immunoblot.

Pretreatment of baicalein (100 μM) for 5 minutes induced significant increase in the expression of phospho-PKC by 1.73 ± 0.25 fold (n=8, P<0.05). Lower concentration of baicalein (50 μM) also increased the expression, although the change was not statistically significant (n=3, P>0.05). The results are shown in Fig3.51.

A

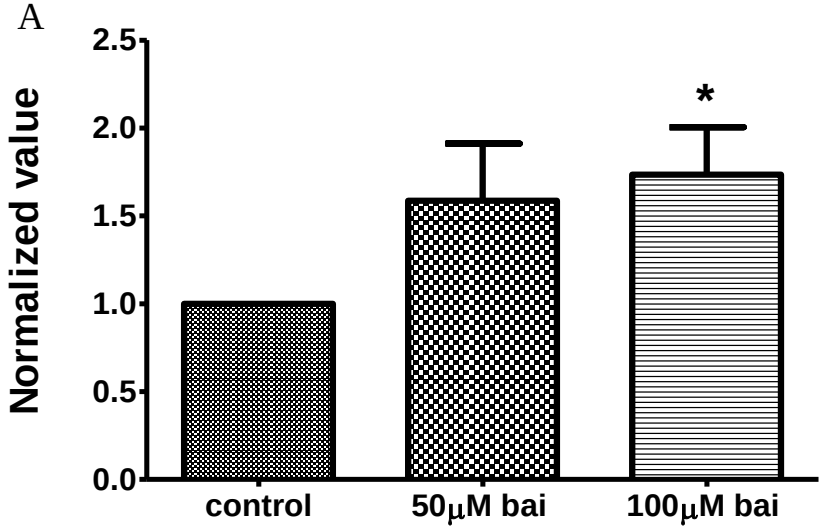

B

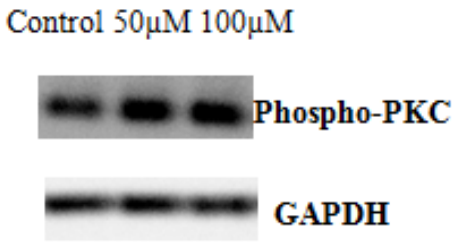

Fig3.51 (A). Effect of 50 and 100 μM baicalein (bai) on phospho-PKC expressions of native porcine ciliary epithelial cells. The relative band intensity normalized to GAPDH was further normalized to the control (expressed as MEAN±SEM). * P<0.05, compared with control (One-way ANOVA, followed by Tukey multiple comparison test). (B) Representative image for one single experiment.

3.7 Effects of baicalein on guinea pig IOP

Clinically, there are two general approaches to lower IOP: to reduce AHF and/or to increase outflow. Based on the inhibitory effect of baicalein on FF, it was hypothesized that baicalein can also decrease IOP. To examine if it is the case, baicalein was used on the eyes of guinea pig and its effects on IOP was investigated.

3.7.1 Effect of topical administration of baicalein on guinea pig IOP

The basel IOP values of baicalein-treated eyes and the contralateral eyes were 18.0 $\pm$ 0.9 and 17.4 $\pm$ 0.6 mmHg respectively, and there was no significant difference between baicalein-treated eyes and the contralateral eyes ($P>0.05$).

As shown in Fig3.52, After topical administration of baicalein (0.3%, dissolved in 10% HP-β-CD), there was a statistically significant decrease in IOP of the experimental eyes at 3 hours post administration, and the reduction at this time point was 2.9 $\pm$ 0.3 mmHg compared with baseline value ($p<0.05$, $n=6$). The changes of contralateral eyes were not significant at all time points ($p>0.05$). The baicalein-treated eyes showed significantly lower IOP than the contralateral eyes

at 3 hours after the administration (P<0.05). The inter-eye IOP difference at 3 hours was 1.5 ± 0.4 mmHg, which was significantly different from the baseline difference (P<0.05, n=6). The change of inter-eye differences between baicalein-treated eyes and contralateral eyes over time was illustrated in Fig3.52.

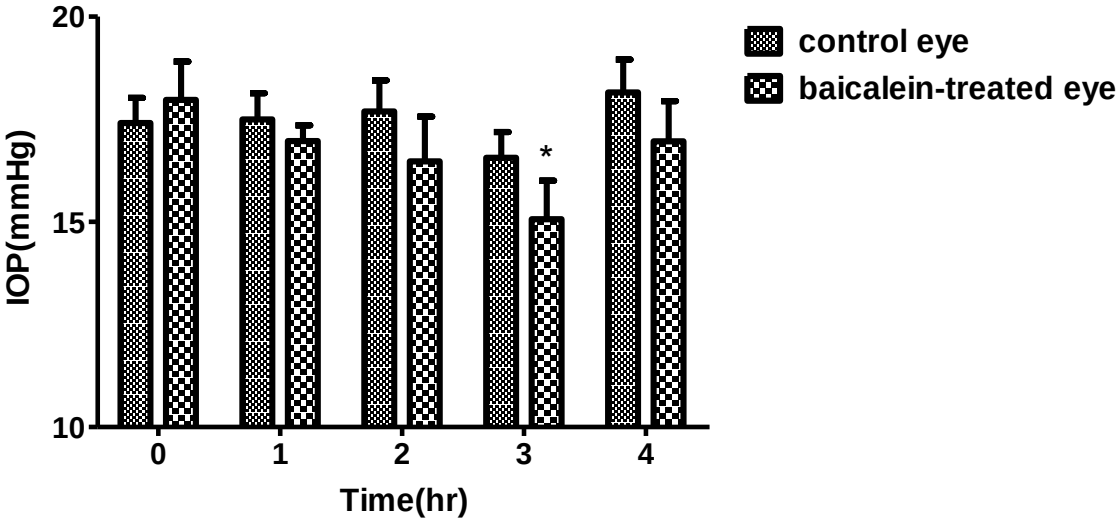

Fig3.52. Effect of topical administration of baicalein on guinea pig IOP. Results were expressed as MEAN±SEM, n=6. *P<0.05, compared with baseline value (Two-way ANOVA, followed by Bonferroni post tests)

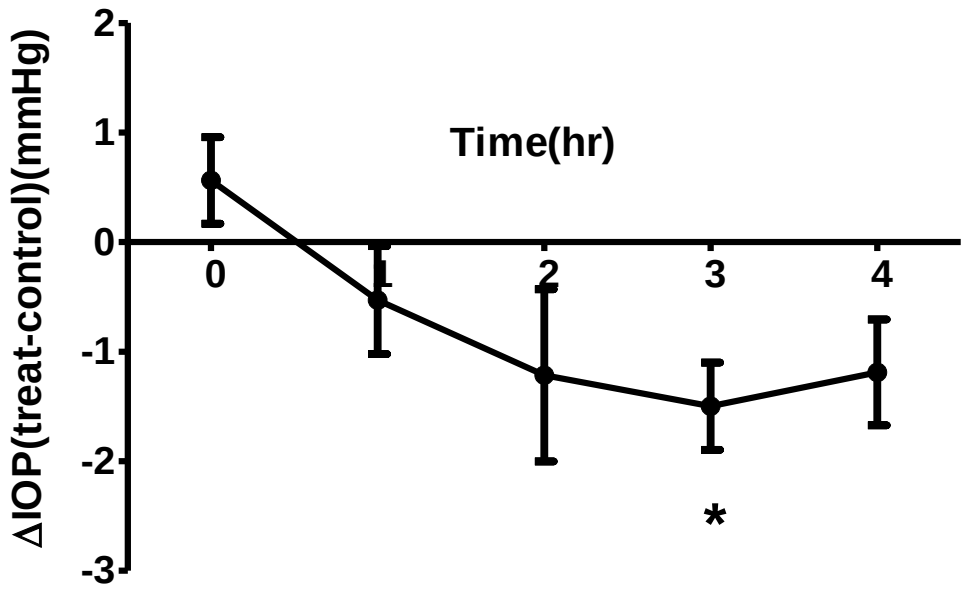

Fig3.53. The change of inter-eye IOP difference after topical administration of baicalein in guinea pig. Results were shown as the IOP differences between baicalein-treated eyes and contralateral eyes (ΔIOP (treat-control)) and expressed as MEAN±SEM, n=6. *P<0.05, compared with baseline value (Repeated measures ANOVA, followed by Bonferroni's multiple comparison test).

3.7.2 Effect of intravitreal injection of baicalein on guinea pig IOP

To further characterize the effect of baicalein on IOP, seven guinea pigs were intravitreally injected with baicalein (2 mM) in one eye, and the contralateral eyes were injected with veicle solution. The basel IOP values of baicalein-treated eyes and the contralateral eyes were 17.5 $\pm$0.7 and 17.9 $\pm$0.9 mmHg respectively, and there was no significant difference between baicalein-treated eyes and the contralateral eyes ($P>0.05$).

As shown in Fig 3.54, baicalein-treated eyes showed significantly lower IOP than the contralateral eyes at 1, 2 and 5 hours post-injection ($P<0.05$). At these time points, the inter-eye IOP difference between baicalein-treated eyes and contraleteral eyes were 2.8 $\pm$0.6, 2.54 $\pm$0.9 and 3.45 $\pm$1.6 mmHg respectively.

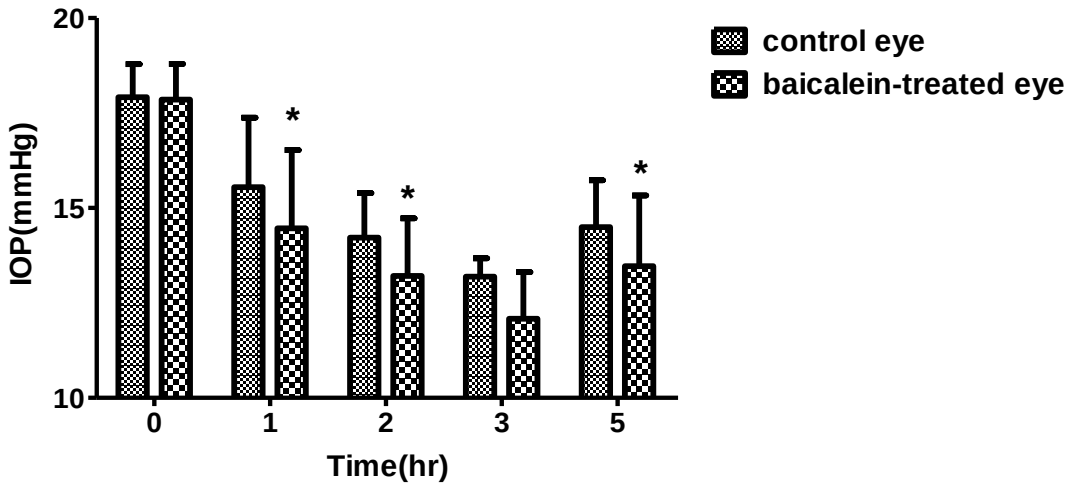

Fig3.54 Effect of intravitreal injection of baicalein on guinea pig IOP. Results were expressed as MEAN±SEM, n=7. *P<0.05, comparison between control eyes and baicalein-teated eyes (Two-way ANOVA, followed by Bonferroni post tests).

Chapter 4 Discussion

4.1. Inhibition of Isc across porcine CBE by baicalein

4.1.1. Structure-activity relationship in flavones induced Isc inhibition

Scutellariae radix is one of the most popular medicinal herbs primarily found in China and Japan. Clinically, it is extensively used for the treatment of various diseases including dysentery, atherosclerosis, hypertension, hyperlipemia and inflammatory diseases. Baicalein and baicalin are the major flavones isolated from Scutellariae radix. Baicalin is the glucuronide derivative of baicalein and both of them can transform into each other at suitable conditions. Chrysin is one of the minor flavones found in Scutellariae radix (Zhang et al., 1997) which is structurally related with baicalein and baicalin. All of the three flavones possess similar broad spectrum of bioactivities, such as anti-inflammatory (Kaneko et al., 2010), antioxidant and anticancer activities (Cai et al., 2004; Khoo et al., 2010). The chemical structures of baicalein, baicalin and chysin are illustrated in Fig.4.1.

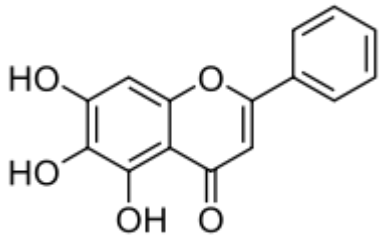

Baicalein: 5, 6, 7-trihydroxy-flavone

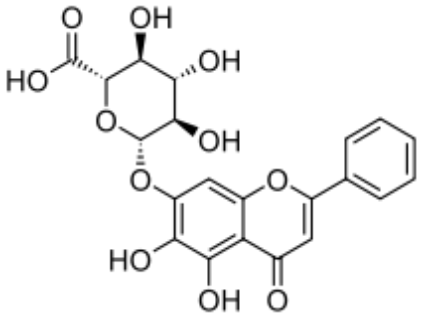

Baicalin: 5, 6-dihydroxy-7-O-glucuronide

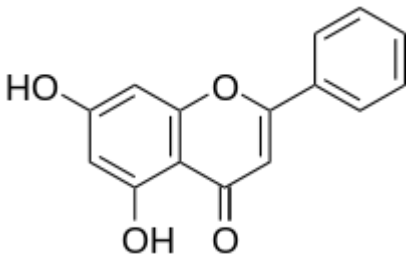

Chrysin: 5, 7-dihydroxyflavone

Fig.4.1. The chemical structures of baicalein, baicalin and chrysin

Several studies suggested that the specific structures of these flavones are key to their diverse bioactivities. The o-di-hydroxyl group in the A ring is thought to be

responsible for its antioxidant activity (Gao et al., 1999); 5, 6, 7-trihydroxy structure may play a key role in inhibitory effect on rat intenstinal α- glucosidase (Gao et al., 2004); whereas 5, 7-dihydroxy group has been linked to the regulation of convulsion (Yoon et al., 2011).

Our results showed that all of these three flavones (baicalein, baicalin and chrysin) inhibited the Isc across porcine CBE when applied to the aqueous side (see Fig3.2; 3.5; 3.7). Baicalein produced the strongest inhibition, while the baicalin and chrysin showed weaker inhibition. They all share the same 5-OH group in their structures, indicating the 5-OH structure may be important in regulating ion transport activity. The varied potency among them in terms of inhibition of Isc may be due to the presence of 7-O-glucuronide group in baicalin and the absence of 6-OH group in chrysin. When 5-OH, 6-OH and 7-OH were present at the same time, it has the strongest inhibition of ion transport activity as seen in the case of baicalein.

4.1.2. Transport mechanism underlying baicalein induced Isc inhibition across porcine CBE

To investigate the ionic basis of baicalein induced inhibition of Isc, chloride substitution experiments were conducted. This inhibitory response was Cl^- –dependent because depletion of most Cl^- ion in the bathing solution dramatically attenuated baicalein induced inhibition (see Fig3.9), indicating transmembrane Cl^- transport was involved and possibly modulated by baicalein. Transepithelial chloride transport across CBE involves three steps: (1) entry into the PE cells, (2) transport from the PE to NPE and (3) secretion from the NPE cells. Several transport inhibitors and channel blockers were used to unravel the transport mechanisms underlying baicalein induced inhibition of Isc across porcine CBE.

Uptake of Cl^-: NKCC is proposed to be the predominant way for uptake of Cl^- by PE cells in porcine CBE (Kong et al., 2006). Pretreatment of the NKCC inhibitor bumetanide failed to stop baicalein from further reducing Isc (see Fig3.11), indicating NKCC may play a minor role in the baicalein triggered responses. However, another loop diuretic furosemide almost abolished baicalein induced inhibition (see Fig3.13). The phenomenon was complicated by the non-specific

nature of furosemide as ion transport blocker, since besides NKCC, active Cl^- transport (Burg et al., 1973; Candia, 1973), Cl^-/HCO_3^- exchanger (Guelrud et al., 1972) and anion exchangers (Deuticke and Gerlach, 1967; Brazy and Gunn, 1976) could be down-regulated by furosemide as well. It has been shown that addition of 4,4'-diisothiocyanatostilbene-2,2'-disulfonic acid (DIDS) to the aqueous side of the CBE induced significant increase of Isc but produced no significant change when applied to the stromal side (Kong et al., 2006), indicating that Cl^-/HCO_3^- exchanger may play a minor part in the Cl^- uptake pathway; so it precluded the effect of furosemide through inhibiting the Cl^-/HCO_3^- exchanger in porcine CE. Therefore, it is plausible that furosemide may have inhibited Isc through a reduction of Cl^- efflux (by acting as a Cl^- channel inhibitor), instead of Cl^- influx. The fact that furosemide abolished the baicalein induced Isc decrease suggested that baicalein may also act on the Cl^- efflux pathway.

Cl^- efflux: Chloride efflux has been suggested to be the rate-limiting step in tranepithelial chloride transport across CE (Civan et al., 1997), and Cl^- channels are suggested to play a vital role in this process. To examine if baicalein exerted its inhibitory effect over Cl^- efflux of porcine CBE, two Cl^- channel blockers (DPC

and NFA) were used. Complete blockades of baicalein's effect were found after the pretreatment of DPC (see Fig3.15) and NFA (see Fig3.17), indicating baicalein may inhibit Isc across porcine CBE by attenuating Cl^- efflux, possibly through suppressing these DPC-, NFA- or furosemide-sensitive Cl^- channels.

4.1.3. Signaling pathways involved in baicalein induced Isc inhibition across porcine CBE

Lipoxygenase pathway

The presence of arachidonic acid metabolism in CE has been reported in studies with rabbit (King et al., 1992) and pig (Sakamoto and Shichi, 1991). In porcine CE, besides the presence of 5- and 12-LOX products such as 5-hydroxyeicosatetraenoic acid (5-HETE) and 12-HETE, the activities of 5- and 12- LOX in NPE cells were higher than that in the PE cells (Sakamoto and Shichi, 1991).

Baicalein is often used as a selective 12/15-LOX inhibitor in previous studies (Wong et al., 2001; van Leyen et al., 2006; Leung et al., 2007; Xu et al., 2013). If baicalein had exerted its inhibitory effect on Isc through the LOX pathway, the inhibition should have been markedly reduced by the common LOX inhibitor-NDGA. However, the findings failed to support this hypothesis. After the pretreatment of NDGA, baicalein still induced further significant inhibition of the Isc (see Fig3.19), suggesting LOX pathway may not be likely involved in baicalein elicited inhibition of Isc. It has to be said that the selectivity and potency to inhibit different LOXs by both baicalein and NDGA may be cell-type specific.

Baicalein may have been a more potent inhibitor for 12- or 15-LOX than NDGA for CE, leading to further reduction of Isc after NDGA addition. As a result, the precise role of LOX pathway in baicalein induced transport inhibition awaits further verification.

Protein kinases

Baicalein was found to exert multiple biological functions via modulating the activities of several protein kinases. In the intestinal epithelia, the phospho-PKA expression was significantly up-regulated by baicalein (Yue et al., 2004). PKC activity was reported to be inhibitable by baicalein in several studies (Kimata et al., 2000; Kimura *et al.*, 2001; Chiu et al., 2011). Moreover, baicalein was found to inhibit the phosphorylation of PKCα of human hepatoma cells (Chiu et al., 2011) but activated it in a cellular model of Parkinson's disease (Zhang, et al., 2012).

To investigate if the protein kinases were involved in baicalein evoked actions in porcine CBE, a number of protein kinases inhibitors were used in the present study. H-89 is the most potent and selective inhibitor for PKA among the H-series compounds (Hidaka et al., 1991; Hidaka and Kobayashi, 1992). However, H89 failed to induce any change over baicalein induced inhibition of Isc (see Fig3.21), excluding any possible participation of PKA in baicalein's actions.

Contrary to PKA, PKC appeared to be important in baicalein's effect on the CBE. Pretreatment of staurosporine (a PKC inhibitor) almost abolished baicalein induced response (see Fig3.25). Similar results were obtained with another potent and selective PKC inhibitor calphostin C (see Fig3.23), supporting the notion that PKC and its signaling pathway may be involved in baicalein elicited inhibition. Both staurosporine and calphostic C are potent PKC inhibitors, but they act at different functional domains of PKC to down-regulate PKC activity. Staurosporine acts on the highly conserved catalytic domain among all PKC isoforms (Nishizuka, 1992; Hug and Sarre, 1993), while calphostin C acts on the regulatory domain of a broad spectrum of PKC subtypes (Ozawa et al., 1993). These different actions of staurosporine and calphostin C may have accounted for the discrepancy between their potencies in inhibiting baicalein induced responses. Since the selectivity of staurosporine over PKC isozymes and ATP-dependent kinases were not exclusive (Gribble et al., 1993), staurosporine may have acted on other protein kinases (PKG, CAMK Ⅱ and tyrosine kinases) and in turn contributed to the calphostin C-insensitive portion of inhibition. There remains room for further study as to better understand the PKC-dependent and/or PKC-independent signaling pathway in baicalein triggered responses on Isc.

4.2 Inhibition of FF across porcine CBE induced by baicalein

Fluid transport across CBE has been detected in several species including rabbit, ox (Candia et al., 2005) and pig (Candia et al., 2007). In rabbit and ox, FF of CE is primarily dependent on bicarbonate (HCO_3^-) and Cl^- respectively (Candia et al., 2005). In pig, FF was found to be dependent on both HCO_3^- and Cl^-, with Cl^- replacement induced more drastic effect. It indicated Cl^- transport played a more important role in the FF across porcine CBE (Candia et al., 2007). Moreover, Law et al. (2009) found that NFA markedly decreased the FF by 62%, demonstrating the essential role of Cl^- channel activities in fluid movement, and further supporting the FF is primarily driven by active Cl^- transport.

Based on the results from Ussing chamber studies, baicalein probably reduced the Isc across porcine CBE by inhibiting Cl^- secretion via unsepcified Cl^- channels. Since baicalein exerted significant inhibition over Cl^- transport across porcine CBE, it followed that the transepithelial FF would be reduced as well. The findings of FF measurement confirmed this hypothesis. When applied to the aqueous side, baicalein inhibited both PD and FF across porcine CBE by around 50% and 31% respectively (see Table3.16 & Fig3.26).

Since the *in vitro* FF measurements in our study precluded the influence of certain factors such as ultrafiltration and osmotic or other pressure gradients, the fluid transport detected can be totally attributed to the secretory activity of the isolated CBE. Therefore, the baicalein induced reduction in the FF reflected a direct inhibition of the secretory activity of porcine CBE. Moreover, since active Cl^- transport is supposed to be the primary driving force for AHF, and the fact that baicalein markedly inhibited transepithelial Cl^- transport and the fluid secretion across porcine CBE strongly suggested that it can inhibit *in vivo* AHF as well.

However, there is uncertainty in defining the quantitative effect on *in vivo* AHF from the present *in vitro* study. The FF rates measured in our experiments were around 3 μL/h, which are consistent with previous studies of FF across CBE reported in rabbit, ox and pig (Candia et al., 2005; Law et al., 2009). However, this value was too small when compared with the *in vivo* AHF value measured in human (165 μL/h) (Brubaker, 1991). The exact reason is unknown but it may be due to a lack of blood circulation and/or limited exposed area when the CBE was mounted in an artificial chamber. Furthermore, the relative contribution of active ion transport to AHF is not fully understood. In a perfused bovine eye model, active ionic transport was proposed to contribute at least 60% of the *in vitro* AHF

(Shahidullah et al., 2003). As a result, although baicalein significantly inhibited the FF rate across porcine CBE, the exact quantitative effect on *in vivo* AHF could not be predicted precisely.

Nevertheless, the results on baicalein induced inhibition of Isc and FF across porcine CBE have provided evidence to support an ocular hypotensive property of baicalein.

4.3. Dye-compound interaction

In $[Cl^-]_i$ measurement of native porcine NPE cells, 100 μM baicalein markedly decreased the fluorescence which corresponded to an increase in $[Cl^-]_i$. However, addition of baicalein, even at 10 μM, caused significant decrease of the fluorescence in the calibration solution. The calibration solution contained high K^+ and free of Cl^- with ionophores (nigericin and tributyltin) which rendered cells unviable. Therefore, the decrease of fluorescence by baicalein in this solution was likely an artifact, implying that baicalein had interacted with MQAE and quenched the fluorescence. This interaction may be due to the yellow color and cell permeable nature of baicalein. As a result, it was difficult to discriminate the physiological response from artifacts induced by baicalein.

Similar interaction also happened in the membrane potential recordings with DiBAC4(3). In the absence of cell, baicalein quenched the fluorescence of DiBAC4(3) in NRR by about 20%. Although the exact physiological effect of baicalein on membrane potential was compromised by this interaction, one can still quantify the change in fluorescence induced by various interventions in the presence of baicalein; for example, the study of Cl^- substitution in preparations pretreated by baicalein.

To circumvent this problem, intracellular recording with microelectrodes and/or whole-cell current measurement instead of fluorescence dye method can be used for membrane potential measurements. Alternatively, novel potential-sensitive dyes such as FLIPR Membrane Potential Assay Kit (FMP) and Fluorescence Resonance Energy Transfer **(**FRET**)** probes can be tried, which have less quenching effect (Wolff et al., 2003). As to the $[Cl^-]_i$ measurement, SPQ can also be tried because of its dissimilar structure with MAQE. However, due to the chemical nature and yellow color, the compound-dye interaction may still happen between baicalein and these dyes. It has been estimated that about 1% of compounds (at 10 μM) may have undesirable dye-compound interaction that causes a change in fluorescence (Gonzalez and Maher, 2002). Dye-compound interaction remains one of the major limitations in the application of fluorescent indicators; therefore the development of chemically stable fluorescent probes of different colors will be useful for accurate intracellular recordings.

4.4. Membrane potential properties of porcine ciliary epithelial cells

Transepithelial ion transport (Crook et al., 2000; Do et al., 2000; Kong et al., 2006) and transmembrane electrogenic transport (Edelman et al., 1995; Do et al., 2004; Do et al., 2006) of ciliary body have been intensively studied previously. Membrane potential measurement constitutes another approach to study intracellular electrophysiologic characteristics of CE. The membrane potentials of ciliary epithelial cells of shark (Wiederholt and Zadunaisky, 1986), rabbit (Green et al., 1985), ox (Helbig et al., 1987; Helbig et al., 1989a) and human NPE cell lines (Helbig et al., 1989b) have been reported previously. Our study was the first to report the intracellular potential in native porcine ciliary epithelial cells, as well as the first attempt to use the potential-sensitive fluorescence probe [DiBAC4(3)] for simultaneously recording membrane potential of NPE and PE cells.

The baseline resting membrane potential of porcine NPE and PE cells were -69 mV and -61 mV respectively, and the difference between the values of these two cell types was not statistical significant. The values were also similar to that of the rabbit, which was -65 mV for the NPE cells (Green et al., 1985). However it was quite different from other species; the membrane potential of bovine (Helbig et al.,

1987; Helbig et al., 1989a) and shark (Wiederholt and Zadunaisky, 1986) NPE and PE cells were about -40 mV and -50 mV respectively, while for a cell line derived from human NPE cells, the value was -50 mV(Helbig et al., 1989b). While species difference may be a possible reason for the discrepancies, these studies mainly employed the intracellular microelectrode technique for intracellular potential recordings instead of using intracellular dye as in the present study. These two methods differ in several aspects. The measurements with microelectrodes are associated with certain mechanical breaks in the plasma membrane and the accuracy of measurements depends on matching of the ionic composition in the pipette solution with that of the cytosol. On the other hand, fluorescent dye method is subjected to unknown influence of microenvironments of the cells and dye distribution. Moreover, the fluorescence signal may be interfered by cellular pigmentation as in the case of the PE cells. Therefore, these two methods could act to complement each other, rather than displace the other, in the study of intracellular potentials.

In addition to recording the membrane potentials, it was noted that both the PE and NPE cells displayed similar responses towards ion substitution, transporter inhibitors and channel blockers. Taken together with the facts of similar

intracellular potentials, the results indicated the intracellular environments of both the NPE and PE cells are effectively coupled and homogeneous.

Na^+: Lowering of extracellular Na^+ concentration into 2 mM induced a fast hyperpolarization (around 7 mV) followed by a slow depolarization towards baseline value (see Fig3.28). This response indicated that the membrane potentials of both NPE and PE cells were dependent on extracellular Na^+ concentration. This Na^+ dependent characteristic was also observed in human NPE cell line (Helbig et al., 1989b). However, in rabbit cultured NPE cells, there was no apparent response to the change of Na^+ concentration in the bathing solution (Green et al., 1985). The reason for this lack of response in rabbit tissue is unclear. The transient hyperpolarization was supposed to be due to a massive Na^+ efflux from the cells via sodium channels because of the low sodium outside of the cell. However, some nonspecific cation channels was proposed to account for such response as well, because Na^+ channel blockers failed to block this hyperpolarization (Helbig et al., 1989b). This massive Na^+ efflux resulted in significant decrease of $[Na^+]_i$, which may trigger several secondary electrogenic transport from some sodium-related transportors and channels. The interaction of all these transport activities may

constitute the slow depolarization. The precise mediation behind Na^+ replacement induced response in porcine ciliary epithelial cells has yet to be elucidated.

Potassium channel: The presence of K^+ conductance has been detected in the CE of shark (Wiederholt and Zadunaisky, 1986), ox (Helbig et al., 1987; Helbig et al., 1989a), rabbit (Green et al., 1985) and human NPE cell line (Helbig et al., 1989b). In porcine ciliary epithelial cells, addition of the potassium channel blocker (Ba^{2+}) caused immediate and marked depolarization of the intracellular potential (see Fig3.30). Similar magnitude of depolarization was reported with human NPE cell line (Helbig et al., 1989b). The present data showed that porcine NPE and PE cells possess K^+ channels that can generate K^+ conductance and contribute to the resting potentials.

Na^+/K^+-ATPase: Ouabain, a specific Na^+/K^+-ATPase inhibitor, depolarized the membrane potential by about 10 mV (see Fig3.31) , which is consistent with the responses in shark ciliary body (Wiederholt and Zadunaisky, 1986), rabbit ciliary epithelial cells (Green et al., 1985) and human NPE cell lines (Helbig et al., 1989b). The significant depolarization induced by ouabain indicated the existence of

Na^+/K^+-ATPases. Na^+/K^+-ATPases is a primary active transporter generating sodium gradients for secondary active transport. Under resting conditions, after the activity of Na^+/K^+-ATPase was blocked by ouabain, all the secondary active transport was halted as well. Therefore, Na^+/K^+-ATPases along with the secondary transport contributes to about 10 mV of the intracellular potential in pocine ciliary epithelial cells.

Cl^- conductance: Chloride transport plays an essential role in AHF. The Isc across bovine and porcine CBE both showed strong dependence on bathing Cl^- concentration (Do and To., 1998; Kong et al., 2006). In terms of membrane potentials, except for rabbit NPE cells (Green et al., 1985), both cultured bovine NPE (Helbig et al., 1989a) and human NPE cell lines (Helbig et al., 1989b) were depolarized upon extracellular Cl^- replacement. This response was also evident in the present study. After extracellular Cl^- substitution, both NPE and PE cells exhibited a depolarization which was followed by a hyperpolarization of variable speed (see Fig3.29). After extracellular Cl^- was depleted, an instant and massive Cl^- efflux in accordance with the electrochemical gradient took place, resulting in the fast depolarization of intracellular potential. Meanwhile, the significant

decrease of $[Cl^-]_i$ induced by the flux may activate a host of other transporter and channels. The interaction of Cl^- efflux and concomitant secondary ion transport may contribute to the hyperpolarization phase. The characteristics of the initial depolarization have been investigated previously and it was effectively blocked by the Cl^- channel blocker DIDS (Helbig et al., 1989a; Helbig et al., 1989b). Similarly, a nonspecific Cl^- channel blocker (NFA) dramatically attenuated the magnitude of the depolarization upon Cl^- removal in porcine ciliary epithelial cells (see Fig3.35). These findings support the presence of a Cl^- conductance that is sensitive to certain Cl^- channel blockers (DIDS or NFA). Pretreatment of baicalein induced similar significant reduction of the depolarization of porcine NPE cells upon Cl^- removal, while the responses in PE cells were not statistical significantly changed (see Fig3.36), indicating the Cl^- current induced by Cl^- substitution in NPE cells was reduced by baicalein, and the Cl^- transport in NPE cells was more sensitive to baicalein than PE cells. The results further supported baicalein elicited inhibition of Isc across porcine CBE was probably via blockade of Cl^- channels at the NPE.

Cl^- channels: Three Cl^- channel inhibitors (NFA, DPC and IAA94) caused significant hyperpolarization of CE (see Fig3.34; 3.32; 3.33), demonstrating the

presence of Cl^- channels in native porcine NPE and PE cells. Although Cl^- channels at the NPE cells are known of its vital importance in AHF, PE cells have also been reported to express Cl^- channels like large-conductance maxi-Cl^- channels (Do et al., 2004). One possible reason for the different responses induced by the three Cl^- channels blockers may be due to their different potencies in down-regulating Cl^- channels' activities. Moreover, the relatively high concentrations used (500 μM) for both NFA and DPC applications may have elicited non-specific inhibition over exchangers or transporters besides Cl^- channels. Nevertheless, the consistent hyperpolarization induced by all of the Cl^- channels blockers has provided strong evidence of the presence of Cl^- channels in porcine NPE and PE cells.

4.5. Modulation of whole cell current of native porcine NPE cells by baicalein

4.5.1. Inhibition of swelling-activated Cl^- current by baicalein

The Cl^- secretion from the NPE cells is the last and rate-limiting step of transepithelial Cl^- transport across CE (Civan et al, 1997). To identify the types of Cl^- channels, a number of investigations have been carried out (Jacob and Civan, 1996; Do and Civan, 2006). Swelling-activated Cl^- channels are broadly and functionally characterized in ciliary epithelial cells of various species, including cultured human NPE cells (Carre et al., 2000) and native bovine NPE cells (Do et al., 2004) and rabbit NPE cells (Vessay et al., 2004).

In the present study, swelling-stimulated current in native porcine NPE cells possessed properties similar to that of previous reports: outward rectification and significant inactivation during large positive voltage clamps. The calculated reversal potentials were around -25 mV, which is also close to the equilibrium potential of Cl^-. Moreover, the stimulated currents could also be dramatically suppressed by Cl^- channel blocker NPPB and NFA (see Fig3.37-3.40). These findings indicated that the swelling-activated current in native porcine NPE cells should primarily be a Cl^- current driven by swelling-activated Cl^- channels.

Therefore, it is plausible here to use swelling-activated Cl^- current as the probe for the Cl^- channel activities at NPE cells..

Addition of baicalein in the bath elicited a dose-dependent inhibition of swelling-activated Cl^- current of native porcine NPE cells (see Fig3.42). At 200 μM, the baicalein induced inhibition was almost comparable to NFA treatment. The marked inhibitory effect caused by baicalein indicated that baicalein may reduce the swelling-activated Cl^- conductance of native porcine NPE cells by down-regulating the activities of swelling-triggered Cl^- channels.

However, the molecular identity of these swelling-activated Cl^- channels at NPE cells has not been clearly identified. Cl^- channel regulator pICln and ClC-3 are two possible candidates proposed by several studies. The swelling-activated Cl^- current was inhibited after down-regulation of pICln with antisense oligonucleotides (Chen et al., 1999). Nevertheless, the predominant location of pICln at cytoplasm of NPE cells and the lack of expression or translocation from cytoplasm to plasma membrane during hypotonic swelling (Sanchez-Torres et al., 1999) ruled it out as the dominant Cl^- channels.

In NPE cells, the activity of swelling-activated Cl^- channels was found inhibited by antisense oligonucleotides that down-regulated message for ClC-3 (Wang et al.,

2000). Functional blockade of ClC-3 by a anti-ClC-3 antibody (Wang et al., 2003) reduced swelling-activated Cl^- current in cultured rabbit (Vessey et al., 2004) and native bovine (Do et al., 2005) NPE cells. Sensitivity to PKC is another feature of ClC-3 related Cl^- current. In cultured rabbit NPE cells, the swelling-activated Cl^- current was potentiated by PKC inhibitors and inhibited by PKC activator and (Shi et al., 2002). In native bovine NPE cells, the onset of swelling-activated Cl^- current was significantly delayed by PKC activation (Do et al., 2005), indicating the swelling-activated Cl^- current was ClC-3 associated. However, the distribution of ClC-3 is found mainly within the nucleus of NPE cells, and suggested to only account partially for of the swelling-activated Cl^- channels (Wang et al., 2000). Therefore the molecular identity of swelling-activated Cl^- channels of NPE cells remains to be identified.

In the present study, PKC inhibitor staurosporine did not induce any significant change on the magnitude of hypotonic swelling triggered current or baicalein induced inhibition (see Fig3.43). The PKC insensitivity indicated that ClC-3 was not likely to be the candidate for swelling-activated Cl^- channels at NPE cells. Moreover, PKC was not likely to participate in the signaling cascade through which baicalein exerted inhibitory activity over swelling-activated Cl^- channels.

At 1 μM, staurosporine could down-regulate activities of many other protein kinases besides PKC, so the inhibitory action of baicalein may be through some signaling transduction pathway without the participation of staurosporine-sensitive protein kinases, or even through a direct blockade of the swelling-activated Cl^- channels.

However, in Ussing chamber study, staurosporine almost abolished baicalein evoked inhibition of Isc, indicating the participation of signaling pathway involving PKC. The discrepancy between the PKC involvement in the baicalein induced inhibition of Isc and swelling-activated Cl^- current may suggest different underlying mechanisms were at work. Swelling-activated Cl^- channels at NPE cells were not likely to be the cellular targets of baicalein exerting Isc inhibition. If baicalein inhibited Isc via blockade the chloride channels identical to the swelling-activated ones, the inhibition of activated current should also be significantly suppressed by staurosporine pretreatment. It is plausible therefore that under physiological condition, the molecular identities of those active Cl^- channels sensitive to baicalein may be quite different from swelling-activated ones. The distinct mechanism underlying baicalein induced inhibition of Isc was still unclear and need further investigation.

4.5.2. Inhibition of basal whole cell current by baicalein with increased $[Cl^-]_i$

Under physiological condition, CE is bathed in isotonic instead of hypotonic solution. In addition, swelling-activated Cl^- current of porcine NPE cells was significantly inhibited by the Cl^- channel blocker NPPB. However, the Isc across porcine CBE was totally insensitive to it (Kong et al., 2006). This discrepancy further support these swelling-activated Cl^- channels may not be operational under isotonic condition and therefore unlikely to be the conduit through which baicalein exhibits Isc inhibition. Rather, baicalein was likely acting on those NPE Cl^- channels that are active in isotonic solution. To examine the hypothesis, the effect of baicalein on the basal whole cell current of NPE cells was studied.

The basal whole cell current of native porcine NPE cells was so small that some inhibition may be too weak to be noticed. Increasing $[Cl^-]_i$ was reported to be able to increase the cAMP stimulated outward and inward current, as well as Cl^- channel conductance of bovine PE cells (Do et al., 2004). Therefore, to enhance the basal current and Cl^- channel activity, $[Cl^-]_i$ of NPE cells was increased. In the present study, after the $[Cl^-]_i$ was increased from 25 mM to 100 mM, the basal outward current of porcine NPE cells was markedly enhanced, while the change of inward current was not statistically significant. Since Cl^- was the only anion

present in the solution, the markedly enhanced basal outward current with the increase of $[Cl^-]_i$ may indicate more Cl^- channels were up-regulated, thereby generating extra Cl^- current. The reduction induced by baicalein in such case should be due to inhibition of these activated Cl^- channels (see Fig3.44).

After the pretreatment of staurosporine (1 μM), baicalein induced inhibition of basal current still persisted (see Fig3.45), indicating the inhibitory effect of baicalein here is either rather upstream and unlikely through indirect regulation of protein kinases, or through some staursporine-insensitive signaling moleculars. Therefore, these Cl^- channels activated by elevated $[Cl^-]_i$ were not likely to be the cellular targets of baicalein in inhibiting Isc across porcine CBE.

Nevertheless, together with the blockade of swelling-activated Cl^- channels, the results corroborated that baicalein is a novel and potent Cl^- channel inhibitors, although the precise regulatory mechanism still awaits further investigation.

4.5.3. Inhibition of basal whole cell current by baicalein

Since the involvement of Cl^- channels activated by increased $[Cl^-]_i$ in the baicalein induced Isc inhibition was excluded as well, the effect of baicalein on basal whole cell current of native porcine NPE cells with normal $[Cl^-]_i$ was therefore examined. The basal whole cell current of native porcine NPE cells was very small. Significant suppression of basal outward current was still observed with NFA (see Fig3.46). The data suggested that under physiological condition, NFA-sensitive Cl^- channels at NPE cells are active and contributing to the basal Cl^- current. However, there was residue current insensitive to NFA, which may attribute to some basal cation movement. Moreover, the presence of leakage of the patch could also have constituted partial of the residue whole cell current.

Similarly, application of baicalein to the bath also significantly inhibited the basal current of native porcine NPE cells (see Fig3.47), indicating that some active Cl^- channels under basal condition were also sensitive to baicalein, and this down-regulation of the Cl^- channel activities was significant enough to be detected in the whole cell current. Accordingly, the reduced inward current may arise from the concomitant reduction in cation movement secondary to the baicalein induced blockade of Cl^- channels. Although the exact mechanism still remains to be

elucidated by single channel analysis, the effects of PKC inhibitors on baicalein induced inhibition of basal current have further supported this hypothesis.

Consistent with the Isc results, pretreatment of PKC inhibitors (staurosporine and calphostin C) almost abolished baicalein evoked inhibition of basal current (see Fig3.48-49), indicating the involvement of PKC related signaling pathway in these responses. Those baicalein-sensitive Cl^- channels under basal condition were likely to be the cellular targets of baicalein, and their molecular identities have yet to be characterized. Given the association with PKC (Kawasaki et al., 1994; Coca-Prados et al., 1995; Duan et al., 1999; Do et al., 2005), both pICln and ClC-3 Cl^- channels are possible candidates of these Cl^- channels.

4.6. Baicalein induced up-regulation of phospho-PKC in porcine ciliary epithelial cells

PKC is a family of protein kinase participating in signaling cascades in multiple cellular functions (Nakamura and Nishizuka, 1994). There are three subfamilies of PKC, including classic PKC isoforms (α, β and γ), novel PKC isoforms (δ, ε, η and θ) and atypical isoforms (ζ and ι).

The present data suggested that baicalein exerts inhibitory effect on Isc and whole cell current of native porcine NPE cells by regulating PKC activity. To characterize the details of modulation of baicalein on PKC, the effect of baicalein on phospho-PKC expression of primary porcine ciliary epithelial cells was examined by western-blot analysis. The results indicated that the phospho-PKC expression was markedly increased by PKC activator PMA and baicalein (see Fig3.50-51), which confirmed the activation of PKC by baicalein in porcine ciliary epithelial cells. However, the work was carried out with a mixture of native NPE and PE cells, further investigations are required to discriminate whether this up-regulation was originated from PE cells, NPE cells or both. Nevertheless, based on the present results together with those of Isc and whole cell current results, it is speculated that baicalein induced PKC related phosphorylation in the NPE cells.

Another limitation lies in the antibody used in the present study. It is useful for screening the phosphorylation of all PKC subtypes, but did not differentiate amongst various PKC isoforms. While phospho-PKCα has been reported to be up-regulated by baicalein in a cellular model of Parkinson's disease (Zhang, et al., 2012), future work is needed to clarify their contributions in ciliary epithelial chloride transport. Besides the issue of unknown isotypes, the phosphorylation sites in PKC remained to be identified as well. Specific functional domains which are responsible for phosphorylation of PKC have been identified in several studies. These sites include the activation loop, the hydrophobic C-terminal site and the autophosphorylation site. PKC inhibitors staurosporine and calphostin C inhibit PKC activity through catalytic and regulatory domain respectively, yet exerted similar inhibitory effect over baicalein-induced reduction of Isc across porcine CBE and whole cell current in NPE cells, which also complicated the speculation about the specific phosphorylation sites targeted by baicalein.

Since both membrane and cytosol proteins were analyzed together, the promotion of PKC translocation from cytosol to membrane would not likely result in the increase of phosphor-PKC expression, precluding it as the mechanism for baicalein induced PKC activity.

Whole cell current results suggested that those PKC-sensitive Cl^- channels at the NPE cells were likely to be the downstream targets of PKC in the inhibitory activity of baicalein of Isc and whole cell current. However, the upstream signals are still unknown. Several isoforms of PKC are reported to differ in their requirements of cofactors for activation. Classic PKC isotypes dependent on Ca^{2+}, diacylglycerol (DAG), and phospholipid (especially phosphatidylserine); novel family (δ, ε, η and θ) requires DAG and phospholipid; the atypical isoforms (ζ and ι) need only phospholipid. These cofactors may play an essential role in facilitating baicalein in regulating PKC activity. Moreover, the signaling cascade involving PKC is well defined; that is operating by binding to the receptors of phosphatidylinositol-specific phospholipase C (PLC) and then through Ins(1, 4, 5)P3/Ca^{2+} or DAG to regulate the activity of PKC (Nishizuka, 1986; Hug *et al*., 1993; Dekker and Parker, 1994; Jaken, 1996). However, so far there is no direct evidence on baicalein being able to activate Ins(1, 4, 5) P3/Ca^{2+} or DAG in any cell types. The missing link between baicalein and PKC in the signaling transduction pathway has yet to be elucidated.

4.7. Effect of baicalein on guinea pig IOP

Guinea pigs are used in our studies as to investigate the effect of baicalein on intraocular pressure. Compared with mouse, guinea pig has bigger eye and easier to handle without anesthetization, which help to obtain more repeatable and accurate IOP reading by tonolab measurement. Moreover, guinea pig has been reported to have more similar gene expression pattern with human than mouse (Zhou et al., 2007). Furthermore, besides the similar range of IOP (8-22 mmHg) as human (Taskintuna et al., 1997), topical administration of Cosopt eye drop induced fast and sustained reduction of guinea pig IOP in our preliminary studies, further supporting that guinea pigs may be a promising animal model for IOP study.

In guinea pigs, topical administration of baicalein induced IOP reduction and the difference between the baicalein-treated eye and control eye (see Fig3.52-53) did not appear to be as large or sustaining as expected. The exact reason is unknown. Some possible reasons are discussed here.

Although baicalein induced significant inhibition of FF across porcine CBE in the present study, its effect on *in vivo* AHF is yet to be established. IOP is maintained by the balance between AH secretion and outflow. Inhibition in AHF by baicalein

was anticipated because of its significant inhibitory effect on FF across porcine CBE. However, the effect of baicalein on outflow is unknown. If baicalein had induced obstruction in the outflow facilities in addition to inhibition of AH secretion, it would be translated to a slight change of IOP only.

Species difference should also be taken into account. Porcine CBE and ciliary epithelial cells were used in the present study. Although both pig and guinea pig eye showed good similarities with human eye, their CE still showed different sensitivities to baicalein. Guinea pig CBE may be less responsive to baicalein and therefore led to a much smaller IOP lowering effect than expected.

Moreover, the bioavailability of baicalein may be low due to its poor water solubility. HP-β-CD, which is a widely used derivative of cyclodextrins, was used in dissolving baicalein in our studies. By forming complex with HP-β-CD, dexamethasone/dexamethasone acetate (Usayapant et al., 1991) and mycophenolate mofetil (Knapp et al., 2003) showed enhanced bioavailability, while hydrocortisone (Bary et al., 2000) and pilocarpine prodrug (Siefert et al., 1999) were attenuated. Despite the inclusive action of HP-β-CD, several studies found the bioavailability of baicalein was enhanced after dissolved in HP-β-CD (Liu et al., 2006; Zhang et al., 2009). Inhibition of PGE_2-induced aqueous flare by

topical addition of baicalein in HP-β-CD also provided evidence of the increased bioavailability (Nagaki et al., 2003). However, although cornea penetration of baicalein was facilitated by HP-β-CD, the maximum concentration detected in AH was only 4.11 $\pm$0.75 μg/mL (Zhang et al., 2009), which was much lower than the effective concentration used in our studies. Therefore, insufficient local concentration of baicalein at the ciliary body may be another reason for the limited and transient IOP lowering effect. Besides HP-β-CD, much effort has been devoted to improve bioavalability of baicalein. Recently, the baicalein-phospholipid complex has been proposed (Rawat et al., 2013). It will be interesting to see if such novel delivery system may enhance the local concentration of baicalein to yield a more potent hypotensive effect.

To improve the local concentration, baicalein was directly injected into the vitreous body. Apparently, the difference between the baicalein-treated eye and control eye was significantly increased after intravitreal injection (see Fig3.54) when compared to that with topical administration. However, there was transient IOP increase due to extra volume of injected fluid and that the anaesthetizing agent, ketamine, gave a short-time decrease in the IOP have made the comparisons with baseline value very difficult. Although both topical administration and intravitreal

injection have their own limitations, the results still strongly implied baicalein may be a potent IOP-lowering pharmacological agent. To explore further the application of baicalein as a hypotensive drug, future development of the compound and characterization of its clinical efficacy are required.

Chapter 5 Summary and Conclusions

5.1 Summary

5.1.1. Effect of baicalein on Isc across porcine CBE

Baicalein has a significant inhibitory effect on Isc across porcine CBE, so did baicalin and chrycin although with much smaller magnitude. The presence of 5, 6, 7-trihydroxy group in the structure may be functionally essential in the inhibitory activity on transepithelial ion transport across CE. The transport mechanism and signaling pathway of this baicalein induced effect were further investigated.

Baicalein induced Isc inhibition was totally dependent on Cl^- concentration in the bath. Besides, it was almost completely abolished by NFA and DPC (Cl^- channels blockers) instead of bumetanide (NKCC inhibitor). The results suggested that baicalein may have inhibited Isc through blocking Cl^- channels and reducing Cl^- secretion of porcine CBE, while NKCC may play a minor role in this response.

Baicalein evoked Isc reduction was not suppressed by the LOX inhibitor NDGA or the PKA inhibitor H89. Instead, it could be significantly attenuated by calphostin C and abolished by staurosporine, which indicated PKC, rather than PKA or LOX pathway, was involved in the signaling cascade of baicalein induced effect.

5.1.2. Effect of baicalein on fluid movements across porcine CBE

A significant portion (31%) of *in vitro* FF was reduced by the application of baicalein to the aqueous side, indicating the tranepithelial Cl^- transport and fluid secretion across porcine CBE were significantly inhibited by baicalein.

5.1.3. Dye-compound interaction

The color of baicalein (yellow) led to quenching of the fluorescence of both MQAE and DiBAC4(3), indicating the limitation of using fluorescent probes for intracellular recording and suggesting alternative techniques other than fluorescent indicators (e.g. microelectrode recording) should be employed to investigate baicalein's bioactivities.

5.1.4. Membrane potential of native porcine NPE and PE cells

Membrane potential of native porcine NPE and PE cells was recorded simultaneously by using a potential-sensitive fluorescence dye DiBAC4(3). The average value of intracellular potential in porcine NPE and PE cells were -69 mV and -61 mV. The intracellular environment of the NPE and PE cells appeared to be homogeneous.

Membrane potential of porcine NPE and PE cells was dependent on extracellular Na^+ and Cl^- concentration. The NFA-sensitive depolarization induced by Cl^- replacement was also inhibited by baicalein, indicating Cl^- permeability of porcine NPE cells, more precisely the Cl^- channels, was possibly supressed by baicalein.

Marked depolarization caused by Ba^{2+} and ouabain indicated the presence of Na^+/K^+-ATPase and K^+ channel, as well as their functional contribution to the intracellular potential of porcine NPE and PE cells. The functional presence of Cl^- channels was demonstrated by the similar significant hyperpolarization elicited by three Cl^- blockers (NFA, DPC and IAA94).

These results indicated that the fluorescent probe DiBAC4(3) can be a useful tool to measure membrane potential and unravel cellular transport mechanisms of pharmacological agents such as anti-glaucoma drugs. Intracellular potential was significantly dependent on extracellular Cl^- concentration, and driven by Cl^- channel activities, consistent with the notion that Cl^- transport is of vital importance in AHF.

5.1.5. Effect of baicalein on whole cell current in native porcine NPE cells

Whole-cell recordings in native porcine NPE cells showed that baicalein markedly reduced the whole cell Cl^- currents activated by hypotonic swelling and raised $[Cl^-]_i$ (100 mM), indicating it may have down-regulated related Cl^- channels that were activated by hypotonic swelling and high $[Cl^-]_{i.}$ Neither of these inhibitory effects could be blocked by staurosporine, indicating irrelevance of PKC and other protein kinases sensitive to staurosporine in both processes. Basal whole cell current was markedly inhibited by baicalein as well. This inhibition was abolished by pretreatment of PKC inhibitors (staurosporine and calphostin C), suggesting baicalein may inhibit these active Cl^- channels at NPE cells via signaling cascades involving PKC.

5.1.6. Effect of baicalein on phospho-PKC expression in native porcine ciliary epithelial cells

The phospho-PKC expression of native porcine ciliary epithelial cells was significantly increased by baicalein, confirming the ability of baicalein in up-regulating PKC activity. Together with the results of Isc and basal whole cell current, this up-regulation of PKC may be involed in baicalein induced reduction of whole cell current in NPE cells and Isc across porcine CBE.

5.1.7. Effect of baicalein on guinea pig IOP

Baicalein treated eyes showed significant lower IOP than the contralateral eyes with topical administration or intravitreal injection, which indicated the hypotensive property of baicalein.

5.2 Conclusions

This study demonstrated that baicalein could significantly inhibit transepithelial Cl^- secretion and FF cross porcine CBE. The underlying cellular mechanism may involve the blockage of NPE Cl^- channels through PKC-associated signaling pathway, yet the upstream cascades and exact molecular targets still need to be elucidated. Baicalein also demonstrated ocular hypotensive property in guinea pigs, suggesting that it may be a potent and potential hypotensive agent that can be further developed for controlling human glaucoma.

References

Agarwal, S., Achari, C., Praveen, D., Roy, K. R., Reddy, G. V. and Reddanna, P. (2009). Inhibition of 12-LOX and COX-2 reduces the proliferation of human epidermoid carcinoma cells (A431) by modulating the ERK and PI3K-Akt signalling pathways. *Exp Dermatol* 18(11): 939-946.

Ahn, H. C., Lee, S. Y., Kim, J. W., Son, W. S., Shin, C. G. and Lee, B. J. (2001). Binding aspects of baicalein to HIV-1 integrase. *Mol Cells* 12(1): 127-130.

Akarsu, C. and Bilgili, M. Y. (2004). Color Doppler imaging in ocular hypertension and open-angle glaucoma. *Graefes Arch Clin Exp Ophthalmol* 242(2): 125–129.

Al-Shabrawey, M., Mussell, R., Kahook, K., Tawfik, A., Eladl, M., Sarthy, V., Nussbaum, J., El-Marakby, A., Park, S. Y., Gurel, Z., Sheibani, N. and Maddipati, K. R. (2011). Increased Expression and Activity of 12-Lipoxygenase in Oxygen-Induced Ischemic Retinopathy and Proliferative Diabetic Retinopathy: Implications in Retinal Neovascularization. *Diabetes* 60(2): 614-624.

Anguita, J., Chalfant, M. L., Civan, M. M. and Coca-Prados, M. (1995). Molecular cloning of the human volume-sensitive chloride conductance regulatory protein, pICln, from ocular ciliary epithelium. *Biochem Biophys Res Commun* 208(1): 89-95.

Avila, M. Y., Stone, R. A. and Civan, M. M. (2002). Knockout of A3 adenosine receptors reduces mouse intraocular pressure. *Invest Ophthalmol Vis Sci* 43(9): 3021-3026.

Bar-Ilan, A., Pessah, N. I. and Maren, T. H. (1984). The effects of carbonic anhydrase inhibitors on aqueous humor chemistry and dynamics. *Invest Ophthalmol Vis Sci* 25(10):1198–1205.

Barros, F., Lopez-Briones, L. G., Coca-Prados, M. and Belmonte, C. (1991). Detection and characterization of Ca^{2+}-activated K^{+} channels in transformed cells of human non-pigmented ciliary epithelium. *Curr Eye Res* 10(8): 731-738.

Bary, A. R., Tucker, I. G. and Davies, N. M. (2000). Considerations in the use of hydroxypropyl-beta-cyclodextrin in the formulation of aqueous ophthalmic solutions of hydrocortisone. *Eur J Pharm Biopharm* 50(2): 237–244.

Baudouin, J. E. and Tachon, P. (1996). Constitutive nitric oxide synthase is present in normal human keratinocytes. *J Investig Dermatol* 106(3): 428-431.

Becker, B. (1960). Hypothermia and aqueous humor dynamics of the rabbit eye. *Trans Am Ophthalmol Soc* 58: 337-363.

Becker, B. (1963). Ouabain and Aqueous Humor Dynamics in the Rabbit Eye. *Invest Ophthalmol* 2(4): 325-331.

Becker, B. (1980). Vanadate and aqueous humor dynamics. Proctor Lecture. *Invest Ophthalmol Vis Sci* 19(10): 1156-65.

Bill, A. (1973). The role of ciliary blood flow and ultrafiltration in aqueous humor formation. *Exp Eye Res* 16(4): 287-98.

Bill, A. (1975). Blood circulation and fluid dynamics in the eye. *Physiol Rev* 55(3): 383-417.

Bonham, M., Posakony, J., Coleman, I., Montgomery, B., Simon, J. and Nelson, P. S. (2005). Characterization of chemical constituents in Scutellaria baicalensis with antiandrogenic and growth-inhibitory activities toward prostate carcinoma. *Clin Cancer Res* 11(10): 3905–3914.

Bowler, J. M., Peart, D., Purves, R. D., Carre, D. A., Macknight, A. D. and Civan, M. M. (1996). Electron probe X-ray microanalysis of rabbit ciliary epithelium. *Exp Eye Res* 62(2): 131-9.

Bräuner, T., Hülser, D. F. and Strasser, R. J. (1984). Comparative measurements of membrane potentials with microelectrodes and voltage-sensitive dyes. *BBA-Biomembranes* 771(2): 208-216.

Brazy, P. C. and Gunn, R. B. (1976). Furosemide inhibition of chloride transport in human red blood cells. *J. Gen. Physiol*. 68(6): 583–599.

Brown, J. E., Khodr, H., Hider, R. C. and Rice-Evans, C. A. (1998). Structural dependence of flavonoid interactions with Cu^{2+} ions: implications for their antioxidant properties. *Biochem*. 330(Pt3): 1173–8.

Brubaker, R. F. (1991). Flow of aqueous humor in humans [The Friedenwald Lecture]. *Invest Ophthalmol Vis Sci* 32(13): 3145-66.

Brubaker, R. F. (1998). Clinical measurements of aqueous dynamics: implications for addressing glaucoma. *Curr Top Membr* 45: 234-284.

Burg, M., Stone, L., Cardinal, J. and Green, N. (1973). Furosemide effect on isolated perfused tubules. *Am. J. Physiol* 225(1): 119–124.

Butler, G. A., Chen, M., Stegman, Z. and Wolosin, J. M. (1994). Na^+- Cl^-- and HCO_3^-dependent base uptake in the ciliary body pigment epithelium. *Exp Eye Res* 59(3): 343-349.

Cai, Y., Luo, Q., Sun, M., and Corke, H. (2004). Antioxidant activity and phenolic compounds of 112 traditional Chinese medicinal plants associated with anticancer. *Life Sciences* 74(17): 2157-2184.

Candia, O. A. (1973). Short-circuit current related to active transport of chloride in frog cornea: Effects of furosemide and ethacrynic acid. *Biochim Biophys Acta* 298(4):1011–1014.

Candia, O. A., Shi, X. P. and Chu, T. C. (1991). Ascorbate-stimulated active Na+ transport in rabbit ciliary epithelium. *Curr Eye Res* 10(3): 197-203.

Candia, O. A., To, C. H., Gerometta, R. M. and Zamudio, A. C. (2005). Spontaneous fluid transport across isolated rabbit and bovine ciliary body preparations. *Invest Ophthalmol Vis Sci* 46(3): 939-947.

Candia, O. A., To, C. H., and Law, C. S. (2007). Fluid Transport across the Isolated Porcine Ciliary Epithelium. *Invest Ophthalmol Vis Sci* 48(1): 321-327.

Carre, D. A., Mitchell, C. H., Peterson-Yantorno, K., Coca-Prados, M. and Civan, M. M. (1997). Adenosine stimulates Cl- channels of nonpigmented ciliary epithelial cells. *Am J Physiol* 273(4 Pt 1): C1354-61.

Carre, D. A., Mitchell, C. H., Peterson-Yantorno, K., Coca-Prados, M. and Civan, M.M. (2000). Similarity of A3-adenosine and swelling-activated Cl^- channels in nonpigmented ciliary epithelial cells. *Am J Physiol Cell Physiol* 279(2): C440-51.

Carre, D. A., Mitchell, C. H., Peterson-Yantorno, K., Coca-Prados, M. and Civan, M. M. (2000). Similarity of A3-adenosine and swelling-activated Cl^- channels in nonpigmented ciliary epithelial cells. *Am J Physiol Cell Physiol* 279(2): C440-51.

Chang, W. H., Chen, C. H. and Lu, F. J. (2002). Different effects of Baicalein, Baicalin and Wogonin on mitochondrial function, glutathione content and cell cycle progression in human hepatoma cell lines. *Planta Med* 68(2): 128-132.

Chang, Z. Y., Yeh, M. K., Chiang, C. H., Chen, Y. H. and Lu, D.W. (2013). Erythropoietin Protects Adult Retinal Ganglion Cells against NMDA-, Trophic Factor Withdrawal-, and TNF-α-Induced Damage. *PLoS ONE* 8(1): e55291.

Chao, H. M., Chuang, M. J., Liu, J. H., Liu, X. Q., Ho, L. K., Pan, W. H., Zhang, X. M., Liu, C. M., Tsai, S. K., Kong, C. W., Lee, S. D., Chen, M. M. and Chao, F. P. (2013). Baicalein protects against retinal ischemia by antioxidation, antiapoptosis, downregulation of HIF-1α, VEGF, and MMP-9 and upregulation of HO-1. *J Ocul Pharmacol Ther* 29(6): 539-549.

Chauhan, B. C., Pan, J., Archibald, M. L., LeVatte, T. L., Kelly, M. E. and Tremblay, F. (2002). Effect of intraocular pressure on optic disc topography,

electroretinography, and axonal loss in a chronic pressure-induced rat model of optic nerve damage. *Invest Ophthalmol Vis Sci* 43(9): 2969–2976.

Chen, C. J., Raung, S. L., Liao, S. L., and Chen, S. Y. (2004). Inhibition of inducible nitric oxide synthase expression by baicalein in endotoxin/cytokine-stimulated microglia. *Biochem Pharmacol* 67(5): 957-965.

Chen, H., Pellegrini, J., Aggarwal, S., Lei, S., Warach, S., Jensen, F., and Lipton, S. (1992). Open-channel block of N-methyl-D-aspartate (NMDA) responses by memantine: therapeutic advantage against NMDA receptor-mediated neurotoxicity. *J Neurosci* 12(11): 4427-4436.

Chen, H. S. V., Wang, Y. F., Rayudu, P. V., Edgecomb, P., Neill, J. C., Segal, M. M., Lipton, S. A. and Jensen, F. E. (1998). Neuroprotective concentrations of the N-methyl-D-aspartate open-channel blocker memantine are effective without cytoplasmic vacuolation following post-ischemic administration and do not block maze learning or long-term potentiation. *Neuroscience* 86(4): 1121-1132.

Chen, L., Wang, L. and Jacob, T. J. (1999). Association of intrinsic pICln with volume-activated Cl- current and volume regulation in a native epithelial cell. *Am J Physiol* 276(1 Pt 1): C182-92.

Chen, S. and Sears, M. (1997). A low conductance chloride channel in the basolateral membranes of the non-pigmented ciliary epithelium of the rabbit eye. *Curr Eye Res* 16(7): 710-8.

Chen, S., Inoue, R., Inomata, H. and Ito, Y. (1994). Role of cyclic AMP-induced Cl conductance in aqueous humour formation by the dog ciliary epithelium. *Br J Pharmacol* 112(4): 1137-45.

Chen, S., Ruan, Q., Bedner, E., Deptala, A., Wang, X., Hsieh, T. C., Traganos, F. and Darzynkiewicz, Z. (2001). Effects of the flavonoid baicalin and its metabolite baicalein on androgen receptor expression, cell cycle progression and apoptosis of prostate cancer cell lines. *Cell Proliferat* 34(5): 293-304.

Chen, Y. Q., Pan, W. H. T., Liu, J. H., Chen M. M., Liu, C. M., Yeh, M. Y., Tsai, S. K., Young, M. S., Zhang, X. M. and Chao, H. M. (2012). The effects and underlying mechanisms of S-allyl L-cysteine treatment of the retina after ischemia/reperfusion. *J Ocul Pharmacol Ther* 28(2): 110-117.

Cheng, P. Y., Lee, Y. M., Wu, Y. S., Chang, T. W., Jin, J. S., and Yen, M. H. (2007). Protective effect of baicalein against endotoxic shock in rats in vivo and in vitro. *Biochem Pharmacol* 73(6): 793-804.

Cheng, Y. H., Li, L. A., Lin, P., Cheng, L. C., Hung, C. H., Chang, N. W. and Lin, C. (2012). Baicalein induces G1 arrest in oral cancer cells by enhancing the degradation of cyclin D1 and activating AhR to decrease Rb phosphorylation. *Toxicol Appl Pharm* 263(3): 360-367.

Chiu, Y. W., Lin, T. H., Huang, W. S., Teng, C. Y., Liou, Y. S., Kuo, W. H., Lin, W. L., Huang, H. I., Tung, J. N., Huang, C. Y., Liu, J. Y., Wang, W. H., Hwang, J. M. and Kuo, H. C. (2011). Baicalein inhibits the migration and invasive properties of human hepatoma cells. *Toxicol Appl Pharmacol* 255(3): 316–326

Chu, T. C. and Candia, O. A. (1987). Electrically silent Na^+ and Cl^- fluxes across the rabbit ciliary epithelium. *Invest Ophthalmol Vis Sci* 28(3): 445-50.

Chu, T. C. and Candia, O. A. (1988). Active transport of ascorbate across the isolated rabbit ciliary epithelium. *Invest Ophthalmol Vis Sci* 29(4): 594-9.

Chung, H. S., Harris, A., Kagemann, L. and Martin, B. (1999). Peripapillary retinal blood flow in normal-tension glaucoma. *Br J Ophthalmol* 83(4): 466–9.

Ciesielska, E., Gwardys, A. and Metodiewa, D. (2002). Anticancer, antiradical and antioxidative actions of novel Antoksyd S and its major components, baicalin and baicalein. *Anticancer Res* 22(5): 2885-2891.

Civan, M. M. (2003). The fall and rise of active chloride transport: implications for regulation of intraocular pressure. *J Exp Zoolog Part A Comp Exp Biol* 300(1): 5-13.

Civan, M. M., Coca-Prados, M. and Peterson-Yantorno, K. (1994). Pathways signaling the regulatory volume decrease of cultured nonpigmented ciliary epithelial cells. *Invest Ophthalmol Vis Sci* 35(6): 2876-86.

Civan, M. M., Peterson-Yantorno, K., Sanchez-Torres, J. and Coca-Prados, M. (1997). Potential contribution of epithelial Na^+ channel to net secretion of aqueous humor. *J Exp Zool* 279(5): 498-503.

Civan, M. M., Coca-Prados, M. and Peterson-Yantorno, K. (1994). Pathways signaling the regulatory volume decrease of cultured nonpigmented ciliary epithelial cells. *Invest Ophthalmol Vis Sci* 35(6): 2876-2886.

Coca-Prados, M., Anguita, J., Chalfant, M. L. and Civan, M. M. (1995). PKC-sensitive Cl- channels associated with ciliary epithelial homologue of pICln. *Am J Physiol* 268(3 Pt 1): C572-9.

Coca-Prados, M., Ghosh, S., Gilula, N. B. and Kumar, N. M. (1992). Expression and cellular distribution of the alpha 1 gap junction gene product in the ocular pigmented ciliary epithelium. *Curr Eye Res* 11(2): 113-22.

Coca-Prados, M., Sanchez-Torres, J., Peterson-Yantorno, K. and Civan, M. M. (1996). Association of ClC-3 channel with Cl^- transport by human nonpigmented ciliary epithelial cells. *J Membr Biol* 150(2): 197-208.

Coffey, K. L., Krushinsky, A., Green, C. R. and Donaldson, P. J. (2002). Molecular profiling and cellular localization of connexin isoforms in the rat ciliary epithelium. *Exp Eye Res* 75(1): 9-21.

Cole, D. F. (1961). Electrical Potential across the Isolated Ciliary Body Observed in Vitro. *Br J Ophthalmol* 45(10): 641-53.

Cole, D. F. (1962). Transport across the Isolated Ciliary Body of Ox and Rabbit. *Br J Ophthalmol* 46(10): 577-91.

Cole, D. F. (1964). Location of Ouabain-Sensitive Adenosine Triphosphatase in Ciliary Epithelium. *Exp Eye Res* 3(1): 72-5.

Cole, D. F. (1969). Evidence for active transport of chloride in ciliary epithelium of the rabbit. *Exp Eye Res* 8(1): 5-15.

Collaborative Normal-Tension Glaucoma Study Group (1998a). Comparison of glaucomatous progression between untreated patients with normal-tension glaucoma and patients with therapeutically reduced intraocular pressures. *Am J Ophthalmol* 126(4): 487-97.

Collaborative Normal-Tension Glaucoma Study Group (1998b). The effectiveness of intraocular pressure reduction in the treatment of normal-tension glaucoma. *Am J Ophthalmol* 126(4): 498-505.

Cotin, S., Calliste, C. A., Mazeron, M. C., Hantz, S., Duroux, J. L., Rawlinson, W. D., Ploy, M. C. and Alain, S. (2012). Eight flavonoids and their potential as inhibitors of human cytomegalovirus replication. *Antivir Res* 96(2): 181-186.

Counillon, L., Touret, N., Bidet, M., Peterson-Yantorno, K., Coca-Prados, M., Stuart-Tilley, A., Wilhelm, S., Alper, S. L. and Civan, M. M. (2000). Na+/H+ and CI-/HCO3- antiporters of bovine pigmented ciliary epithelial cells. *Pflugers Arch* 440(5): 667-78.

Crook, R. B., Takahashi, K., Mead, A., Dunn, J. J. and Sears, M. L. (2000). The role of NaKCl cotransport in blood-to-aqueous chloride fluxes across rabbit ciliary epithelium. *Invest Ophthalmol Vis Sci* 41(9): 2574-83..

Crook, R. B., Von Brauchitsch, D. K., and Polansky, J. R. (1992). Potassium transport in nonpigmented epithelial cells of ocular ciliary body: Inhibition of a Na^+, K^+, Cl^- cotransporter by protein kinase C. *J Cell Physiol* 153(1): 214-220.

Crosson, C. E. and Petrovich, M. (1999). Contributions of adenosine receptor activation to the ocular actions of epinephrine. *Invest Ophthalmol Vis Sci* 40(9): 2054-61.

Dailey, R. A., Brubaker, R. F. and Bourne, W. M. (1982). The effects of timolol maleate and acetazolamide on the rate of aqueous formation in normal human subjects. *Am J Ophthalmol* 93(2): 232-7.

Davson, H. (1990). The aqueous humor and the intraocular pressure. Physiology of the Eye. H. Davson. London, *Macmillan Press*: 3-95.

Davson, H. and Luck, C. P. (1956). A comparative study of the total carbon dioxide in the ocular fluids, cerebrospinal fluid, and plasma of some mammalian species. *J Physiol* 132(2): 454-64.

Dekker, L. V. and Parker, P. J. (1994). Protein kinase C—a question of specificity. *Trends Biochem Sci* 19(2): 73–77.

Delamere, N. A. and King, K. L. (1992). The influence of cyclic AMP upon Na^+, K^+-ATPase activity in rabbit ciliary epithelium. *Invest Ophthalmol Vis Sci* 33(2): 430-5.

Detry-Morel, M. L., Van Acker, E., Pourjavan, S., Levi, N. and De Potter, P. (2006). Anterior segment imaging using optical coherence tomography and ultrasound biomicroscopy in secondary pigmentary glaucoma associated with in-the-bag intraocular lens. *J Cataract Refract Surg* 32(11): 1866-1869.

Deuticke, B and Gerlach, E. (1967). Beeinflussung von Form und Phosphat-Permeabilität menschlicher Erythrocyten durch Hämolysine, Benzol-Derivate und pharmakologisch aktive Substanzen. *Klin. Wschr* 45(19): 977-983.

Devor, D. C., Simasko, S. M. and Duffey, M. E. (1990). Carbachol induces oscillations of membrane potassium conductance in a colonic cell line, T84. *Am J Physiol Cell Physiol* 258(2): C318-C326.

Do, C. W. and To, C. H. (2000). Chloride secretion by bovine ciliary epithelium: a model of aqueous humor formation. *Invest Ophthalmol Vis S*ci 41(7): 1853-60.

Do, C. W., Kong, C. W. and To, C. H. (2004). cAMP inhibits transepithelial chloride secretion across bovine ciliary body/epithelium. *Invest Ophthalmol Vis Sci* 45(10): 3638-43.

Do, C. W., Lu, W., Mitchell, C. H. and Civan, M. M. (2005). Inhibition of swelling-activated Cl^- currents by functional anti-ClC-3 antibody in native bovine non-pigmented ciliary epithelial cells. *Invest Ophthalmol Vis Sci* 46(3): 948-55.

Do, C. W., Peterson-Yantorno, K. and Civan, M. M. (2006). Swelling-activated Cl^- channels support Cl- secretion by bovine ciliary epithelium. *Invest Ophthalmol Vis Sci* 47(6): 2576-82.

Do, C. W., Peterson-Yantorno, K., Mitchell, C. H. and Civan, M. M. (2004). cAMP-activated maxi-Cl channels in native bovine pigmented ciliary epithelial cells. *Am J Physiol Cell Physiol* 287(4): C1003-11.

Dobbs, P. C., Epstein, D. L. and Anderson, P. J. (1979). Identification of isoenzyme C as the principal carbonic anhydrase in human ciliary processes. *Invest Ophthalmol Vis Sci* 18(8): 867-70.

Dong, J., and Delamere, N. A. (1994). Protein kinase C inhibits Na(+)-K(+)-2Cl-cotransporter activity in cultured rabbit nonpigmented ciliary epithelium. *Am J Physiol Cell Physiol* 267(6): C1553-C1560.

Dou, W., Mukherjee, S., Li, H., Venkatesh, M., Wang, H., Kortagere, S., Peleg, A., Chilimuri, S. S., Wang, Z. T., Feng, Y., Fearon, E. R. and Mani, S. (2012). Alleviation of gut inflammation by Cdx2/Pxr pathway in a mouse model of chemical colitis. *PLoS ONE* 7(7): e36075.

Duan, D., Cowley, S., Horowitz, B., and Hume, J. R. (1999). A serine residue in ClC-3 links phosphorylation–dephosphorylation to chloride channel regulation by cell volume. *J Gen Physiol.* 113(1): 57-70.

Dunn, J. J., Lytle, C. and Crook, R. B. (2001). Immunolocalization of the Na^+-K^+-Cl^--cotransporter in bovine ciliary epithelium. *Invest Ophthalmol Vis Sci* 42(2): 343-53.

Edelman, J. L., Loo, D. D. and Sachs, G. (1995). Characterization of potassium and chloride channels in the basolateral membrane of bovine nonpigmented ciliary epithelial cells. *Invest Ophthalmol Vis Sci* 36(13): 2706-16.

Edelman, J. L., Sachs, G. and Adorante, J. S. (1994). Ion transport asymmetry and functional coupling in bovine pigmented and nonpigmented ciliary epithelial cells. *Am J Physiol* 266(5 Pt 1): C1210-21.

Ellis, D. Z., Nathanson, J. A., Rabe, J. and Sweadner, K. J. (2001). Carbachol and nitric oxide inhibition of Na,K-ATPase activity in bovine ciliary processes. *Invest Ophthalmol Vis Sci* 42(11): 2625-31.

Flammer, J. and Mozaffarieh, M. (2007). What is the present pathogenetic concept of glaucomatous optic neuropathy? *Surv Ophthalmol* 52(Suppl. 2): S162–73.

Fleischhauer, J. C., Mitchell, C. H., Peterson-Yantorno, K., Coca-Prados, M. and Civan, M. M. (2001). PGE2, Ca^{2+} and cAMP mediate ATP activation of Cl^{-} channels in pigmented ciliary epithelial cells. *Am J Physiol Cell Physiol* 281: C1614-C1623.

Flugel, C. and Lutjen-Drecoll, E. (1988). Presence and distribution of Na^{+} /K^{+} -ATPase in the ciliary epithelium of the rabbit. *Histochemistry* 88(3-6): 613-21.

Friedenwald, J. S. (1949). The formation of the intraocular fluid. *Am J Ophthalmol 32 Pt* 2(6): 9-27.

Fuchshofer, R. and Tamm, E. R. (2012). The role of TGF-b in the pathogenesis of primary open-angle glaucoma. *Cell Tissue Res* 347(1): 279-290.

Gonzalez, J. E. and Maher, M. P. (2002) Cellular fluorescent indicators and voltage/ion probe reader (VIPR™): Tools for ion channel and receptor drug discovery. *Receptors and Channels* 8(5-6): 283-295.

Gao, D., Sakurai, K., Chen, J. and Ogiso, T. (1995). Protection by baicalein against ascorbic acid-induced lipid peroxidation of rat liver microsomes. *Res Commun Mol Pathol Pharmacol* 90(1): 103–114.

Gao, D., Sakurai, K., Katoh, M., Chen, J. and Ogiso, T. (1996). Inhibition of microsomal lipid peroxidation by baicalein: A possible formation of an iron-baicalein complex. *IUBMB Life* 39(2): 215-225.

Gao, H., Nishioka, T., Kawabata, J. and Kasai, T. (2004). Structure-activity Relationships for alpha-Glucosidase inhibition of Baicalein, 5, 6, 7-Trihydroxyflavone: the Effect of A-Ring Substitution. *Bios Biotechnol Biochem* 68(2): 369-375.

Gao, Z., Huang, K., Yang, X. and Xu, H. (1999). Free radical scavenging and antioxidant activities of flavonoids extracted from the radix of Scutellaria baicalensis Georgi. *Biochim Biophys Acta* 1472(3): 643-650.

Garg, L. C. and Oppelt, W. W. (1970). The effect of ouabain and acetazolamide on transport of sodium and chloride from plasma to aqueous humor. *J Pharmacol Exp Ther* 175(2): 237-47.

Geyer, O., Podos, S. M. and Mittag, T. (1997). Nitric oxide synthase activity in tissues of the bovine eye. *Graefes Arch Clin Exp Ophthalmol* 235(12): 786–93.

Gherghel, D., Griffiths, H. R., Hilton, E. J., Cunliffe, I. A. and Hosking, S. L. (2005). Systemic reduction in glutathione levels occurs in patients with primary open-angle glaucoma. *Invest Ophthalmol Vis Sci* 46(3): 877–883.

Ghosh, S., Freitag, A. C., Martin-Vasallo, P. and Coca-Prados, M. (1990). Cellular distribution and differential gene expression of the three alpha subunit isoforms of the Na^+, K^+-ATPase in the ocular ciliary epithelium. *J Biol Chem* 265(5): 2935-40.

Ghosh, S., Hernando, N., Martin-Alonso, J. M., Martin-Vasallo, P. and Coca-Prados, M. (1991). Expression of multiple Na^+, K^+-ATPase genes reveals a gradient of isoforms along the nonpigmented ciliary epithelium: functional implications in aqueous humor secretion. *J Cell Physiol* 149(2): 184-94.

Ghosh, S., Mukherjee, A., Sadler, P. J. and Verma, S. (2008). Periodic Iron Nanomineralization in Human Serum Transferrin Fibrils. *Angew Chem Int Ed* 47(2): 2217-2221.

Glynn, I. M. (2002). A hundred years of sodium pumping. *Annu Rev Physiol* 64: 1-18.

Green, K. and Pederson, J. E. (1972). Contribution of secretion and filtration to aqueous humor formation. *Am J Physiol* 222(5): 1218-26.

Green, K., Bountra, C., Georgiou, P. and House, C. R. (1985). An electrophysiologic study of rabbit ciliary epithelium. *Invest Ophthalmol Vis Sci* 26(3): 371-81.

Gribble, G. W. and Berthel, S., Studies in Natural Products Chemistry, Elsevier, New York, vol. 12 (1993) 365

Guelrud, M., Rudick, J and Janowitz, H. D. (1972). Effects of some inhibitors of sodium transport (adenosine triphosphate inhibitors) on pancreatic secretion. *Gastroenterology* 62: 540-546.

Guo, L., Moss, S. E., Alexander, R. A., Ali, R. R., Fitzke, F. W. and Cordeiro, M. F. (2005). Retinal ganglion cell apoptosis in glaucoma is related to intraocular pressure and IOP-induced effects on extracellular matrix. *Invest Ophthalmol Vis Sci* 46(1): 175–182.

Hamada, H., Hiramatsu, M., Edamatsu, R. and Mori, A. (1993). Free radical scavenging action of baicalein. *Arch Biochem Biophys* 306(1): 261–266.

Hanneken, A., Lin, F. F., Johnson, J. and Maher, P. (2006). Flavonoids Protect Human Retinal Pigment Epithelial Cells from Oxidative-Stress–Induced Death. *Invest Ophthalmol Vis Sci* 47(7): 3164-3177.

Hänninen, V. A., Pantcheva, M. B., Freeman, E. E., Poulin, N. R., and Grosskreutz, C. L. (2002). Activation of caspase 9 in a rat model of experimental glaucoma. *Curr Eye Res* 25(6): 389-395.

Haufschild, T., Nava, E., Meyer, P., Flammer, J., Lüscher, T. F., and Haefliger, I. O. (1996). Spontaneous calcium-independent nitric oxide synthase activity in porcine ciliary processes. *Biochem Biophys Res Commu* 222(3): 786-789.

Havsteen, B. H. (2002). The biochemistry and medical significance of the flavonoids. *Pharmacol Ther* 96(2-3): 67–202.

Helbig, H., Korbmacher, C., Stumpff, F., Coca-Prados, M. and Wiederholt, M. (1989b). Role of HCO3- in regulation of cytoplasmic pH in ciliary epithelial cells. *Am J Physiol* 257(4 Pt 1): C696-705.

Helbig, H., Korbmacher, C., Wohlfarth, J., Coroneo, M. T., Lindschau, C., Quass, P., Haller, H., Coca-Prados, M. and Wiederholt, M. (1989). Effect of acetylcholine on membrane potential of cultured human nonpigmented ciliary epithelial cells. *Invest Ophthalmol Vis Sci* 30(5): 890-6.

Hidaka, H. and Kobayashi, R. (1992). Pharmacology of protein kinase inhibitors. *Annu Rev Pharmacol Toxicol* 32: 377-97.

Hidaka, H., Watanabe, M. and Kobayashi, R. (1991). Properties and use of H-series compounds as protein kinase inhibitors. *Methods Enzymol* 201: 328-39.

Hobbs, A. J., Higgs, A. and Moncada, S. (1999). Inhibition of nitric oxide synthase as a potential therapeutic target. *Annu Rev Pharmacol Toxicol* 39: 191-220.

Hochgesand, D. H., Dunn, J. J. and Crook, R. B. (2001). Catecholaminergic regulation of Na^+-K^+-Cl^- cotransport in pigmented ciliary epithelium: differences between PE and NPE. *Exp Eye Res* 72(1): 1-12.

Holland, M. G. (1970). Chloride ion transport in the isolated ciliary body. II. Ion substitution experiments. *Invest Ophthalmol Vis Sci* 9(1): 30-41.

Holland, M. G. and Gipson, C. C. (1970). Chloride ion transport in the isolated ciliary body. *Invest Ophthalmol Vis Sci* 9(1): 20-9.

Hosseini, A., Lattanzio, F. A., Schellenberg, K., Shaeffer, J., Samudre, S. S. and Williams, P. B. (2006). Effects of novel free radical scavengers on intraocular pressure and electroretinograms in rat glaucoma models. *FASEB J* 20: 689.

Howard, M., Sen, H. A., Capoor, S., Herfel, R., Crooks, P. A. and Jacobson, M. K. (1998). Measurement of adenosine concentration in aqueous and vitreous. *Invest Ophthalmol Vis Sci* 39(10): 1942-6.

Huang, P., Qi, Y., Xu, Y. S., Liu, J., Liao, D., Zhang, S. S. and Zhang, C. (2010). Serum cytokine alteration is associated with optic neuropathy in human primary open angle glaucoma. *J Glaucoma* 19(5): 324-330.

Huang, P., Zhang, S. S. and Zhang, C. (2009). The two sides of cytokine signaling and glaucomatous optic neuropathy. *J Ocul Biol Dis Infor* 2(2): 78-83.

Huang, W., Dobberfuhl, A., Filippopoulos, T., Ingelsson, M., Fileta, J. B., Poulin, N. R., and Grosskreutz, C. L. (2005b). Transcriptional Up-Regulation and Activation of Initiating Caspases in Experimental Glaucoma. *Am J Pathol* 167(3): 673-681.

Huang, W., Fileta, J. B., Dobberfuhl, A., Filippopolous, T., Guo, Y., Kwon, G., and Grosskreutz, C. L. (2005a). Calcineurin cleavage is triggered by elevated intraocular pressure, and calcineurin inhibition blocks retinal ganglion cell death in experimental glaucoma. *Proc Natl Acad Sci* 102(34): 12242-12247.

Hug, H. and Sarre, T. F. (1993). Protein kinase C isoenzymes: divergence in signal transduction? *Biochem J* 291(Pt 2): 329 –343.

Hwang, K. Y., Oh, Y. T., Yoon, H., Lee, J., Kim, H., Choe, W. and Kang, I. (2008). Baicalein suppresses hypoxia-induced HIF-1α protein accumulation and activation through inhibition of reactive oxygen species and PI 3-kinase/Akt pathway in BV2 murine microglial cells. *Neurosci Lett* 444(3): 264-269.

Iizuka, S., Kishida, K., Tsuboi, S., Emi, K. and Manabe, R. (1984). Electrical characteristics of the isolated dog ciliary body. *Curr Eye Res* 3(3): 417-421.

Ikemoto, S., Sugimura, K., Kuratukuri, K. and Nakatani, T. (2004). Antitumor Effects of Lipoxygenase Inhibitors on Murine Bladder Cancer Cell Line (MBT-2). *Anticancer Res* 24(2B): 733-736.

Izzotti, A., Bagnis, A. and Sacca, S. C. (2006). The role of oxidative stress in glaucoma. *Mutat. Res.* 612(2): 105–114.

Izzotti, A., Sacca, S. C., Cartiglia, C., and De Flora, S. (2003). Oxidative deoxyribonucleic acid damage in the eyes of glaucoma patients. *Am J Med* 114(8): 638–646.

Jacob, T. J. (1991). Two outward K^+ currents in bovine pigmented ciliary epithelial cells: IK(Ca) and IK(V). *Am J Physiol* 261(6 Pt 1): C1055-62.

Jaken, S. (1996) Protein kinase C isozymes and substrates. *Curr Opin Cell Biol* 8(2): 168–173.

Johari, J., Kianmehr, A., Mustafa, M., Abubakar, S. and Zandi, K. (2012). Antiviral Activity of Baicalein and Quercetin against the Japanese Encephalitis Virus. *Int J Mol Sci* 13(12): 16785-16795.

Kahn, M. G., Giblin, F. J and Epstein, D. L. (1983). Glutathione in calf trabecular meshwork and its relation to aqueous humor outflow facility. *Invest Ophthalmol Vis Sci* 24(9): 1283-1287.

Kaneko, T., Chiba, H., Horie, N., Kato, T., Kobayashi, M., Hashimoto, K., Kusama, K., and Sakagami, H. (2010). Inhibition of Prostaglandin E2 Production by Flavone and its Related Compounds. *In Vivo* 24(1): 55-58.

Kass, M. A., Heuer, D. K., Higginbotham, E. J., Johnson, C. A., Keltner, J. L., Miller, J. P., Parrish, R. K., Wilson, M. R. and Gordon, M. O. (2002). The ocular hypertension treatment study: A randomized trial determines that topical ocular hypotensive medication delays or prevents the onset of primary open-angle glaucoma. *Arch Ophthalmol* 120(6): 701-713.

Kawasaki, M., Uchida, S., Monkawa, T., Miyawaki, A., Mikoshiba, K., Marumo, F. and Sasaki, S. (1994). Cloning and expression of a protein kinase C-regulated chloride channel abundantly expressed in rat brain neuronal cells. *Neuron* 12(3):597–604.

Khoo, B. Y., Chua, S. L. and Balaram, P. (2010). Apoptotic effects of chrysin in human cancer cell lines. *Int J Mol Sci* 11(5): 2188-2199.

Kimata, M., Shichijo, M., Miura, T., Serizawa, I., Inagaki, N. and Nagai, N. (2000). Effects of luteolin, quercetin and baicalein on immunoglobulin E-mediated mediator release from human cultured mast cells. *Clin Exp Allergy* 30(4): 501–508.

Kimura, Y., Matsushita, N., Yokoi-Hayashi, K. and Okuda, H. (2001) Effects of baicalein isolated from Scutellaria baicalensis Radix on adhesion molecule expression induced by thrombin and thrombin receptor agonist peptide in cultured human umbilical vein endothelial cells. *Planta Med* 67(4): 331–334.

King, K. L., Delamere, N. A., Csukas, S. C., and Pierce Jr, W. M. (1992). Metabolism of arachidonic acid by isolated rabbit ciliary epithelium. *Exp Eye Res* 55(2): 235-241.

Kishida, K., Sasabe, T., Iizuka, S., Manabe, R. and Otori, T. (1982). Sodium and chloride transport across the isolated rabbit ciliary body. *Curr Eye Res* 2(3): 149-52.

Kishida, K., Sasabe, T., Manabe, R. and Otori, T. (1981). Electric characteristics of the isolated rabbit ciliary body. *Jpn J Ophthalmol* 25: 407-416.

Knapp, S., Bertelmann, E., Hartmann, C., Keipert, S. and Pleyer, U. (2003) Intraocular availability of topically applied mycophenolate mofetil in rabbits. *J Ocul Pharmacol Ther* 19(2): 181–192.

Ko, M. L., Hu D. N., Ritch R. and Sharma, S. C. (2000). The combined effect of brain-derived neurotrophic factor and a free radical scavenger in experimental glaucoma. *Invest Ophthalmol. Vis. Sci* 41(10): 2967–2971.

Ko, W. H., Law, V. W. Y., Yip, W. C. Y., Yue, G. G. L., Lau, C. W., Chen, Z. Y. and Huang, Y. (2002). Stimulation of chloride secretion by baicalein in isolated rat distal colon. *Am J Physiol Gastrointest Liver Physiol* 282(3): G508-G518.

Kodama, T., Reddy, V. N. and Macri, F. J. (1985). Pharmacological study on the effects of some ocular hypotensive drugs on aqueous humor formation in the arterially perfused enucleated rabbit eye. *Ophthalmic Res* 17(2): 120-4.

Kong, C. W., Li, K. K. and To, C. H. (2006). Chloride secretion by porcine ciliary epithelium: new insight into species similarities and differences in aqueous humor formation. *Invest Ophthalmol Vis Sci* 47(12): 5428-36.

Kong, M. C. W., Tse, D. Y. and To, C. H. (2005). Regulation of Nitric Oxide (NO) on the chloride (Cl^-) secretion across the porcine ciliary body epithelium (CBE) via both cGMP-dependent and -independent Pathway. *Invest Ophthalmol Vis Sci* 46(5): E-Abstract 2414.

Koseki, Y., Kitano, S. and Podos, S. M. (1994). A nitric oxide synthase inhibitor protects against anoxia in cultured rat retinal ganglion cells. *Invest Ophthalmol Vis Sci* 35: 1968.

Krupin, T. and Civan, M. M. (1996). Physiologic basis of aqueous humor formation. The Glaucomas: Basic Sciences, vol 1. R. Ritch, M. B. Shields and T. Krupin. St. Louis, Mosby: 251-280.

Krupin, T., Reinach, P. S., Candia, O. A. and Podos, S. M. (1984). Transepithelial electrical measurements on the isolated rabbit iris-ciliary body. *Exp Eye Res* 38(2): 115-23.

Kvanta, A., Seregard, S., Sejersen, S., Kull, B. and Fredholm, B. B. (1997). Localization of adenosine receptor messenger RNAs in the rat eye. *Exp Eye Res* 65(5): 595-602.

Larsson, L. I. and Alm, A. (1998). Aqueous humor flow in human eyes treated with dorzolamide and different doses of acetazolamide. *Arch Ophthalmol* 116(1): 19-24.

Law, C. S., Candia, O. A. and To, C. H. (2009). Inhibitions of chloride transport and gap junction reduce fluid flow across the whole porcine ciliary epithelium. *Invest Ophthalmol Vis Sci* 50(3): 1299-306.

Lee, H. Z., Leung, H. W., Lai, M. Y. and Wu, C. H. (2005). Baicalein-induced cell cycle arrest and apoptosis in human lung squamous carcinoma CH27 cells. *Anticancer Res* 25(2A): 959–964.

Lee, S. W., Song, G. S., Kwon, C. H. and Kim, Y. K. (2005). Beneficial effect of flavonoid baicalein in cisplatin-induced cell death of human glioma cells. *Neurosci Lett* 382(1-2): 71-5.

Lee, J. H., Li, Y. C., Ip, S. W., Hsu, S. C., Chang, N. W., Tang, N. Y., Yu, C. S., Chou, S. T., Lin, S. S., Lin, C. C., Yang, J. S. and Chung, J. G. (2008). The Role of Ca^{2+} in Baicalein-induced Apoptosis in Human Breast MDA-MB-231 Cancer Cells through Mitochondria- and Caspase-3-dependent Pathway. *Anticancer Res* 28(3A): 1701-1711.

Leung, H. W., Yang, W. H., Lai, M. Y., Lin, C. J. and Lee, H. Z. (2007). Inhibition of 12-lipoxygenase during Baicalein-induced human lung nonsmall carcinoma H460 cell apoptosis. *Food Chem Toxicol* 45(3): 403–11.

Levin, L. A. and Louhab, A. (1996). Apoptosis of retinal ganglion cells in anterior ischemic optic neuropathy. *Arch. Ophthalmol* 114(4): 488-491.

Levkovitch-Verbin, H., Quigley, H.A., Martin, K. R., Valenta, D., Baumrind, L. A. and Pease, M. E. (2002). Translimbal laser photocoagulation to the trabecular meshwork as a model of glaucoma in rats. *Invest Ophthalmol Vis Sci* 43(2): 402–10.

Li, Z. F., Xia, X. M., Huang, C., Zhang, S., Zhang, J. and Zhang, A. J. (2009). Emodin and baicalein inhibit pancreatic stromal derived factor-1 expression in rats with acute pancreatitis. *Hepatobiliary Pancreat Dis Int* 8(2): 201-208.

Li, X., Alvarez, B., Casey, J. R., Reithmeier, R. A. and Fliegel, L. (2002). Carbonic anhydrase II binds to and enhances activity of the Na^+/H^+ exchanger. *J Biol Chem* 277(39): 36085-91.

Lipton, S. A. (2004). Paradigm shift in NMDA receptor antagonist drug development: Molecular mechanism of uncompetitive inhibition by memantine in the treatment of Alzheimer's disease and other neurologic disorders. *J Alzheimers Dis* 6(6 suppl): S61–74.

Liton, P. B., Luna, C., Bodman, M., Hong, A., Epstein, D. L. and Gonzalez, P. (2005). Induction of IL-6 by mechanical stress in the trabecular meshwork. *Biochem Biophys Res Commun* 337(4):1229-1236.

Liu, J., Qiu, L., Gao, J. and Jin, Y. (2006). Preparation, characterization, and in vivo evaluation of formulation of baicalein with hydroxypropylbeta-cyclodextrin. *Int J Pharm* 312(1-2):137–143.

Liu, J. H., Wann, H., Chen, M. M., Pan, W. H., Chen, Y. C., Liu, C. M., Yeh, M. Y., Tsai, S. K, Young, M. S., Chuang, H. Y., Chao, F. P. and Chao, H. M. (2010). Baicalein Significantly Protects Human Retinal Pigment Epithelium Cells Against H_2O_2-Induced Oxidative Stress by Scavenging Reactive Oxygen Species and Downregulating the Expression of Matrix Metalloproteinase-9 and Vascular Endothelial Growth Factor. *J Ocul Pharmacol Ther* 26(5): 421-429.

Liu, B., Jian, Z., Li, Q., Li, K., Wang, Z., Liu, L., Tang, L., Yi, X., Wang, H., Li, C. and Gao, T. (2012). Baicalein protects Human melanocytes from H_2O_2-induced apoptosis via inhibiting mitochondria-dependent caspase activation and the p38 MAPK pathway. *Free Radic Biol Med* 53(2): 183-193.

Lutjen-Drecoll, E. and Lonnerholm, G. (1981). Carbonic anhydrase distribution in the rabbit eye by light and electron microscopy. *Invest Ophthalmol Vis Sci* 21(6): 782-97.

Lutjen-Drecoll, E., Lonnerholm, G. and Eichhorn, M. (1983). Carbonic anhydrase distribution in the human and monkey eye by light and electron microscopy. *Graefes Arch Clin Exp Ophthalmol* 220(6): 285-91.

Ma, Z., Otsuyama, K. I., Liu, S., Abroun, S., Ishikawa, H., Tsuyama, N., Obata, M., Li, F. J., Zheng, X., Maki, Y., Miyamoto, K. and Kawano, M. M. (2005). Baicalein, a component of Scutellaria radix from Huang-Lian-Jie-Du-Tang (HLJDT), leads to suppression of proliferation and induction of apoptosis in human myeloma cells. *Blood* 105(8): 3312-3318.

Mabalirajan, U., Ahmad, T., Rehman, R., Leishangthem, G. D., Dinda, A. K., Agrawal, A., Ghosh, B., and Sharma, S. K. (2013). Baicalein Reduces Airway

Injury in Allergen and IL-13 Induced Airway Inflammation. *PLoS ONE* 8(4): e62916.

Maher, P. and Hanneken, A. (2008). Flavonoids protect retinal ganglion cells from ischemia in vitro. *Exp Eye Res* 86(2): 366-374.

Maher, P. and Hanneken, A. (2005). Flavonoids Protect Retinal Ganglion Cells from Oxidative Stress–Induced Death. *Invest Ophthalmol Vis Sci* 46(12): 4796-4803.

Maren, T. H. (1976). The rates of movement of Na^+, Cl^-, and HCO_3^- from plasma to posterior chamber: effect of acetazolamide and relation to the treatment of glaucoma. *Invest Ophthalmol* 15(5): 356-64.

Maren, T. H. (1977). Ion secretion into the posterior aqueous humor of dogs and monkeys. *Exp Eye Res* 25 Suppl: 245-7.

Marković, Z., Dimitrić Marković, J., Milenković, D., and Filipović, N. (2011). Mechanistic study of the structure–activity relationship for the free radical scavenging activity of baicalein. *J Mol Model* 17(10): 2575-2584.

Marshall, W. S., Bryson, S. E., and Garg, D. (1993). Alpha 2-adrenergic inhibition of Cl- transport by opercular epithelium is mediated by intracellular Ca^{2+}. *Proc Natl Acad Sci* 90(12): 5504-5508.

Martin, S., and Shuttleworth, T. (1994). Muscarinic-receptor activation stimulates oscillations in K^+ and Cl^- currents which are acutely dependent on extracellular Ca^{2+} in avian salt gland cells. *Pflugers Arch* 426(3-4): 231-238.

McKinnon, S. J., Lehman, D. M., Kerrigan-Baumrind, L. A., Merges, C. A., McLaughlin, C. W., Peart, D., Purves, R. D., Carre, D. A., Macknight, A. D. and Civan, M. M. (1998). Effects of HCO3- on cell composition of rabbit ciliary epithelium: a new model for aqueous humor secretion. *Invest Ophthalmol Vis Sci* 39(9): 1631-41.

McLaughlin, C. W., Zellhuber-McMillan, S., Macknight, A. D. and Civan, M. M. (2004). Electron microprobe analysis of ouabain-exposed ciliary epithelium: PE-NPE cell couplets form the functional units. *Am J Physiol Cell Physiol* 286(6): C1376-89.

Medzhitov, R. (2008). Origin and physiological roles of inflammation. *Nature* 454(7203): 428-435.

Meyer, P., Champion, C., Schlotzer-Schrehardt, U., Flammer, J. and Haefliger, I. O. (1999). Localization of nitric oxide synthase isoforms in porcine ocular tissues. *Curr Eye Res* 18(5): 375-80.

Miao, K and Joyner, W. L. (1994). In situ study of the membrane potential in microvascular endothelial cells using a fluorescent probe. *Microvasc Res* 48(1): 135—142.

Michelson, G., Langhans, M. J., Harazny, J. and Dichtl A. (1998). Visual field defect and perfusion of the juxtapapillary retina and the neuroretinal rim area in primary open-angle glaucoma. *Graefes Arch Clin Exp Ophthalmol* 236(2): 80–5.

Middleton, Jr. E., Kandaswami, C. and Theoharides, T. C. (2000). The effects of plant flavonoids on mammalian cells: implications for inflammation, heart disease, and cancer. *Pharmacol Rev* 52(4): 673–751.

Mitchell, C. H., Peterson-Yantorno, K., Carre, D. A., McGlinn, A. M., Coca-Prados, M., Stone, R. A. and Civan, M. M. (1999). A3 adenosine receptors regulate Cl^- channels of nonpigmented ciliary epithelial cells. *Am J Physiol* 276(3 Pt 1): C659-66.

Mito, T., and Delamere, N. A. (1993). Alteration of active Na-K transport on protein kinase C activation in cultured ciliary epithelium. *Invest Ophthalmol Vis Sci* 34(3): 539-546.

Mito, T., Delamere, N. A. and Coca-Prados, M. (1993). Calcium-dependent regulation of cation transport in cultured human nonpigmented ciliary epithelial cells. *Am J Physiol* 264(3 Pt 1): C519-26.

Miyahara, M., Ohtaka, H., Katayama, H., Tatsumi, Y., Miyaichi, Y. and Tomimori, T. (1993). Structure-activity relationship of flavonoids in suppressing rat liver lipid peroxidation. *Yakugaku Zasshi* 113(2): 133–154.

Morel, I., Lescoat, G., Cillard, P. and Cillard, J. (1994). Role of flavonoids and iron chelation in antioxidant action. *Methods Enzymol* 234: 437–43.

Moreno M. C., Campanelli J., Sande P., Sanez D. A., Keller M. I., Sarmiento M. I., and Rosenstein R. E.(2004). Retinal oxidative stress induced by high intraocular pressure, Free Radic. *Biol. Med.* 37(6): 803–812.

Mori, N., Yamada, E. and Sears, M. L. (1991). Immunocytochemical localization of Na/K-ATPase in the isolated ciliary epithelial bilayer of the rabbit. *Arch Histol Cytol* 54(3): 259-65.

Moro, M. A., Russel, R. J., Cellek, S., Lizasoain, I., Su, Y., Darley-Usmar, V. M., Radomski, M. W. and Moncada, S. (1996). cGMP mediates the vascular and platelet actions of nitric oxide: confirmation using an inhibitor of the soluble guanylyl cyclase. *Proc Natl Acad Sci USA* 93(4): 1480-5.

Morrison, J. C., Moore, C. G., Deppmeier, L. M., Gold, B. G., Meshul, C. K. and Johnson, E. C. (1997). A rat model of chronic pressure-induced optic nerve damage. *Exp Eye Res*. 64(1): 85–96.

Moslehi, M., Meshkini, A., and Yazdanparast, R. (2012). Flavonoid Baicalein Modulates H2O2-Induced Mitogen-Activated Protein Kinases Activation and Cell Death in SK-N-MC Cells. *Cell Mol Neurobiol* 32(4): 549-560.

Muther, T. F. and Friedland, B. R. (1980). Autoradiographic localization of carbonic anhydrase in the rabbit ciliary body. *J Histochem Cytochem* 28(10): 1119-24.

Nagaki, Y., Hayasaka, S., Kadoi, C., Nakamura, N. and Hayasaka, Y. (2001). Effects of Scutellariae Radix Extract and its Components (Baicalein, Baicalin, and Wogonin) on the Experimental Elevation of Aqueous Flare in Pigmented Rabbits. *Jpn J Ophthalmol* 45(3): 216-220.

Nagaki, Y., Hayasaka, S., Zhang, X.Y., Hayasaka, Y., Nakamura, N. and Terasawa, K. (2003). Effects of Topical Instillation of Traditional Herbal Medicines, Herbal Extracts, and Their Components on Prostaglandin E2-induced Aqueous Flare Elevation in Pigmented Rabbits. *Jpn J Ophthalmol* 47(3): 249-253.

Nakamura, S. and Nishizuka, Y. (1994). Lipid mediators and protein kinase C activation for the intracellular signaling network. *J Biochem (Tokyo)* 115(6): 1029–1034.

Nakamura, N., Hayasaka, S., Zhang, X.Y., Nagaki, Y., Matsumoto, M., Hayasaka, Y. and Terasawa, K. (2003). Effects of baicalin, baicalein, and wogonin on interleukin-6 and interleukin-8 expression, and nuclear factor-κb binding activities induced by interleukin-1β in human retinal pigment epithelial cell line. *Exp Eye Res* 77(2): 195-202.

Nakano, H., Nakajima, A., Sakon-Komazawa, S., Piao, J. H., Xue, X. and Okumura, K. (2006). Reactive oxygen species mediate crosstalk between NF-kappaB and JNK. *Cell Death Differ* 13(5): 730–7.

Naskar, R., Wissing, M. and Thanos, S. (2002). Detection of early neurondegeneration and accompanying microglial responses in theretina of a rat model of glaucoma. *Invest Ophthalmol Vis Sci* 43(9): 2962–2968.

Naveenkumar, C., Raghunandhakumar, S., Asokkumar, S. and Devaki, T. (2013). Baicalein abrogates reactive oxygen species (ROS)-mediated mitochondrial dysfunction during experimental pulmonary carcinogenesis in vivo. *Basic Clin Pharmacol Toxicol* 112(4): 270-281.

Ni, Y., Wu, R., Xu, W., Maecke, H., Flammer, J. and Haefliger, I. O. (2006). Effect of cAMP on porcine ciliary transepithelial short-circuit current, sodium transport, and chloride transport. *Invest Ophthalmol Vis Sci* 47(5): 2065-74.

Nicolela, M. T., Walman, B. E., Buckley, A. R. and Drance, S. M. (1996). Ocular hypertension and primary open-angle glaucoma: a comparative study of their retrobulbar blood flow velocity. *J Glaucoma* 5(5): 308–10.

Nishizuka, Y. (1992). Intracellular signalling by hydrolysis of phospholipids and activation of protein kinase C. *Science* 258(5082): 607– 614.

Nishizuka, Y. (1986). Studies and perspectives of protein kinase C. *Science* 233(4761): 305–312.

Oh, J., Krupin, T., Tang, L.Q., Sveen, J., and Lahlum, R.A. (1994). Dye coupling of rabbit ciliary epithelial cells in vitro. *Invest Ophthalmol Vis Sci* 35(5): 2509-2514.

Ong, K., Farinelli, A., Billson, F., Houang, M. and Stern, M. (1995). Comparative study of brain magnetic resonance imaging findings in patients with low-tension glaucoma and control subjects. *Ophthalmol* 102(11): 1632–8.

Oppelt, W. W. and White, E. D., Jr. (1968). Effect of ouabain on aqueous humor formation rate in cats. *Invest Ophthalmol* 7(3): 328-33.

Osborne, N. N., Casson, R. J., Wood, J. P. M., Chidlow, G., Graham, M., and Melena, J. (2004). Retinal ischemia: mechanisms of damage and potential therapeutic strategies. *Prog Retin Eye Res* 23(1): 91-147.

Osborne, N. N., Li, G. Y., Ji, D., Mortiboys, H. J. and Jackson, S. (2008). Light affects mitochondria to cause apoptosis to cultured cells: possible relevance to ganglion cell death in certain optic neuropathies. *J. Neurochem* 105(5): 2013–2028.

Ozawa, K., Szallasi, Z., Kazanietz, M. G., Blumberg, P. M., Mischak, H., Mushinski, J. F. and Beaven, M. A. (1993) Ca^{2+}-dependent and Ca^{2+}-independent isozymes of protein kinase C mediate exocytosis in antigen-stimulated rat basophilic RBL-2H3 cells. *J Biol Chem* 268(3): 1749 –1756.

Paris, S., and Pouysségur, J. (1986). Growth factors activate the bumetanide-sensitive $Na^+/K^+/Cl^-$ cotransport in hamster fibroblasts. *J Biol Chem* 261(14): 6177-6183.

Peng, P. H., Chao, H. M., Juan, S. H., Chen, C. F., Liu, J. H., and Ko, M. L. (2011). Pharmacological Preconditioning by Low Dose Cobalt Protoporphyrin Induces Heme Oxygenase-1 Overexpression and Alleviates Retinal Ischemia-Reperfusion Injury in Rats. *Curr Eye Res* 36(3): 238-246.

Perez, C. A., Wei, Y., and Guo, M. (2009). Iron-binding and anti-Fenton properties of baicalein and baicalin. *J Inorg Biochem 103*(3): 326-332.

Pesin, S. R. and Candia, O. A. (1982). Na^+ and Cl^- fluxes, and effects of pharmacological agents on the short-circuit current of the isolated rabbit iris-ciliary body. *Curr Eye Res* 2(12): 815-27.

Pidgeon, G. P., Kandouz, M., Meram, A., and Honn, K. V. (2002). Mechanisms controlling cell cycle arrest and induction of apoptosis after 12-Lipoxygenase inhibition in prostate cancer cells. *Cancer Res* 62(9): 2721-2727.

Quigley, H. A. (1996). Number of people with glaucoma worldwide. *Br J Ophthalmol* 80(5): 389-93.

Raviola, G. and Raviola, E. (1978). Intercellular junctions in the ciliary epithelium. *Invest Ophthalmol Vis Sci* 17(10): 958-81.

Rawat, D. S., Thakur, B. K., Semalty, M., Semalty, A., Badoni, P. and Rawat, M. S. (2013). Baicalein-phospholipid Complex: A novel drug delivery technology for phytotherapeutics. *Curr Drug Discov Technol* 10(3):224-32.

Reitsamer, H. A. and Kiel, J. W. (2003). Relationship between ciliary blood flow and aqueous production in rabbits. *Invest Ophthalmol Vis Sci* 44(9): 3967-71.

Flammer, J., Orgül, S., Costa, V. P., Orzalesi, N., Krieglstein, G. K., Serra, L. M., Renard, J. P. and Stefánsson, E. (2002). The impact of ocular blood flow in glaucoma. *Prog Retin Eye Res* 21(4): 359-393.

Richardson, D. R. (2004). Novel chelators for central nervous system disorders that involve alterations in the metabolism of iron and other metal ions. *Ann NY Acad Sci* 1012:326-341.

Riley, M. V. and Kishida, K. (1986). ATPases of ciliary epithelium: cellular and subcellular distribution and probable role in secretion of aqueous humor. *Exp Eye Res* 42(6): 559-68.

Ryan, J. S., Tao, Q. P. and Kelly, M. E. (1998). Adrenergic regulation of calcium-activated potassium current in cultured rabbit pigmented ciliary epithelial cells. *J Physiol* 511 (Pt 1): 145-57.

Sacca, S. C., Centofanti, M. and Izzotti, A. (2012). New proteins as vascular biomarkers in primary open angle glaucomatous aqueous humor. *Invest Ophthalmol Vis Sci* 53(7): 4242-4253.

Sacca, S. C., Izzotti, A., Rossi, P., and Traverso, C. (2007). Glaucomatous outflow pathway and oxidative stress. *Exp Eye Res* 84(3): 389–399.

Sacca S. C., Pascotto A., Camicione P., Capris P., and Izzotti A. (2005). Oxidative DNA damage in human trabecular meshwork and its correlation with intraocular pressure and visual field in primary open angle glaucoma, *Arch. Ophthalmol*. 123(4): 458–463.

Sakamoto, S and Shichi, H. (1991). Regional distribution of lipoxygenase activities in porcine ciliary epithelium. *J Ocul Pharmacol Ther* 7(2): 141-145.

Saito, Y. and Watanabe, T. (1979). Relationship between short-circuit current and unidirectional fluxes of Na^+ and Cl^- across the ciliary epithelium of the toad: demonstration of active Cl^- transport. *Exp Eye Res* 28(1): 71-9.

Samples, J. R., Binder, P. S., and Nayak, S. (1989). The effect of epinephrine and benzalkonium chloride on culture corneal endothelial and trabecular meshwork cells. *Exp Eye Res* 49(1): 1-12.

Sanchez-Torres, J., Huang, W., Civan, M. M. and Coca-Prados, M. (1999). Effects of hypotonic swelling on the cellular distribution and expression of pICln in human nonpigmented ciliary epithelial cells. *Curr Eye Res* 18(6): 408-16.

Satilmis, M., Orgul, S., Doubler, B. and Flammer, J. (2003). Rate of progression of glaucoma correlates with retrobulbar circulation and intraocular pressure. *Am J Ophthalmol* 135(5): 664–9.

Schlamp, C. L., Li, Y., Dietz, J. A., Janssen, K. T. and Nickells, R. W. (2006). Progressive ganglion cell loss and optic nerve degeneration in DBA/2J mice is variable and asymmetric. *BMC Neurosci* 7: 66.

Schuier, M., Sies, H., Illek, B., and Fischer, H. (2005). Cocoa-Related Flavonoids Inhibit CFTR-Mediated Chloride Transport across T84 Human Colon Epithelia. *J Nutr* 135(10): 2320-2325.

Schwartz, G. F. (2005). Compliance and persistency in glaucoma follow-up treatment. *Curr Opin Ophthalmol* 16(2): 114-21.

Shahidullah, M. and Delamere, N. A. (2006). NO donors inhibit Na^+, K^+-ATPase activity by a protein kinase G-dependent mechanism in the nonpigmented ciliary epithelium of the porcine eye. *Br J Pharmacol* 148(6): 871-80.

Shahidullah, M., Tamiya, S. and Delamere, N. A. (2007). Primary culture of porcine nonpigmented ciliary epithelium. *Curr Eye Res* 32(6): 511-22.

Shahidullah, M., Wilson, W. S., Yap, M. and To, C. H. (2003). Effects of ion transport and channel-blocking drugs on aqueous humor formation in isolated bovine eye. *Invest Ophthalmol Vis Sci* 44(3): 1185-91.

Shahidullah, M., Yap, M. and To, C. H. (2005). Cyclic GMP, sodium nitroprusside and sodium azide reduce aqueous humour formation in the isolated arterially perfused pig eye. *Br J Pharmacol* 145(1): 84-92.

Shi, C., Barnes, S., Coca-Prados, M. and Kelly, M. E. (2002). Protein tyrosine kinase and protein phosphatase signaling pathways regulate volume-sensitive chloride currents in a nonpigmented ciliary epithelial cell line. *Invest Ophthalmol Vis Sci* 43(5): 1525-32.

Shi, C., Ryan, J. S., French, A. S., Coca-Prados, M. and Kelly, M. E. (1999). Hyposmotically activated chloride channels in cultured rabbit non-pigmented ciliary epithelial cells. *J Physiol* 521(Pt 1): 57-67.

Shi, C., Szczesniak, A., Mao, L., Jollimore, C., Coca-Prados, M., Hung, O. and Kelly, M. E. (2003). A3 adenosine and CB1 receptors activate a PKC-sensitive Cl^- current in human nonpigmented ciliary epithelial cells via a G-coupled MAPK signaling pathway. *Br J Pharmacol* 139(3): 475-86.

Shi, Y. (2002). Mechanisms of caspase activation and inhibition during apoptosis. *Molecular Cell* 9(3): 459-470.

Shieh, D. E., Liu, L. T. and Lin, C. C. (2000). Antioxidant and free radical scavenging effects of baicalein, baicalin and wogonin. *Anticancer Res* 20(5A): 2861-2865.

Siefert, B., Pleyer, U., Muller, M., Hartmann, C. and Keipert, S. (1999). Influence of cyclodextrins on the in vitro corneal permeability and in vivo ocular distribution of thalidomide. *J Ocul Pharmacol Ther* 15(5): 429–438.

Sithisarn, P., Michaelis, M., Schubert-Zsilavecz, M., and Cinatl Jr, J. (2013). Differential antiviral and anti-inflammatory mechanisms of the flavonoids biochanin A and baicalein in H5N1 influenza A virus-infected cells. *Antivir Res* 97(1): 41-48.

Slater, B. J., Mehrabian, Z., Guo, Y., Hunter, A., and Bernstein, S. L. (2008). Rodent Anterior Ischemic Optic Neuropathy (rAION) induces regional retinal ganglion cell apoptosis with a unique temporal pattern. *Invest Ophthalmol Vis Sci* 49(8): 3671-3676.

So, F. V., Guthrie, N., Chambers, A. F., Moussa, M., and Carroll, K. K. (1996). Inhibition of human breast cancer cell proliferation and delay of mammary tumorigenesis by flavonoids and citrus juices. *Nutr and Cancer* 26(2): 167-181.

Stavniichuk, R., Drel, V. R., Shevalye, H., Maksimchyk, Y., Kuchmerovska, T. M., Nadler, J. L., and Obrosova, I. G. (2011). Baicalein alleviates diabetic

peripheral neuropathy through inhibition of oxidative–nitrosative stress and p38 MAPK activation. *Exp Neurol* 230(1): 106-113.

Stein, A., Pinke, R., Krupin, T., Glabb, E., Podos, S. M., Serle, J., and Maren, T. H. (1983). The effect of topically administered carbonic anhydrase inhibitors on aqueous humor dynamics in rabbits. *Am J Ophthalmol* 95(2): 222-228.

Stelling, J. W. and Jacob, T. J. (1996). Transient activation of K^+ channels by carbachol in bovine pigmented ciliary body epithelial cells. *Am J Physiol* 271(1 Pt 1): C203-9.

Stelling, J. W. and Jacob, T. J. (1997). Functional coupling in bovine ciliary epithelial cells is modulated by carbachol. *Am J Physiol* 273(6 Pt 1): C1876-81.

Sterling, D., Reithmeier, R. A. and Casey, J. R. (2001). A transport metabolon. Functional interaction of carbonic anhydrase II and chloride/bicarbonate exchangers. *J Biol Chem* 276(51): 47886-94.

Suh, J. and Rabson, A. B. (2004). NF-kappaB activation in human prostate cancer: important mediator or epiphenomenon? *J Cell Biochem* 91(1): 100–17.

Taskintuna, I., Banker, A. S., Rao, N. A., Wiley, C. A., Flores-Aguilar, M., Munguia, D., Bergeron-Lynn, G., De Clercq, E., Keefe, K. and Freeman, W. R. (1997). An Animal Model for Cidofovir (HPMPC) Toxicity: Intraocular Pressure and Histopathologic Effects. *Exp Eye Res* 64(5): 795-806.

Tezel, G. (2008). TNF-alpha signaling in glaucomatous neurodegeneration. *Prog Brain Res* 173: 409-421.

Tezel, G. (2006). Oxidative stress in glaucomatous neurodegeneration: mechanisms and consequences. *Prog Retin Eye Res* 25(5): 490–513.

The AIGS Investigators (2000). The Advanced Glaucoma Intervention Study (AGIS): 7. The relationship between control of intraocular pressure and visual field deterioration.The AGIS Investigators. *Am J Ophthalmol* 130(4): 429-40.

To, C. H., Do, C. W., Zamudio, A. C. and Candia, O. A. (2001). Model of ionic transport for bovine ciliary epithelium: effects of acetazolamide and HCO. *Am J Physiol Cell Physiol* 280(6): C1521-30.

To, C. H., Kong, C. W., Chan, C. Y., Shahidullah, M. and Do, C. W. (2002). The mechanism of aqueous humour formation. *Clin Exp Optom* 85(6): 335-49.

To, C. H., Mok, K. H., Do, C. W., Lee, K. L. and Millodot, M. (1998). Chloride and sodium transport across bovine ciliary body/epithelium (CBE). *Curr Eye Res* 17(9): 896-902.

Tunon, M. J., Garcia-Mediavilla, M. V., Sanchez-Campos, S. and Gonzalez-Gallego, J. (2009). Potential of Flavonoids as Anti-inflammatory Agents: Modulation of Pro- Inflammatory Gene Expression and Signal Transduction Pathways. *Curr Drug Metab* 10(3): 256-271.

Usayapant, A., Karara, A. H. and Narurkar, M. M. (1991). Effect of 2-hydroxypropyl-beta-cyclodextrin on the ocular absorption of dexamethasone and dexamethasone acetate. *Pharm Res* 8(12): 1495–1499.

Usukura, J., Fain, G. L. and Bok, D. (1988). [^{3}H] ouabain localization of Na^{+}/K^{+}-ATPase in the epithelium of rabbit ciliary body pars plicata. *Invest Ophthalmol Vis Sci* 29(4): 606-14.

van Leyen, K., Kim, H. Y., Lee, S. R., Jin, G., Arai, K., and Lo, E. H. (2006). Baicalein and 12/15-Lipoxygenase in the Ischemic Brain. *Stroke* 37(12): 3014-3018.

Vessey, J. P., Shi, C., Jollimore, C. A., Stevens, K. T., Coca-Prados, M., Barnes, S. and Kelly, M. E. (2004). Hyposmotic activation of $I_{Cl,swell}$ in rabbit nonpigmented ciliary epithelial cells involves increased ClC-3 trafficking to the plasma membrane. *Biochem Cell Biol* 82(6): 708-18.

Waitzman, M. B. and Jackson, R. T. (1965). Effects of topically administered ouabain on aqueous humor dynamics. *Exp Eye Res* 4(3): 135-45.

Wakabayashi, I. (1999). Inhibitory effects of baicalein and wogonin on lipopolysaccharide-induced nitric oxide production in macrophages. *Pharmacol Toxicol* 84(6): 288–291.

Wan, X. L., Chen, S. and Sears, M. (1997). Cloning and functional expression of a swelling-induced chloride conductance regulatory protein, plCln, from rabbit ocular ciliary epithelium. *Biochem Biophys Res Commun* 239(3): 692-6.

Wang, L., Chen, L. and Jacob, T. J. (2000). The role of ClC-3 in volume-activated chloride currents and volume regulation in bovine epithelial cells demonstrated by antisense inhibition. *J Physiol* 524 (Pt 1): 63-75.

Wang, R., Serle, J. B., Podos, S. M., and Sugrue, M. F. (1990). The ocular hypotensive effect of the topical carbonic anhydrase inhibitor l-671,152 in glaucomatous monkeys. *Arch Ophthalmol* 108(4): 511-513.

Wang, R., Serle, J. B., Podos, S. M., and Sugrue, M. F. (1991). MK-507 (l-671,152), a topically active carbonic anhydrase inhibitor, reduces aqueous humor production in monkeys. *Arch Ophthalmol* 109(9): 1297-1299.

Watanabe, T. and Saito, Y. (1978). Characteristics of ion transport across the isolated ciliary epithelium of the toad as studied by electrical measurements. *Exp Eye Res* 27(2): 215-26.

Wei, Y. and Guo, M. (2007). Hydrogen peroxide triggered prochelator activation, subsequent metal chelation, and attenuation of the fenton reaction. *Angew Chem Int Ed* 46(25):4722–4725.

Wetzel, R. K. and Sweadner, K. J. (2001). Immunocytochemical localization of the Na^+/K^+-ATPase α and γsubunits in the rat kidney. *Am J Physiol* 281(3): F531–F545.

Wiederholt, M. and Zadunaisky, J. A. (1986). Membrane potentials and intracellular chloride activity in the ciliary body of the shark. *Pflugers Arch* 407 Suppl 2: S112-5.

Wiederholt, M., Helbig, H. and Korbmacher, C. (1991). Ion transport across the ciliary epithelium: Lessons from cultured cells and proposed role of the carbonic anhydrase. *Carbonic Anhydrase. F. Botre', G. Gross and B. T. Storey. New York, VCH*: 232-44.

Williams, R. J., Spencer, J. P. and Rice-Evans, C. (2004). Flavonoids: antioxidants or signaling molecules? *Free Radic Biol Med* 36(7): 838–49.

Wilson, W. S., Shahidullah, M. and Millar, C. (1993). The bovine arterially-perfused eye: an in vitro method for the study of drug mechanisms on IOP, aqueous humour formation and uveal vasculature. *Curr Eye Res* 12(7): 609–20.

Wistrand, P. J. and Garg, L. C. (1979). Evidence of a high-activity C type of carbonic anhydrase in human ciliary processes. *Invest Ophthalmol Vis Sci* 18(8): 802-6.

Wistrand, P. J., Schenholm, M. and Lonnerholm, G. (1986). Carbonic anhydrase isoenzymes CA I and CA II in the human eye. *Invest Ophthalmol Vis Sci* 27(3): 419-28.

WoldeMussie, E., Ruiz, G., Wijono, M., and Wheeler, L. A. (2001). Neuroprotection of retinal ganglion cells by brimonidine in rats with laser-induced chronic ocular hypertension. *Invest Ophthalmol Vis Sci* 42(12): 2849-2855.

Wolff, C., Fuks, B., and Chatelain, P. (2003). Comparative study of membrane potential-sensitive fluorescent probes and their Use in ion channel screening assays. *J Biomol Screen* 8(12): 533-543.

Wolosin, J. M., Bonanno, J. A., Hanzel, D. and Machen, T. E. (1991). Bicarbonate transport mechanisms in rabbit ciliary body epithelium. *Exp Eye Res* 52(4): 397-407.

Wolosin, J. M., Candia, O. A., Peterson-Yantorno, K., Civan, M. M. and Shi, X. P. (1997). Effect of heptanol on the short circuit currents of cornea and ciliary body

demonstrates rate limiting role of heterocellular gap junctions in active ciliary body transport. *Exp Eye Res* 64(6): 945-52.

Wolosin, J. M., Chen, M., Gordon, R. E., Stegman, Z. and Butler, G. A. (1993). Separation of the rabbit ciliary body epithelial layers in viable form: identification of differences in bicarbonate transport. *Exp Eye Res* 56(4): 401-9.

Wong, B. C. Y., Wang, W. P., Cho, C. H., Fan, X. M., Lin, M. C. M., Kung, H. F. and Lam, S. K. (2001). 12-Lipoxygenase inhibition induced apoptosis in human gastric cancer cells. *Carcinogenesis* 22(9): 1349-1354.;

Woo, K. J., Lim, J. H., Suh, S. I., Kwon, Y. K., Shin, S. W., Kim, S. C., Choi, Y. H., Park, J. W. and Kwon, T. K. (2006). Differential inhibitory effects of baicalein and baicalin on LPS-induced cyclooxygenase-2 expression through inhibition of C/EBPβ DNA-binding activity. *Immunobiology* 211(5): 359-368.

Wu, Q., Delamere, N. A. and Pierce, W., Jr. (1997). Membrane-associated carbonic anhydrase in cultured rabbit nonpigmented ciliary epithelium. *Invest Ophthalmol Vis Sci* 38(10): 2093-102.

Wu, Q., Pierce, W. M., Jr. and Delamere, N. A. (1998). Cytoplasmic pH responses to carbonic anhydrase inhibitors in cultured rabbit nonpigmented ciliary epithelium. *J Membr Biol* 162(1): 31-8.

Wu, R., Yao, K., Flammer, J. and Haefliger, I. O. (2004). Role of anions in nitric oxide-induced short-circuit current increase in isolated porcine ciliary processes. *Invest Ophthalmol Vis Sci* 45(9): 3213-22.

Xu, H., Chen, M. and Forrester, J. V. (2009). Para-inflammation in the aging retina. *Prog Retin Eye Res* 28(5): 348-368.

Xu, J., Zhang, Y., Xiao, Y., Ma, S., Liu, Q., Dang, S., Jin, M., Shi, Y. and Wan, B. (2013). Inhibition of 12/15-lipoxygenase by baicalein induces microglia PPAR[beta]/[delta]: a potential therapeutic role for CNS autoimmune disease. *Cell Death Dis* 4(4): e569.

Yang, H., Avila, M. Y., Peterson-Yantorno, K., Coca-Prados, M., Stone, R. A., Jacobson, K. A. and Civan, M. M. (2005). The cross-species A3 adenosine-receptor antagonist MRS 1292 inhibits adenosine-triggered human nonpigmented ciliary epithelial cell fluid release and reduces mouse intraocular pressure. *Curr Eye Res* 30(9): 747-54.

Yang, L. P., Sun, H. L., Wu, L. M., Guo, X. J., Dou, H. L., Tso, M. O. M., Zhao, L. and Li, S. M. (2009). Baicalein Reduces Inflammatory Process in a Rodent Model of Diabetic Retinopathy. *Invest Ophthalmol Vis Sci* 50(5): 2319-2327.

Yantorno, R. E., Carre, D. A., Coca-Prados, M., Krupin, T. and Civan, M. M. (1992). Whole cell patch clamping of ciliary epithelial cells during anisosmotic swelling. *Am J Physiol* 262(2 Pt 1): C501-9.

Yee, R. W. (2007). The effect of drop vehicle on the efficacy and side effects of topical glaucoma therapy: a review. *Curr Opin Ophthalmol* 18(2): 134-139

Yildirim, O., Ates, N. A., Ercan, B., Muslu, N., Unlu, A., Tamer, L., Atik, U. and Kanik, A. (2005). Role of oxidative stress enzymes in open-angle glaucoma. *Eye* 19(5): 580–583.

Yoo, S., Han, S., Park, Y., Lee, J. H., Oh, U., and Hwang, S. (2009). Lipoxygenase inhibitors suppressed carrageenan-induced Fos-expression and inflammatory pain responses in the rat. *Mol Cells* 27(4): 417-422.

Yoon, S. Y., dela Peña, I.C., Shin, C. Y., Son, K. H., Lee, Y. S., Ryu, J. H., Cheong, J. H. and Ko, K. H. (2011). Convulsion-related activities of Scutellaria flavones are related to the 5, 7-dihydroxyl structures. *Eur J Pharmacol* 659(2-3): 155-160.

Yoshino, M. and Murakami, K. (1998). Interaction of iron with polyphenolic compounds: application to antioxidant characterization. *Anal Biochem* 257(1): 40–44.

Yue, G. G. L., Yip, T. W. N., Huang, Y. and Ko, W. H. (2004). Cellular Mechanism for Potentiation of Ca^{2+} -mediated Cl^{-} Secretion by the Flavonoid Baicalein in Intestinal Epithelia. *J Biol Chem* 279(38): 39310-39316.

Zandi, K., Teoh, B. T., Sam, S. S., Wong, P. F., Mustafa, M. and AbuBakar, S. (2012). Novel antiviral activity of baicalein against dengue virus. *BMC Complement Altern Med.* 9(12): 214.

Zhang, H. B., Lu, P., Guo, Q. Y., Zhang, Z. H. and Meng, X. Y. (2013). Baicalein induces apoptosis in esophageal squamous cell carcinoma cells through modulation of the PI3K/Akt pathway. *Oncol Lett* 5(2): 722-728.

Zhang, Y. Y., Guo, Y. Z. and Ageta, H. (1997). A new flavones C-glycoside from Scutellariaaicalensis. *J Chin Pharm Sci* 6: 182–186.

Zhang, J. J. and Jacob, T. J. (1997). Three different Cl^- channels in the bovine ciliary epithelium activated by hypotonic stress. *J Physiol* 499 (Pt 2): 379-89.

Zhang, L., Zhang, J., Wang, L., and Xia, H. (2009). Ocular Pharmacokinetics and Availability of Topically Applied Baicalein in Rabbits. *Curr Eye Res* 34 (4): 257-263.

Zhang, S., Ye, J., and Dong, G. (2010). Neuroprotective Effect of Baicalein on Hydrogen Peroxide-Mediated Oxidative Stress and Mitochondrial Dysfunction in PC12 Cells. *J Mol Neurosci* 40(3): 311-320.

Zhang, Z., Cui, W., Li, G., Yuan, S., Xu, D., Hoi, M. P. M., Lin, Z., Dou, J., Han, Y., and Lee, S. M. Y. (2012). Baicalein Protects against 6-OHDA-Induced Neurotoxicity through Activation of Keap1/Nrf2/HO-1 and Involving PKCα and PI3K/AKT Signaling Pathways. *J Agric Food Chem* 60(33): 8171-8182.

Zhong, L., Bradley, J., Schubert, W., Ahmed, E., Adamis, A. P., Shima, D. T., Robinson, G. S. and Ng, Y. S. (2007). Erythropoietin Promotes Survival of Retinal Ganglion Cells in DBA/2J Glaucoma Mice. *Invest Ophthalmol. Vis. Sci* 48(3): 1212-1218.

Zhou, Q. M., Wang, S., Zhang, H., Lu, Y. Y, Wang, X. F., Motoo, Y. and Su, S. B. (2009). The combination of baicalin and baicalein enhances apoptosis via the ERK/p38 MAPK pathway in human breast cancer cells. *Acta Pharmacol Sin* 30(12): 1648-1658.

Zhou, X., Wang, W., Lu, F., Hu, S., Jiang, L., Yan, D., Zhang, X., Yu, X., Yu, J. and Qu, J. (2007). A comparative gene expression profile of the whole eye from human, mouse, and guinea pig. *Mol Vis* 28(13): 2214–21.

Zhou, L., Li, Y., and Yue, B. Y. J. T. (1999). Oxidative stress affects cytoskeletal structure and cell-matrix interactions in cells from an ocular tissue: The trabecular meshwork. *J Cell Physiol* 180(2): 182-189.

Zimmerman, T. J., Garg, L. C., Vogh, B. P. and Maren, T. H. (1976). The effect of acetazolamide on the movement of sodium into the posterior chamber of the dog eye. *J Pharmacol Exp Ther* 199(3): 510-7.